IDENTIFICATION AND CHARACTERIZATION OF ADULT *AEDES AEGYPTI* MIDGUT PERITROPHIC MATRIX HEME-BINDING PROTEINS

A Dissertation

by

SHAVONN REEZALE WHITEN

Submitted to the Office of Graduate and Professional Studies of
Texas A&M University
in partial fulfillment of the requirements for the degree of

DOCTOR OF PHILOSOPHY

Chair of Committee,	Zachary N. Adelman
Committee Members,	Kevin M. Myles
	Pete D. Teel
	Carmen D. Tekwe
Head of Department,	David W. Ragsdale

December 2018

Major Subject: Entomology

ABSTRACT

Bloodfeeding is a high risk, high reward process that has evolved in many arthropods. The adult female *Aedes aegypti* mosquito- a hematophagous arthropod, is the principle vector of dengue, chikungunya, yellow fever and Zika viruses. While these viruses must transverse the midgut to be transmitted, the ingested blood meal must also be digested, absorbed, or excreted, as aggregation of blood meal metabolites (heme) potentiates a toxic environment for the female mosquito midgut. The midgut peritrophic matrix (PM), a semipermeable extracellular layer comprised of chitin fibrils, glycoproteins and proteoglycans, has been shown to facilitate heme binding, and thereby serves as a protective mechanism after blood meal feeding. However, the protein composition, and specifically heme-binding proteins, of this structure have not been characterized for adult female *Ae. aegypti*. Therefore, as part of this dissertation, we: 1) conducted a proteomic analysis to identify constituents of the adult female *Ae. aegypti* early midgut PM, 2) conducted a heme-enrichment proteomic analysis to isolate adult female *Ae. aegypti* midgut PM heme-binding proteins, and 3) conducted reverse genetic analyses to determine the physiological function of known and putative adult female *Ae. aegypti* heme-binding proteins. We identified 474 unique proteins, with 115 predicted as secreted proteins without transmembrane domains in the adult female *Ae. aegypti* early midgut PM. To our surprise, 10% of the peptides identified were known salivary proteins, but most interestingly, we isolated the two known and a novel PM peritrophin. As part of our midgut PM enrichment analysis, we identified 23 heme-enriched proteins, including one known heme-binding protein. Through gene expression profiling experiments, we found that one PM protein (AeAper50; AAEL002467) increased in expression by 300-fold within four hours of blood meal feeding.

However, RNAi-mediated single and multiplex knockdown experiments of this gene and two related PM proteins showed no significant phenotypic effect on mortality, fecundity or hatch rate. Likewise, we found no significant alternations in catalase or ferritin expression with loss of function for the known and putative midgut PM proteins. Taken together, these results suggest that adult female *Ae. aegypti* have evolved many (known and unknown) mechanisms to ensure a favorable environment and avoidance of oxidative damage after bloodfeeding.

DEDICATION

I dedicate this dissertation to my ancestors who fought, bled and died so that I could exercise my humanly right to pursue higher education in America. May this dissertation serve as evidence that your unspeakable suffering, relentless efforts and vision of a brighter tomorrow were not in vain. May your light continue to shine through my vessel. I also dedicate this dissertation to future generations of African-Americans who will fulfill the calling to venture down this challenging and yet rewarding path. I pray each of you are able to find and rise in your true light.

"Bringing the gifts that my ancestors gave, I am the dream and the hope of the slave.

I RISE I RISE I RISE."

~ Maya Angelou

ACKNOWLEDGEMENTS

I first give honor and praise to my Creator for keeping and covering me throughout this journey, which has brought about an unspeakable level of humility, reverence and divine understanding. I next thank my major advisor, Dr. Zach Adelman, for the time and energy invested to assure that when I exit Texas A&M University, I can stand and compete with research scientists around the world. I am grateful to my committee members, Dr. Eric Calvo, Dr. Kevin Myles, Dr. Pete Teel and Dr. Carmen Tekwe for the support and guidance provided throughout the course of my doctoral research and training process. Likewise, thank you to the Texas A&M University Department of Entomology faculty, administrative staff and colleagues for assistance provided during my transition to Texas A&M University and throughout my Ph.D. training. Thanks are also due to the Virginia Tech Department of Entomology faculty, administrative staff and colleagues who helped me navigate and survive the first two years of my doctoral training process.

Sincere thank you to my many mentors who have traveled this journey with me and provided inspiration even when I could not see the light. I am forever grateful to Dr. Randy Grayson and the Virginia Tech George Washington Carver program for providing the platform for my desire to pursue a doctorate degree to become reality. Likewise, I am eternally grateful for my personal mentor, Dr. Estralita Martin, who has served as my guiding light and a living reminder to always KEEP THE FAITH.

Last but certainly not least, I thank my family and village for all of the love, support and prayers provided as I sought to embark upon, endure and overcome some of the most challenging and yet rewarding days of my life. I thank my siblings, Meagan and Michael Whiten for being

sources of earthly strength in times when I was weak and for always being there to encourage me to fight on another day. To the two individuals who gave me earthly life and since then have made every effort to provide me with the continuous financial, emotional and physical support required to be and do all that I aspire to achieve in life, there are not enough ways to say thank you. Therefore, my highest gratitude I extend to my father and mother- Sherman and Gloria Whiten, as without you two, THERE IS NO ME.

CONTRIBUTORS AND FUNDING SOURCES

This research was overseen by my dissertation advisory committee consisting of Dr. Zach N. Adelman (major advisor), Dr. Kevin M. Myles and Dr. Pete D. Teel of the Texas A&M University Department of Entomology. Likewise, outside committee members include Dr. Carmen D. Tekwe of the Texas A&M University School of Public Health and Dr. Eric Calvo of the National Institute of Allergy and Infectious Diseases of the National Institutes of Health.

This research was funded by the National Institute of Allergy and Infectious Diseases (NIAID) of the National Institutes of Health (NIH) under award number AI115138. Chapter 2 research was conducted at Virginia Tech in collaboration with Dr. Richard F. Helm and Dr. William Keith Ray of the Virginia Tech Department of Biochemistry Mass Spectrometry Incubator. Chapter 3 research was conducted in collaboration with Dr. Larry Dangott and the Texas A&M University Department of Biochemistry & Biophysics Protein Chemistry Laboratory. LC-MS/MS data analysis for Chapter 3 was conducted by the University of Texas Health Science Center at San Antonio Mass Spectrometry Laboratory. Preliminary experiments for Chapter 4 gene expression profiling were conducted under the direction of Drs. Eric Calvo and José Ribeiro of the National Institute of Allergy and Infectious Diseases of the National Institutes of Health through the NIH Office of Intramural Training and Education (OITE) Gradate Summer Opportunity to Advance Research (GSOAR) fellowship. The NIH OITE GSOAR fellowship provided funding for all research materials utilized while conducting research at the NIH NIAID Laboratory of Malaria and Vector Research (LMVR) in Rockville, Maryland.

Graduate student funding was supported by the Virginia Tech George Washington Carver Assistantship August 2014-May 2016, and subsequently supported by the Texas A&M University College of Agriculture and Life Sciences Lechner Fellowship August 2016-May 2018. Funds to disseminate research findings at local and international conferences were provided by the Texas A&M University Office of Graduate and Professional Studies (OGAPS) Travel Award (April 2017) and the Texas A&M College of Agriculture and Life Sciences Student Development Grant (June 2018).

TABLE OF CONTENTS

Page

LIST OF FIGURES

Page

LIST OF TABLES

Page

CHAPTER I

INTRODUCTION AND LITERATURE REVIEW*

1.1 Introduction: Evolution of arthropod hematophagy

Estimates suggest there are more than 1 million insect and arachnid species inhabiting planet Earth, approximately 14,000 of which have adapted the ability to feed on vertebrate blood [1]. Commonly known as hematophagy, this adaptation has arisen independently many times over the course of evolution [1]. However, certain features are shared among the ancestors of bloodfeeding arthropods. Traditionally accepted ancestral pre-conditions to bloodfeeding include: 1) living in close proximity to vertebrates, 2) specialized feeding on skin remains, dung or fluids from animal carcasses and 3) specialized mouthparts for piercing and cutting [1]. It is quite interesting that hematophagous arthropods can consume anywhere from 2 to 100x their normal body weight during a single blood meal. Subsequently, this blood meal, comprised largely of proteins, is digested by enzymes secreted from midgut epithelial cells [2-5]. The amino acids that result from blood meal protein digestion are used for lipid, carbohydrate, and egg protein synthesis [6]. While the bloodfeeding process has obvious nutritional advantages for hematophagous arthropods, the digestive process releases the pro-oxidant molecules heme and iron in potentially toxic quantities. In response to this challenge, bloodfeeding arthropods have evolved a number of strategies to limit oxidative damage during blood digestion. This review seeks to compile and compare existing vertebrate and invertebrate literature as it pertains to iron

* Reprinted with permission from "Ironing out the Details: Exploring the Role of Iron and Heme in Blood-Sucking Arthropods" by Whiten, S.R., Eggleston, H., and Adelman, Z.N., 2018. Frontiers in Physiology, Vol. 8, Issue 1134, Copyright 2018 Adelman

and heme processing, with particular interest in applying knowledge gained in other systems to hematophagous arthropods.

1.2 Protective adaptations against oxidative stress after a blood meal: antioxidants

Over time, hematophagous arthropods have honed their antioxidant systems to avoid oxidative stress [7, 8]. Oxidative stress has traditionally been defined as the disturbance in balance between the production of reactive oxygen species (ROSs) and antioxidant defenses [7, 9, 10], which may result in the oxidation of nucleic acids [11], lipids [12, 13] and proteins [13, 14]. However, all cells and organisms naturally produce ROSs [10]. For example, prior to a blood meal, the mosquito *Aedes aegypti*, the most important vector of arboviruses worldwide, generate ROSs for the control of intestinal microbiota proliferation [15]. Oliveira and Oliveira (2002) hypothesized that a decrease in mitochondrial ROSs may be necessary to avoid their interaction with the pro-oxidant products of blood meal digestion, heme and iron [16]. This was confirmed by Goncalves et al. (2009), who reported that bloodfeeding promoted the fusion of *Ae. aegypti* flight muscle mitochondria, which decreased the generation of ROSs [17]. Interestingly, mitochondrial decreases in H_2O_2 followed the digestion process, with mitochondrial function returning to pre-blood meal levels upon the completion of digestion [17]. Oliveira et al. (2011) found that this decrease in ROSs is triggered by heme and no other blood component [15]. To further reduce ROSs generated post bloodfeeding and avoid a milieu prone to oxidative stress, *Ae. aegypti* and other hematophagous arthropods have deployed a number of defenses into the gut lumen and hemolymph (extracellular) as well as in the cytoplasm of midgut epithelial cells or other tissues in the body (intracellular).

1.2.1 Intracellular antioxidants

Intracellularly, Cu, Zn and Mn superoxide dismutases (SOD) catalyze the conversion of superoxide anions into hydrogen peroxide. Subsequently, catalase (CAT) and general peroxidases (POD) are responsible for detoxifying hydrogen peroxide [7]. More specifically, catalase catalyzes the dismutation of hydrogen peroxide to oxygen and water. Paes et al. (2001) found that when compared to other tissues, SOD and CAT activity were highest in the adult female midgut of the kissing bug, *Rhodnius prolixus*. Likewise, subsequent inhibition of CAT resulted in increased H_2O_2 in midgut extracts [18]. To further test the individual and collective roles of (CAT) and glutathione (GSH), each antioxidant was individually and collectively inhibited. For GSH and CAT, there was a fourfold and twofold increase in H_2O_2 content in *R. prolixus* midgut extracts, respectively. Interestingly, when GSH and CAT synthesis were inhibited simultaneously, the authors saw a tremendous increase in midgut extract H_2O_2 content, confirming the importance of both antioxidants with regards to H_2O_2 control after a blood meal [18]. In a more recent study, through gene expression comparisons, Oliveira, Talyuli [19] found that mRNA levels for the antioxidant enzyme CAT increased 6-fold at 24 and 36 hours after a blood meal and decreased to values equivalent to sugar fed mosquitoes at the end of digestion (72 hours). RNAi-mediated knockdown of CAT resulted in reduced oviposition and lifespan when adult female *Aedes aegypti* were challenged with the pro-oxidant H_2O_2 [19]. This reduced fecundity as a result of RNAi mediated knockdown of CAT was also demonstrated in adult female *Anopheles gambiae,* one of the primary mosquito vectors of malaria parasites [20]. Interestingly, this study found that a single serine to tryptophan polymorphism resulted in decreased CAT activity and stability [20]. The antioxidant role of CAT in ovaries has also been documented in other Dipterans besides mosquitoes, as ovarian CAT was found to accumulate in

developing oocytes of the bloodsucking sand fly, *Lutzomyia longipalpis,* 12 to 48 hours after bloodfeeding [21]. Beyond SOD and CAT, glutathione S-transferase (GST) catalyzes the conjugation between glutathione and other molecules [22]. Through competitive enzymatic-based assays and assays measuring changes in intrinsic fluorescence, *Ae. aegypti* recombinant GSTX2-2 was the first mosquito GST found to *in vitro* bind heme [23]. However, further studies are needed to determine antioxidant functionality for GSTX2-2 after a blood meal. In the cattle tick, *Rhipicephalus* (*Boophilus*) *microplus,* GST activity was confirmed as antioxidant in the eggs and larvae of engorged females. More specifically, GST enzymatic activity significantly increased and O_2 consumption progressively increased during embryonic development and eventually peaked at hatch [22]. These authors reported a strong correlation between O_2 consumption and GST activity, as well as a positive correlation for the antioxidants CAT and GSH with GST in *R. microplus* eggs and larvae. These results suggest that in addition to the antioxidant parameters, which allow for avoidance of oxidative stress in the midgut after a blood meal, increased oxidative stress can be associated with embryogenesis and aging [22].

1.2.2 Extracellular antioxidants

While certain antioxidant molecules work in concert to intracellularly reduce oxidative stress, here we highlight recent advancements regarding extracellular antioxidants. Recently, Lim et al. (2012) suggested a new role for xanthurenic acid (XA) as a heme and iron chelator. XA is product of tryptophan degradation through the kynurenine pathway. Traditionally, in insects, the kynurenine pathway is associated with eye pigment formation. However, reverse phase HPLC and mass spectrometry were used to identify xanthurenic acid (XA) as a component of *Ae. aegypti* midgut homogenates after a blood meal (ABM) [24]. At 24 hours ABM, XA

reached maximum levels. This is also the time of peak of blood meal hemoglobin digestion, when large amounts of heme and iron are present in the midgut lumen. Both heme and iron-induced lipid peroxidation were inhibited by XA through the i*n vitro* binding of XA to both heme and iron, suggesting an antioxidant role for XA in the *Ae. aegypti* midgut after a blood meal. Similarly, an antioxidant function has been demonstrated for a 15 kDa heme-binding protein (RHBP) in *R. prolixus* [25]. Given that RHBP is a hemolymph-localized heme-binding protein, it will be further discussed in this context later in our review. However, using ^{32}P labeling of fat bodies (site of lipid production), Dansa-Petretski et al. (1995) provided evidence that RHBP serves as an antioxidant, allowing for proper functioning of lipophorin as a lipid shuttle from the fat bodies to other organs. Heme negatively affected the functionality of lipophorin, but functionality returned to normal levels when RHBP was present [25]. More specifically, RHBP inhibited the heme-induced reduction of lipophorin ability to transfer phospholipids to the ovaries [25].

The above studies highlight various antioxidant molecules deployed by some bloodfeeding arthropods. Undoubtedly, many additional mechanisms remain to be uncovered, particularly in those bloodfeeding species that do not receive as much attention, such as lice, fleas and bed bugs. We note that the subject of redox homeostasis is even more complicated in context of the microbiota of bloodfeeding arthropods. This topic was the subject of a recent review [8], and thus will not be discussed further.

1.3 Protective adaptations against oxidative stress after a blood meal: Specialized midgut defense mechanisms

Hematophagous arthropods have evolved specialized defense mechanisms to avoid heme toxicity during blood meal digestion such as the extracellular double plasma membrane structure, perimicrovillar membranes (PPM), [26-28] which cover the midgut epithelia and facilitate generation of the heme crystal, hemozoin in the kissing bug [27, 29-33], hemosomes in the cattle tick [34, 35], and Type I peritrophic matrix formation in larval and nymphal *Ixodes sacpularisscapularis* ticks and adult Dipteran mosquitoes (except Tsetse adults which form Type II PM) [36-38]. Interestingly, all of the above-mentioned structures function in heme detoxification through various specialized forms of aggregation or crystalization [1]. Below we have highlighted recent advancements in knowledge regarding each of these structures, but refer the reader to Graça-Souza et al. (2006) for a more detailed review of earlier literature [1].

In the kissing bug *R. prolixus*, transmission electron micrographs of the midgut showed large aggregates of crystalline heme during blood meal digestion [29, 30]. Interestingly, heme crystallization was also found in three other triatomine insects, *Triatoma infestans*, *Dipetalogaster maximus* and *Panstrongylus megistus* [39]. Further investigation identified the perimicrovillar membranes, extracellular double plasma membranes which line the midgut epithelium, as necessary for heme crystallization into hemozoin for *R. prolixus*, *T. infestans*, *D. maximus* and *P. megistus* [31, 33, 39]. Specifically, lipid and protein constituents of the perimicrovillar membrane were necessary for proper hemozoin formation [31, 40, 41]. Hemozoin formation assays and RNAi mediated knock-down of α-glucosidase provided evidence supporting the role of α-glucosidase in the nucleation step of hemozoin formation [42]. α-glucosidase is a membrane-bound enzyme found in the midgut of *R. prolixus* with maximal

activity 7-9 days post blood meal (PBM) [31]. Interestingly, aggregated hemozoin also reached maximum levels at 7 days PBM [31]. More recently, through kinetic analysis of hemozoin formation induced by the perimicrovillar membranes, Stiebler et al. (2010) identified three different stages of hemozoin formation in *R. prolixus*. Through Mössbauer spectroscopy, these authors provided evidence that at least 97% of all iron present in the midguts of *R. prolixus* four days post blood meal was in the form of hemozoin [40]. Follow-up experiments provided evidence that lipids isolated from the perimicrovillar membranes are efficient catalysts of hemozoin formation *in vitro* [40, 41]. More specifically, *in vitro* experiments with two commercial phospholipids, unsaturated 1,2-dilinoleoyl-sn-glycero-3-phosphoethanolamine (uPE) and to a lesser extent unsaturated 1,2-dilinoleoyl-sn-glycero-3-phosphocholine (uPC) produced brick shaped and blunt ended β-hematin crystals similar to those produced by plasma-fed or blood-fed *R. prolixus* midgut lipids [41]. This suggests that uPE and uPC (to lesser extent) play integral roles in the determination of crystal morphology for hemozoin in the midgut of *R. prolixus*. This is in agreement with previous findings, which reported 1,2-dilinoleoyl-sn-glycero-3-phosphoethanolamine as the major phospholipid synthesized by *R. prolixus* midgut epithelium [43]. A similar involvement of lipids in hemozoin formation has been well documented in the parasites *Plasmodium* and *Schistosoma mansoni* (blood fluke) [40, 41, 44, 45]. Taken together, these results emphasize the importance of looking beyond protein components for the mechanistic basis of important biochemical reactions in bloodmeal detoxification.

R. microplus are unable to endogenously synthesize heme [35]. For the first seven days after a blood meal, hemoglobin-derived heme is directly absorbed for vitellogenesis [34]. During this time, the largest amount of heme is concentrated at the basal lamina side of midgut digestive cells (closest to hemocoel) [34]. This contrasts with other hematophagous arthropods where

digestion occurs in the midgut lumen. After the first seven days PBM, the amount of heme absorption decreases and heme concentrates in midgut digestive cell organelles that specialize in heme sequestration, termed hemosomes [34]. By the end of blood meal digestion, the mass of an individual hemosome was reported to be 90% heme [34]. More recently, Lara et al. (2015) proposed a detailed model for heme movement in digestive cells of *R. microplus*. However, there remain unanswered questions regarding movement of heme from digestive vesicles to the intracellular hemosomes [46].

While digestive cell hemosomes (*R. microplus*) and heme crystal hemozoins in association with a perimicrovillar membrane (*R. prolixus*) have been documented as protective mechanisms against oxidative stress, *I. scapularis* ticks (vector of *Borrelia burgdorferi*) [38] and most adult Dipterans (biting flies and mosquitoes) produce a peritrophic matrix in response to bloodfeeding [37, 38, 47-57].

The peritrophic matrix (PM) is a semipermeable extracellular layer, which lines the midgut of most invertebrates [36, 58]. The peritrophic matrix is classified as Type I or Type II based on location of synthesis within the insect midgut [36]. The Type I peritrophic matrix is

completely synthesized by midgut epithelial cells [58]. In contrast, the Type II peritrophic matrix is constitutively secreted by the cardia, a specialized organ found between the foregut and midgut [58-60]. Type I PM formation is induced by midgut distension [61, 62] and it is comprised of proteins, proteoglycans, and chitin fibrils [50, 63]. Peritrophic matrix proteins are integral components of the PM, and are commonly referred to as peritrophins [58]. Peritrophins are characterized by the presence of a secretory signal peptide, multiple chitin-binding domains containing cysteine-proline dipeptides, and intervening mucin-like domains rich in proline, serine, and threonine [58]. The multiple chitin-binding domains of peritrophic matrix peritrophins function as cross-linkers for chitin fibrils, thereby providing structure and support for the peritrophic matrix [47, 64]. In addition, PM peritrophins contain aromatic amino acid residues that facilitate binding with N-acetyl-glucosamine of the chitin fibrils [65]. Several Type I and Type II PM peritrophins have been identified and characterized from hematophagous insects (Fig. 1).

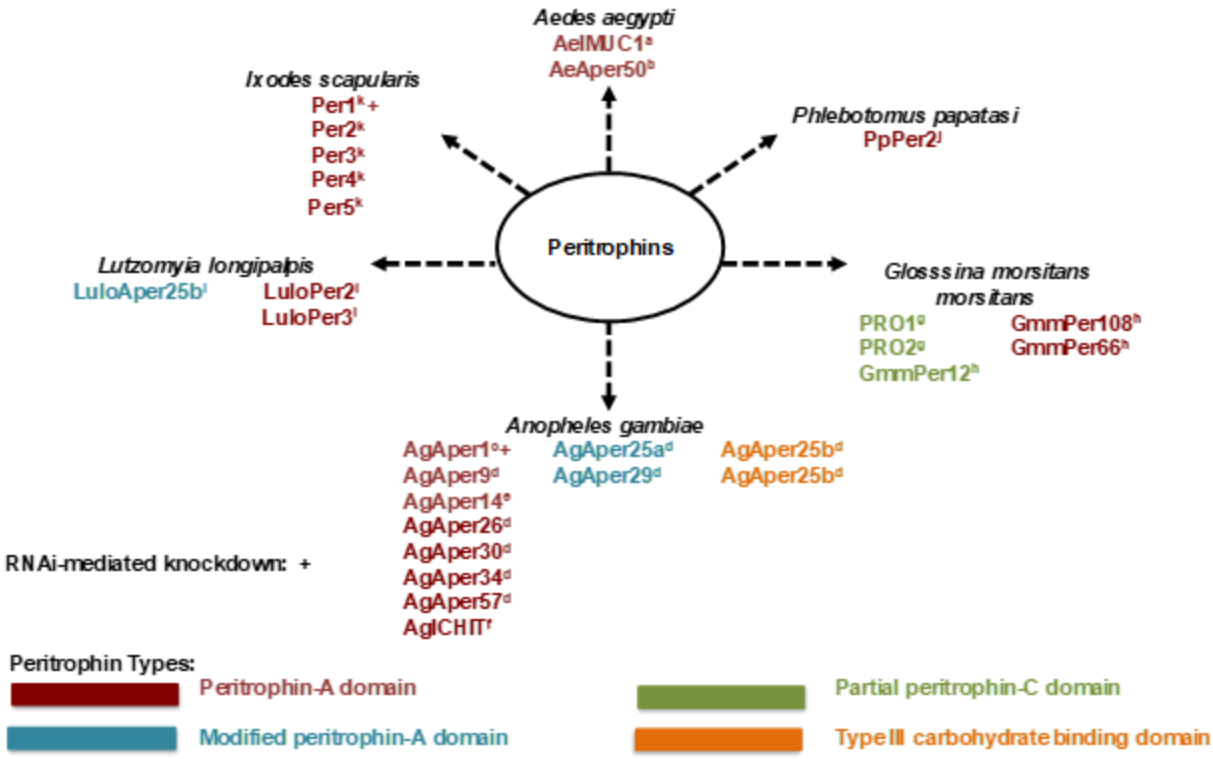

Figure 1. Known hematophagous arthropod peritrophic matrix peritrophins. Peritrophic matrix peritrophin classification according to their chitin-binding domains (CBDs). Peritrophin-A domain (PAD) is the most common type of CBD with six interspersed cysteine residues. Modified peritrophin-A domains (mPADs) have two additional cysteine residues. Peritrophin-C domain (PCD) contains 10 interspersed cysteine residues, and typically 121-122 amino acid residues long. Partial PCDs contain 67-70 amino acids. Type III carbohydrate binding domains (CBDIII) contains 10 interspersed cysteine residues, similar to PCD, this domain is typically 110-117 amino acid residues long. [a]Morlais and Severson, 2001; [b]Shao et al., 2005; [c]Shen and Jacobs-Lorena, 1998; [d]Dinglasan et al., 2009; [e]Devenport et al., 2005; [f]Dimopoulos et al., 1998; [g]Hao and Aksoy, 2002; [h]Rose et al., 2014; [i]Jochim et al., 2008; [j]Ramalho-Ortigão et al., 2007; Narasimhan et al., 2014 [66].

Peritrophic matrix peritrophins can be further classified according to their chitin-binding domains (CBDs). Each CBD is comprised of cysteine residues that allow for disulfide bonds within the CBD, and the number of disulfide bonds within a CBD can range from three to five [58, 65]. The Peritrophin-A domain (PAD) is the most common type of CBD, and contains six interspersed cysteine residues [65]. Typically, an individual PAD contains 48-57 amino acid residues. However, the exact PAD sequence arrangement has been found to vary for different

insect orders [65], and as seen in *Anopheles gambiae* there are cases of modified peritrophin-A domains (mPADs). The mPAD of AgAper25a and AgAper29 are characterized as having two additional cysteine residues, however, these two cysteine residues are not considered significant [65].

While less common, CBDs can also be classified as Peritrophin-B domain (PBD) or Peritrophin-C domain (PCD) according to the number of cysteine residues. An individual PBD contains eight interspersed cysteine amino acid residues, and is 81-88 residues long [65]. In contrast, an individual PCD contains 10 interspersed cysteine residues, and is typically 121-122 amino acid residues long [65]. As seen in the Tsetse (*Glosssina morsitans morsitans*), there are partial PCDs that contain 67-70 amino acids [37, 55]. In addition, as seen in *An. gambiae* AgAper25b, peritrophins can contain a Type III carbohydrate binding domains (CBDIII). While the CBDIII contains 10 interspersed cysteine residues (similar to PCD), this domain is typically 110-117 amino acid residues long.

In addition to binding chitin, one peritrophin has been reported to bind heme. *Ae. aegypti* intestinal mucin 1 (AeIMUC1) is a 275-amino acid glycoprotein that contains three chitin-binding domains and a mucin domain between CBD 1 and CBD 2[51, 67]. Rayms-Keller et al. (2000) first identified AeIMUC1 RNA in metal exposed *Ae. aegypti* mosquito larvae, metal fed adult females and blood-fed adult females [67]. Devenport et al. (2006), confirmed chitin and heme binding for AeIMUC1. Through deletion analysis using recombinant proteins, they also determined that chitin-binding and heme-binding functions are associated with the 3 CBDs of AeIMUC1 [51]. Most importantly, they confirmed AeIMUC1 as an integral PM peritrophin associated with the PM 12 to 24 hours post bloodfeeding [51]. Taken together, results from previous AeIMUC1 studies suggest this protein is important for PM structural integrity [51] and

blood meal heme detoxification [51, 67]. However, studies suggest there are potentially more *Ae. aegypti* midgut peritrophic matrix peritrophins [59, 63].

With advancements in technology such as Multidimensional protein identification technology (MudPIT) [68], the total protein composition of tissues such as the PM can more readily be explored/discovered. For example, a similar approach to MudPIT was utilized by Dinglasan et al. (2009) to determine PM protein composition for *An. gambiae*. By utilizing an artificial protein-free meal enriched with latex beads for midgut distention and subsequent PM formation, Dinglasan et al. (2009) collected more than 750 PMs for sequential extraction, digestion and identification. In total, 209 PM and PM-associated proteins were identified via a mass spectrometry-based proteomic analysis. While the largest majority of identified proteins were associated with peptidase activity, nine PM proteins isolated in this proteomic analysis contained a secretory signal peptide and one or more chitin binding domains, and therefore took the total list of identified peritrophins from three to twelve in *An. gambiae.* Dinglasan et al. (2009) also proposed a model which detailed *An. gambiae* PM formation and putative interactions among the various types of proteins identified in their study [53].

Given the unprecedented level of exploration and discovery of *An. gambiae* PM protein composition, and the relation of the Dinglasan et al. (2009) results to *Ae. aegypti*, another important disease vector, this methodology should be further explored to determine PM protein composition for other hematophagous arthropods of medical importance. To date, only one study with the tsetse fly (*Glossina morsitans morsitans*) has utilized a similar methodology [37]. Interestingly, this study utilized teneral (unfed) male tsetse flies to determine PM protein composition, as only two PM proteins had been identified previously, but were poorly characterized [37, 55]. Given that adult tsetse flies produce a Type II PM, it is constitutively

expressed. Therefore, the requirement of blood meal or artificial meal induction, as seen in Type I PM formation, was found not necessary for PM protein composition analyses. To maximize the number of isolated proteins, the authors conducted in-gel and in-solution tryptic digests using 150 PMs. While their in-gel analysis yielded two highly visible bands at 26 and 21 kDa (identified as midgut trypsin), the most abundant and frequent protein hit was for a novel PM protein, GmmPer6 [37]. As expected, the in –solution analysis yielded substantially more proteins (minimum of 195). Based on putative function, the largest majority of isolated proteins were associated with oxidation/reduction (17%). In total, five PM peritrophins were isolated in this study (two known and three novel). As in the in-gel analysis, GmmPer66 was one of the most abundant proteins isolate din the in-solution analysis with two other novel PM peritrophins isolated (GmmPer12 and GmmPer108) [37].

Despite the identification of these structural components, few studies have utilized reverse genetic approaches such as RNAi mediated knockdown to determine physiological importance of individual peritrophins. *I. scapularis* nymphs were administered dsRNA targeting *peritrophin-1* through their anal pore and subsequently allowed to feed until repletion on *B. burgdorferi*-infected C3H/HeN mice. While peritrophin-1 knockdown nymphs engorged at a comparable rate to control nymphs, knockdown of peritrophin-1 resulted in decreased thickness of the PM and compromised structural integrity [38]. Interestingly, knockdown of peritrophin-1 was associated with decreased *B. burgdorferi* adherence/attachment to midgut epithelial cells. A similar effect was seen via RNAi-mediated knockdown of the signal transducer and activator of transcription (*stat)* gene which encodes STAT (the cytosolic component of the Janus kinase (JAK)/STAT pathway [38], suggesting a modulatory role of STAT in peritritrophin-1 expression, and role of the intact PM in *B. burgdorferi* spirochetes adherence to midgut

epithelium. RNAi-mediated knockdown of *An. gambiae* AgAper1 [most abundant CBD protein from Dinglasan et al. (2009)] was used to determine its role in midgut epithelium response to microbiota in adult *Anopheles coluzzii* [69]. Interestingly, knockdown of AgAper1 resulted in an increased immune response and translocation of bacteria from family *Enterobacteriaceae* into the body cavity. Therefore, these findings suggest that the PM of *An. coluzzii* serves as a barrier which blocks or limits dissemination of certain bacteria throughout the mosquito body [69].

Despite the highly successful strategies deployed by bloodfeeding arthropods to sequester heme during the process of blood digestion, heme and molecular iron are also critical nutrients that must be absorbed during digestion and transported throughout the body. In the following sections, we discuss recent progress on understanding heme and iron transport across cell membranes, as well as trafficking, packaging, signaling and ultimate deposition into the ovaries for oogenesis, in order to systematically track the fate of blood meal heme and iron in medically important hematophagous arthropods.

1.4 Heme uptake across cell membranes

Despite its importance as a nutrient and signaling molecule [70, 71], surprisingly little is known about heme transport/uptake in arthropods. New developments in this area would seem to be promising targets, particularly since this subject has been explored in many other organisms including mammals, fish, yeast and worms, as moving heme from either its point of synthesis (mitochondria) or from the diet (extracellular space) to the cell cytoplasm involves crossing membranes.

The feline leukemia virus subgroup C receptor (FLVCR1) heme transporter has been characterized in both humans and mice [72-75]. Flvcr1a is a 12 transmembrane (TM) domain

protein while Flcvr1b is a 6 TM domain protein which is thought to homo/heterodimerize to form a functional transporter. Recently, Mercurio et al. (2015) found that Flvcr1a and Flvcr1b were both required for development of committed erythroid progenitors with Flvr1a exporting heme through the plasma membrane into the extracellular space while Flvr1b exports heme into the mitochondria [76]. In erythroid cells, heme regulation is particularly important because it ensures the balanced production of the globin chain components [77, 78]. Experiments using knockout mice showed that Flvcr1a and Flvcr1b both play a role in the expansion of committed erythroid progenitors as production of hemoglobin was reduced but only Flvcr1b is indispensable during terminal erythroid differentiation due to a block at the pro-erythroblast stage [76]. RNAi in human lymphoblast K562 cells showed that the coordinated expression of both isoforms controls the cytosolic free heme pool; Flvcr1a deficiency resulted in cytosolic heme accumulation detrimentally effecting cell proliferation but promoted differentiation, while mitochondrial heme accumulation due to Flvcr1b loss was deleterious to both processes. While Flvcr1 has been characterized in vertebrates, a potential role in arthropod heme transport has not been explored.

In 2008, a new family of heme transporters was identified in the nematode *Caenorhabditis elegans*. Rajagopal et al. (2008) performed a genome-wide microarray analysis to identify genes transcriptionally regulated by heme and found F36H1.5 (hrg-4) and its 3 paralogues, R02E12.6 (hrg-1), F36H1.9 (hrg-5) and F36H1.10 (hrg-6) with only two, hrg-1 and hrg-4, found to be highly responsive to heme deficiency and the only genes that were not nematode-specific. White et al. (2013) identified a human/mouse hrg-1 ortholog localized on the macrophage phagolysosomal membranes in mice by immunofluorescence microscopy [79]. Immunohistochemistry showed high levels of hrg-1 in the macrophages present in the tissues

responsible for high levels of recycling of heme iron obtained from degraded red blood cells, the spleen, liver and bone marrow of mice and humans. Knockdown of the gene by siRNA in mice bone marrow-derived macrophages resulted in a reduction of the heme regulatory pool while overexpression increased cellular heme availability. Toh et al (2015) identified and characterized an hrg-1 ortholog in the blood fluke *Schistosoma mansoni* (Smhrg-1), which had a low sequence identity and homology to the *C. elegans* genes hrg-1 and hrg-4 and was found localized via palladium mesoporphyrin IX fluorescence in the vitelline and ovary regions of the females of the species [80]. However, heme transport by Smhrg-1 was only identified in these organs indicating that the heme transport mechanism after digestion to the vitelline and the ovary regions is not due to Smhrg-1 but some other unknown mechanism. A *Leishmania amazonensis* homolog of the *C. elegans* heme transporter hrg-4, LHR1, was identified by Huynh et al. (2012), and was found to localize to both the plasma membrane and the lysosomes as determined by measurement of GFP-LHR1 fusion proteins in cells via confocal laser fluorescence microscopy [81, 82]. Subsequent failure to generate a full knockout of LHR1 was interpreted to indicate the essential nature of this gene to organism survival. Partial knockout and overexpression resulted in reduced heme uptake and increased uptake respectively as measured by zinc mesoporphyrin (ZnMP). Taken together these three observations indicated that LHR1 accounts for the majority of the heme transport activity in *L. amazonensis*. Topology modeling identified four predicted transmembrane domains and cytoplasmic N- and C- termini in *C. elegans* hrg-1 and hrg-4 as well as LHR1 in *L. amazonensis* indicating similar protein structure between hrg family members in these distant eukaryotes [81, 82].The fact that members of the hrg gene family are present in humans, worms and single-cell protozoan parasites suggests that this gene family is

very ancient, however orthologues of this gene family in bloodfeeding arthropods have not been described.

Recently, Lara et al. (2015) identified ATP binding cassette subtype B10 (ABCB10) as a heme transporter in the midgut cells of R. *microplus*. Incubation of midgut cells with Rhodamine 123 (a PgP protein transporter substrate), separately or combined with CsA (an ABC inhibitor) confirmed an ABC transporter was responsible for heme transport after a bloodmeal, while an anti-PgP-1 antibody identified the membrane of digestive vacuoles to be its location in the cells. RNAi of the RmABCB10 transporter in female bloodfed ticks and Zinc protoporphyrin IX (ZnPp) fluorescence showed reduced ZnPp in the hemosomes, but more in the digestive vacuoles, which confirmed RmABCB10 as the transporter characterized above. Lara et al. (2015) confirmed previous reports that identified ABC transporters as key components of detoxification of acaricides by showing that Tin protoporphyrin IX and amitraz transport to the hemosome are increased in the amitraz-resistant Ibirapuã strain when compared to wild type [83-87]. Mangia et al. (2016) expanded this to *Ixodes ricinus* by examining expression of ABCB1, ABCB6, ABCB8 and ABCB10 after ivermectin treatment in cultured cells [88]. The authors' found that only ABCB8 showed changes in expression showing a low-dose stimulation but a high-dose return to control levels after exposure the increasing concentration of ivermectin. These results taken together indicate that ABC transporters transport acaricides in the detoxification pathway of multiple tick species with some family members also transporting heme out of the digestive vacuoles. Like FLVCR and HRG genes, orthologues of ABCB10 have not been described to date in other bloodfeeding arthropods.

Pereira et al., (2007) found evidence of heme transport into the midgut epithelium cells in *Ae. aegypti* and export of its degradation product biglutaminyl-biliverdin back into the lumen for

excretion [89]. The authors observed a change in color from red to green during bloodmeal digestion and upon analysis identified it as a bilin pigment. Heme degradation occurs via the cytosolic heme oxygenase reaction, thus heme must enter the midgut epithelium to be degraded and then the biliverdin biproduct must be secreted, although the mechanisms behind the transport of these 2 molecules are unknown. RNA sequencing following heme exposure in *Ae. aegypti* cultured cells identified several potential transport-related proteins that could be involved in this transport mechanism [70], however their activity has not been characterized to date. Although, strong evidence of the capacity of heme transport is available for bloodfeeding arthropods, only 1 transporter, RmABCB10 had been characterized to date.

1.5 Heme catabolism

After heme is imported into the cell, a conserved heme degradation pathway is present in many organisms, during which heme is broken down into biliverdin IX α (BV α), iron and CO by heme oxygenase (HO) [for recent reviews, see [90, 91]]. However, at least two bloodfeeding arthropods, *Aedes aegypti* and *Rhodnius prolixus*, deviate from this pathway as discussed below. In addition, many species of ticks have completely lost the ability to breakdown heme due to absence of key enzymes in the heme degradation pathway in their genomes [35, 89, 92, 93]. In *Ae. aegypti*, after BV IX, iron and CO are produced, two glutamine residues are added, as determined by electrospray ionization mass spectrometry (ESI-MS)[89]. A BV IX product with one glutamine residue was isolated with the final product in reverse phase HPLC indicating that the glutamines were sequentially added instead of simultaneously. This addition to BV IX yields a more soluble product, and was thought to reduce toxicity caused by the accumulation of the heme byproducts in the midgut by allowing for easier excretion [89]. The formation of a green

pigment identified as biglutaminyl BV IX in the lumen indicates that this byproduct must exit the midgut epithelium cells to be eventually excreted, although the mechanisms behind the transport are unknown. This mechanism is so far unique to *Ae. aegypti*, the pathways utilized by other bloodfeeding dipterans are currently unknown.

In all cases previously reported, heme is broken down by HO prior to any modifications to the porphyrin ring, however the kissing bug contains a unique pathway in which two cysteinylglycine residues are added before oxidative cleavage of the porphyrin ring yielding the end product of dicysteinyl-BV IX ɣ (RpBV) as determined by ESI-MS [92]. While the biological advantage to these added residues is not clear, Paiva-Silva et al. (2006) hypothesized this change in structure is also enacted to increase solubility of the byproducts, easing excretion as confirmed by its elution with a more hydrophilic retention time during reverse-phase HPLC than BV IX α. Also, while RpBV has been identified as the end product, the method of residue addition and the order added are unknown. In mammals, all the degradation products produced by heme play key regulatory roles, for example CO has both anti-inflammatory and anti-apoptotic effects and BV may function as antioxidants, however these roles have not been explored in insects to date [94-100]. Given at least two variations on heme degradation pathways in arthropods have been described so far, it is likely that there are more not yet discovered. Figure 2 details the proposed mechanisms of the *Ae. aegypti* and *R. prolixus* heme degradation pathways.

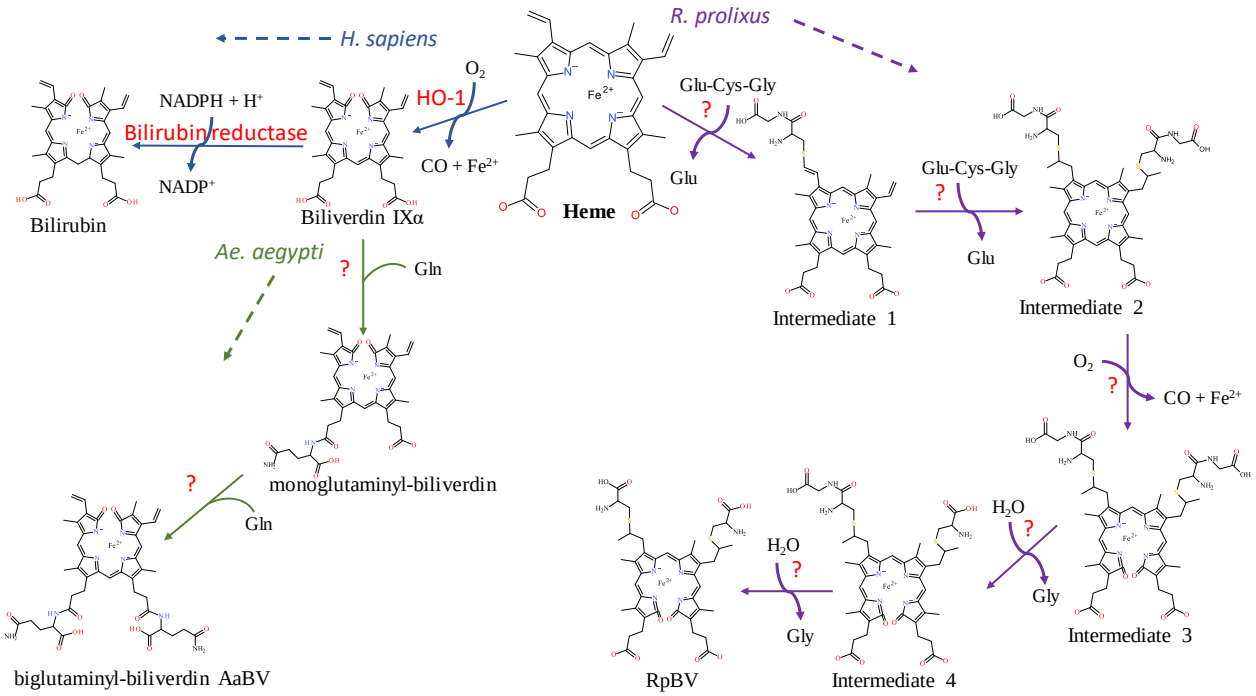

Figure 2. Known heme degradation mechanisms
The arthropods *Ae. aegypti* and *R. prolixus* have alternate heme degradation mechanisms from the shared mechanism of humans, mice and many other organisms. All three mechanisms are detailed above. Enzymes utilized for each reaction are given in red, with unknown enzymes indicated (?). The order in which the modifications are sequentially added to the intermediates in both the *Ae. aegypti* and *R. prolixus* mechanisms is not known, however only one method is detailed here for simplicity. The structural drawings shown here were made using BIOVIA 2017 R2 (Dassault Systemes, San Diego) [66].

In *D. melanogaster*, heme oxygenase expression is necessary for the normal development of tissues. Whole body knockdown of HO in larval and pupal flies results in lethality, evidence of the necessity of heme-iron recycling in tissue development [101]. Cui et al. (2008) observed the effects of tissue specific HO-knockdown utilizing the GMR-GAL4 driver system to target the eye imaginal discs which resulted in abnormal development of the adult eye tissue. Immunostaining the eye tissue of HO knockdown larvae revealed high concentrations of activated caspase-3, an apoptotic marker, as well as larger than normal iron deposits, both of which were thought to contribute to the rough eye phenotype observed. This observed phenotype

was later linked to G1/S arrest of the cell cycle leading to cell death due to increased generation of reactive oxygen species [102]. Ida et al. (2013) also observed a significant drop in proliferating cells and an increase of DNA damage detected in the eye imaginal discs of the larva after treatment with HO dsRNA. Ida et al. (2013) performed a genomic screen leading to the identification of eight genomic regions that suppressed the observed rough eye phenotype during HO knockdown. This indicates that specific genes on these isolated regions may interact with HO and help counteract its loss during a knockdown event, however further work is needed to isolate specific genes. Damulewicz et al. (2017) found that *ho* is a clock-controlled gene as it oscillates in expression during the day peaking at the beginning of the light phase and in the middle of the night [103]. One of the reasons behind this pattern of oscillation was due to HO's protection of the retina photoreceptors against ROS-induced degradation brought on during the transition of the night to day phase at the start of UV and white light exposure. DNA damage was reduced when HO was activated by hemin and increased when HO activity was inhibited by Sn PP [103, 104]. The decline in HO regulated two different canonical clock genes *period* and *clock*, increasing and decreasing respectively. This regulation is potentially mediated through CO as an increase in CO shows the same effect as the increase of HO expression [103]. In conclusion, the results of the loss of HO in *Drosophila* tissues and whole body indicate that HO is very important for the successful development of these tissues. However, HO expression and its regulation of DNA damage response and canonical clock genes has not been examined in other insects. This would be particularly important to study in bloodfeeding arthropods as their ingestion of blood yields a much more iron rich diet than flies.

1.6 Iron transport across cell membranes

Iron-responsive genes including those implicated in membrane bound iron transport have been identified in multiple organisms, including arthropods [for recent reviews see, [105, 106]. A recent study in *G. morsitans* for example, identified 150 iron-responsive genes, only two of which were previously identified, ferritin heavy chain and mRCK-alpha [107, 108]. These genes were predicted by computational analysis of UTR regions searching for the characteristic stem loop structures present in iron regulatory element (IRE) regulated genes. Of these genes, 29 had functions potentially related to iron trafficking, including cell envelope, transport and binding proteins that localized in the extracellular environment or the plasma membrane. Genes involved in iron trafficking are particularly important for bloodfeeding arthropods as the blood meal contains a huge influx of iron in the form of transferrin and hemoglobin, 1884.8ng iron per female on average [109].

Three genes in *Drosophila melanogaster* have been identified as playing a role in membrane bound iron transport, *malvolio (mvl), zip13* and *mco1*. Mvl is a homolog of the human natural resistance-associated macrophage proteins (*Nramp*). Both loss and gain-of-function *mvl* mutants in adult flies resulted in altered taste perception, particularly sugar and salt perception [110]. Fowell et al. (2006) found high expression of *mvl* in adult and larval midgut tissue as well as in the Malpighian tubules, while elucidating its role in iron acquisition at multiple developmental stages and its role in divalent cation reabsorption [110, 111]. Subsequently, an ortholog of *Nramp/mvl* was also characterized in the mosquito *Anopheles albimanus* [112]. Martinez-Barnetche et al. (2007) determined that *anaNramp* localized to the head, midgut, malpighian tubules and ovaries, the highest expression of which was in the malpighian tubules [113]. These authors confirmed the role of *anaNramp* in Fe^{2+} transport by inducing full length

cDNA expression in Xenopus embryos and measuring $^{59}Fe^{2+}$ isotope incorporation. An examination of the *anaNramp* 5' and 3' UTR sequences indicated that unlike *mvl*, no iron responsive elements (IRE) were present suggesting *anaNramp* may not be regulated by cytoplasmic Fe concentration. Few arthropods have been characterized that contain *h-Nramp* homologs, those that do contain the gene require further study as the regulation method behind their iron transport is unidentified.

Xiao et al. (2014) recently characterized the Drosophila ortholog of the human zinc iron permease 13 (*zip13*), an iron efflux pump that moves iron from the cytosol to the ER/Golgi [114]. RNAi knockdown of *dzip13* resulted in iron deficiency in the entire body of the fly with a reduction of about 50% of wild type iron levels except for iron in the cytosol of the gut cells which showed higher than wild type iron levels. On the other hand, *zip13* overexpression in the midgut resulted in increased iron content throughout the body. The authors then examined *ferritin* and *malvolio* as examples of genes involved in iron metabolism that could act as additional indicators of cytosolic iron levels. They found that when *zip13* expression was knocked down, ferritin expression increased and an Mvl expression decreased, with the opposite expression patterns observed when *dZip13* was overexpressed. The overexpression results matched ferritin and Mvl levels observed when larvae were fed an iron-supplemented diet indicating ferritin and Mvl expression levels seem to be a good indicator of cellular iron levels in Drosophila. With the exception of d*zip13* and *malvolio* no other iron transporters have been identified in *Drosophila*. While orthologs of *dzip13* and *malvolio* are present in many bloodfeeding arthropods, involvement in iron transport hasn't been confirmed in any to date, with the exception of *anaNramp* described above.

The multicopper oxidase enzyme family includes oxidases that target different types of substrates including iron, copper, ascorbic acid and bilirubin [115]. dMCO1, while not an iron transporter, facilitates transport by acting as a ferroxidase at the membrane which oxidizes reactive aqueous ferrous iron (Fe^{2+}) to ferric iron (Fe^{3+}) in the hemolymph allowing its binding to transferrin and similar iron binding proteins for transport in *D. melanogaster*. Lang et al. (2012) found dMCO1 localized to both the digestive system and Malpighian tubules, specifically the basal surfaces of each using RT-PCR on organ extracts to calculate expression of the transcript, followed by immunostaining tissues to visualize its location [116]. dMCO1's role in iron homeostasis was confirmed by RNAi knockdown experiments yielding increased longevity when flies fed on high iron food and a decreased iron accumulation in the body. The MCO gene family is conserved in coleopterans, lepidopterans and dipterans [116-119]. *A. gambiae* contains 5 putative multicopper oxidases, with AgMCO1 considered the functional ortholog to dMCO1, though experimental confirmation of this is lacking [120]. Very few putative MCO enzymes have been characterized to date in bloodfeeding arthropods and those that do contain these enzymes, require further work to identify which substrate they target and whether or not they are involved in iron metabolism.

1.7 Iron chaperones

Metallochaperones facilitate metal ion storage in target proteins via specific protein-protein interactions at their docking surface tuned to recognize these partner proteins [121]. Iron metallochaperones could be particularly important to iron homeostasis as they bind and safely transport ferrous iron around the cell, preventing oxidative damage from occurring [122]. Four cytosolic iron metallochaperones were discovered in humans that are thought to aid in ferritin

iron loading: human poly(rC)-binding protein 1 (PCBP1) and its paralogues PCBP2, PCBP3 and PCBP4. When either PCBP1 or PCBP2 and ferritin are expressed in yeast cells, the amount of iron loaded into ferritin drastically increased when compared to ferritin expression by itself [123, 124]. This was confirmed by RNAi knockdown of PCBP1, PCBP2 or both proteins in human cultured cells and observation of the amount of ^{55}Fe incorporated into endogenous cytosolic ferritin, which led to similar reductions in iron uptake into ferritin compared to control cells indicating that both proteins are needed independently for efficient delivery of iron to ferritin [123, 124]. The other two family members, PCBP3 and PCBP4 also showed increased iron loading into ferritin [124]. PCBP2 was also shown to interact with NRAMP2 via its cytoplasmic N-terminal region and with ferroportin, the main ferrous iron exporter, lending further credence to its function as an iron chaperone [125]. Interestingly, HO1 was found to complex with PCBP2 but not any of its paralogues (PCBP1, 3 or 4) or the NADPH-cytochrome P450 reductase (CDR) complex competitively, with PCBP2 affinity to HO1 seeing a significant reduction when in heme loaded cells or when PCBP2 is bound to ferrous iron [126]. While these proteins have been characterized in humans, orthologous proteins have not been characterized in any arthropod species to date. If orthologues of the PCBP family of proteins exist in bloodfeeding arthropods, these could indicate a possible missing link in known mechanisms related to iron homeostasis as they may be involved in ferrous iron transport through the midgut epithelium cells, thus preventing the oxidative damage associated with free ferrous iron in the cell.

1.8 Iron packaging and ferritin shuttling

Free iron can enter the cytosol through direct transport from outside the cell or be released internally following heme catabolism. Fe^{2+} is the reactive soluble form of iron while

Fe^{3+} is both unreactive and insoluble. Ferritins chaperone and transport iron preventing large concentrations of cytosolic Fe^{2+} which can easily react with lipids, proteins and other cellular components causing oxidative damage. The Ferritin-like superfamily is present in many organisms including arthropods, with all individual members thought to be evolved from a rubrerythrin-like ancestor which played a role in the defense against reactive oxygen species [127]. Ferritin is typically composed of 24 subunits, which fold to create a large cavity that can store 1500+ Fe^{3+} molecules as well as smaller amounts of other metals like zinc and magnesium [128]. Insects have two ferritin subunits, very similar to vertebrate ferritin subunits, heavy-chain homolog (HCH) and light-chain homolog (LCH) [129]. HCH, like dMCO1, also has ferroxidase activity and thus catalyzes the oxidization of Fe^{2+} to Fe^{3+} for storage in ferritin; LCH is involved in iron core formation. In most insects, ferritin contains a signal peptide directing it to the endoplasmic reticulum for translation where it stays until iron loaded ferritin is exported out of the cell via secretory vesicles [129-131]. As ferritin loading occurs in the ER and not the basal surface of the midgut epithelial membrane, dMCO1's ferroxidase activity is not utilized to facilitate loading of the iron into ferritin. Excellent reviews are available covering insect ferritins [108, 129, 130], so they are only mentioned briefly here.

Loss of ferritin following gene knockdown or knockout resulted in growth abnormalities ending in death in *D. melanogaster* [132]. Lack of iron present in embryos either due to knockout of ferritin or lack of maternally derived iron also resulted in serious abnormalities often culminating in death during early development. When midgut specific knockdown was performed in *D. melanogaster*, iron accumulated in the iron cell region while systematic iron deficiency was observed throughout the rest of the body, confirming the importance of ferritin in serving as a transport mechanism [133]. However, the exact mechanism of ferritin iron transport

to non-intestinal tissues after export out of the midgut epithelium remains unknown, as while labeled ferritin or its substrate iron has been identified in multiple tissues across both *D. melanogaster* and *Ae. aegypti* their entry method into other cellular tissues remains uncharacterized [109, 133, 134].

In mosquitoes and other bloodfeeding arthropods ferritin is particularly important due to the large influx of iron they obtain during a blood meal. In *Ae. aegypti*, both ferritin subunits, HCH and LCH, increase in expression after an iron overload or a blood meal, indicating that ferritin may serve as a cytotoxic protector [135, 136]. In mosquitoes, different cell types handle ferritin iron storage in different ways. Geiser et al. (2015) found that CCL-125 *Ae. aegypti* larval epithelial-like cells and 4a3b *An. gambiae* larval hemocyte-like cells experienced high levels of iron uptake using Calcein fluorescence assays upon exposure to high levels of iron [132, 137]. However, the inductively coupled plasma mass spectrometry (ICP-MS) they performed showed low levels of cytoplasmic free iron present indicating that upon uptake, iron is immediately bound to proteins like ferritin and secreted [132, 137]. When comparing the two cell types examined, Geiser et al. (2015) noted that after packaging of iron into ferritin occurred, the CCL-125 cells exported the ferritin out of the cell while 4a3b cells retained it. They speculated that since hemocyte cells are involved in the immune response, hoarding an essential nutrient like iron is likely done to prevent foreign cells access to it providing a more hostile environment for their growth. This immune response is observed in both *Ae. aegypti* and *Bombyx mori* (silkworm), when ferritin is upregulated during bacterial infection lending evidence that host-bacteria regulatory mechanisms involving ferritin production do exist in these organisms [138, 139]. However, the signaling mechanism which determines when secretion occurs or which cell types secrete iron loaded ferritin or retain it has not been identified to date.

Ticks and insects have evolved different mechanisms to ensure free heme is dealt with during digestion, however they both utilize ferritin to package and transport the molecular iron absorbed from the blood meal [140]. Recently, Galay et al. (2013, 2014) characterized two distinct ferritins in the hard tick, *Haemaphysalic longicornis* [141, 142]. Hlfer1 and Hlfer2 both have unique functions: storage of iron in the midgut, and secretion from the midgut for transport to other organs with the subunit composition of each potentially controlling their different functions [141]. Unlike *hlfer1*, the sequence of *hlfer2* lacks an IRE, indicating that it may not be regulated by cytoplasmic Fe concentration, and contains a signal peptide much like the secretory ferritin characterized by Hajdusek et al. (2009) in the hard tick *Ixodes ricinus* [141, 143]. RNAi experiments showed the importance of both ferritins present to successful feeding and reproduction in both *H. longicornis* and *I. ricinus*. While intestinal cell types have been studied extensively, knowledge of the regulation of ferritin subunits in non-intestinal cell types and whether multiple subunits work together in different situations is lacking.

Transferrin is an iron binding glycoprotein that is also conserved between vertebrates and arthropods. Unlike ferritin, transferrin can only carry two molecules of Fe^{3+} at a time. In mammals, transferrin is primarily utilized in iron transport in the blood to bring iron to the erythrocytes to be utilized in heme production [144]. *D. melanogaster* transferrin and *Ae. aegypti* transferrin 1 were both found to be expressed in larval, pupal and adult stages but not in embryos, with expression in *Ae. aegypti* found mainly in the fat body where it is secreted into the hemolymph with high levels of juvenile hormone acting as a negative regulator of its expression [145, 146]. A second transferrin gene was described in *Ae. aegypti* with weaker iron binding due to key amino acid mutations in the binding pocket as compared to other members of the transferrin family [147]. Expression of both genes differ in the adult female mosquitoes, with

AaTf1 expression highest at 24 hours post bloodmeal and *AaTf2* expression highest at 72 hours post bloodmeal compared to sugar fed females [147]. This difference in expression suggests distinct roles in iron metabolism, however the precise roles these genes play remains to be determined. Bacterial infection of *Ae. aegypti* also increases transferrin expression, particularly of *AaTf1*, suggesting that *AaTf1* may play a role in sequestering iron during pathogen infection [147]. Other studies have also shown transferrin upregulation in mosquito host response to pathogen infection, particularly *Wuchereria bancrofti*, in *Ae. aegypti* and *C. quinquefasciatus* females [148, 149]. An early genome survey by Dunkov et al (2006) identified members of the transferrin family in several insect species; including four in *A. gambiae* and *Ae. aegypti* [130]. However, little is known about the biological role or specialization of these transferrin genes. In summary, transferrin has been identified as an important regulator of iron homeostasis during blood digestion, larval and pupal development and bacterial infection in arthropods. However, most of the underlying data derives from inferred similarity with vertebrate transferrins. The exact signaling mechanism that activates transferrin expression upon pathogen infection has not been identified nor has the role of transferrin as an iron transporter been extensively studied in bloodfeeding insects.

1.9 Heme/iron signaling

In addition to its role as a nutrient, heme acts as a signaling molecule triggering many biological pathways. In *Ae. aegypti* cultured cells, heme was found to regulate the expression of several hundred transcripts, including those associated with redox stress, metabolism and transport related proteins, suggesting the existence of distinct signaling pathways regulated by heme [70]. Analysis of these genes found that several immune genes were downregulated in

response to heme exposure, indicating that the exposed cells may be more susceptible to immune challenge. This was confirmed both *in vitro* and *in vivo* by introduction of *E. cloacae* to heme incubated cultured cells and by orally challenging heme-fed females with *Serratia marcescens* resulting in diminished expression of immune genes both in cells and the midgut and a two-fold increase in microbial growth. However, the mechanism by which heme is effects the immune pathways and the molecular mechanisms behind certain induced genes are not currently well understood.

While the role of heme signaling in regulating the immune response of bloodfeeding arthropods is just being appreciated, the role of heme in regulating reproduction in bloodfeeding mosquitoes is well established. In the arthropods *D. melanogaster* and *Ae. aegypti*, heme binding to the nuclear receptor E75 can result in the activation of the steroid hormone 20-hydroxyecdysone (20E), a key component in molting, metamorphosis and vitellogenesis [150-152]. Cruz et al. (2012) found that heme was required for mediating 20E action via its stabilization of E75, implying its role as a signaling molecule to indicate the availability of a blood meal for vitellogenesis. E75's ligand binding pocket was characterized by Reinking et al. in *D. melanogaster*, where a single heme molecule was identified as a tightly bound prosthetic group [153]. The *Ae. aegypti* ortholog, like its *Drosophila* counterpart, has three isoforms, all three of which are vital to the regulation of multiple genes [154-156]. Aicart-Ramos [157] examined the heme binding of E75 hemoproteins in four different species of insect, *D. melanogaster, B. mori, O. fasciatus* and *B. germanica*. In the first two insects, heme is only tightly bound while in the latter two it is covalently attached [153, 157]. In all four insects, heme is so tightly bound that E75 could not be purified without it. Reinking et al. (2005) also described E75 as a potential heme sensor, because upon treatment of cultured cells with an increased

concentration of heme, the cells induced up to 8-fold increase of E75 expression indicating that the expression of E75 is directly proportional to the available heme level [153]. Aicart-Ramos et al (2012), however disagreed with this definition, stating that heme's tightly bound nature precludes it from acting as a heme sensor, since a heme sensor must be able to reversibly bind heme [for a detailed review of heme sensor proteins see [158]]. However, this appears to be a disagreement concerning the definition of a heme sensor, not experimental evidence disproving the evidence collected by Reinking et al (2005) [153, 157].

The regulation of E75 by·NO and CO, common in many organisms, occurs when either gas binds the heme-E75 complex, which blocks the heme active site and prevents binding to E75's other regulatory targets [for detailed reviews on NO and CO signaling see [159-161]]. Therefore, E75 is likely to act as a cellular oxidative state sensor since these gaseous molecules can only bind to ferrous iron not ferric, thus binding would only occur when the cellular state was reduced enough to allow the heme iron to be in its ferrous state (Fig. 3). To determine E75's status as a redox sensor, further work must be completed to determine if the cellular environment can actually affect the binding capacity of the protein.

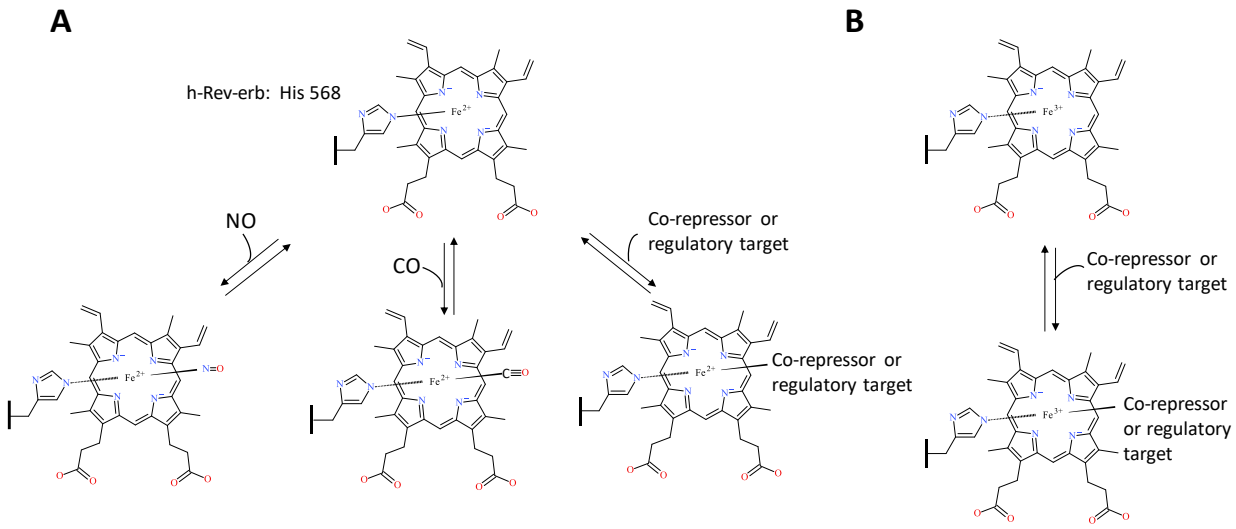

Figure 3. E75-Heme as a cellular oxidative state sensor
The human ortholog of insect E75, h-Rev-erb, acts as a carbon monoxide and nitric oxide sensor when the cell exists in a reducing environment, inhibiting binding of Rev-erb to its co-repressors and regulatory targets (**A**). Rev-erb's gas sensor ability is not present during a cellular oxidizing environment allowing uninhibited binding to its co-repressors and regulatory targets (**B**). The structural drawings shown here were made using BIOVIA 2017 R2 (Dassault Systemes, San Diego) [66].

1.10 The role of hemolymph heme and iron-binding proteins: heme, iron and oogenesis in anautogenous arthropods

In addition to the iron carrier proteins, transferrin and ferritin, many arthropods utilize heme/iron carrier proteins which chaperone maternal heme/iron to the developing eggs. This is especially important in ticks, as many species lack key enzymes in the heme synthesis pathway requiring heme to be acquired entirely exogenously[35, 93]. Perner et al. (2016) showed that hemoglobin was not necessary for egg production, but was essential for embryo survival in *Ixodes scapularis* [93]. Female ticks were fed with whole blood or hemoglobin-free serum; eggs were laid by both sets, however only those laid by the bloodfed females hatched and developed normally. Hemoglobin was confirmed as the critical factor by performing rescue experiments with females fed on serum + 10%, 1% and 0.1% hemoglobin added prior to the rapid

engorgement phase which showed that as little as one hundredth of the physiological concentration of hemoglobin was sufficient to rescue tick reproduction. Likewise, Perner et al. (2016) demonstrated that IrCP3 is the major heme-binding protein in *Ixodes ricinus* hemolymph [93]. Expression profiling over *I. ricinus* developmental stages and tissues revealed that *ircp3* mRNA was consistently up-regulated by bloodfeeding and was predominantly expressed in the trachea-fat body complex, and to a lesser extent, in salivary glands and ovaries of adult females. The authors also confirmed IrCP3 as the most abundant protein in tick hemolymph via SDS PAGE and Western blot analysis. Interestingly, the hemolymph lipoglycoheme-carrier protein from the American dog tick, *Dermacentor variabilis*, was also found to bind heme suggesting that *D. variabilis* carrier protein may function to sequester heme derived from the digestion of the blood meal [162]. Likewise, through spectrophotometric titrations, Maya Monteiro et al. (2000) found an analogous heme lipoprotein (HeLp) to be the main heme-binding protein in the hemolymph of male and female *R. microplus* [163]. To determine if HeLp is involved in extracellular transport, specifically to the ovaries, ^{55}Fe-heme-HeLp was injected into the hemocoel of female ticks. Decreased radioactivity was seen in the hemolymph of injected females by 210 minutes. Most interestingly, by 4 hours after hemocoel injection, radioactivity was found associated with the ovaries of female *R. microplus*. However, *R. microplus* females maintained at 4^{o}C after injections lacked clearance of ^{55}Fe-heme-HeLp from the hemolymph or incorporation into the ovaries. Therefore, this suggests active metabolism is involved [163]. Vitellin (VN), the main yolk protein, has also been associated with heme-binding function in *R. microplus* ovaries [164]. Through heme-binding assays with purified VN, Logullo et al. (2002) demonstrated that a single VN bound 30 or more heme molecules [164]. Given that both HeLp and vitellin have been ascribed heme-binding functionally and associated with egg development

in *R. microplus*, this raises the questions as to whether these two proteins are necessary and sufficient to provide the developing *R. microplus* egg with heme reserves.

Walter-Nuno et al. (2013) found that the *R. prolixus* heme binding protein (RHBP) is an essential transporter of heme to the embryos. RNAi mediated knockdown of RHBP did not alter fecundity, however the resultant eggs were not viable and were white in color. This is in contrast to the dark red embryos oviposited by controls. Taken together, the above studies shed light on the sheer importance of heme-binding and iron-binding proteins in terminal incorporation of heme and iron into the developing eggs of hematophagous arthropods, in particular ticks, which lack the *de novo* heme synthesis pathway. Whether corresponding heme carrier proteins are utilized by bloodfeeding arthropods that maintain the ability to synthesize heme remains unknown.

1.11 Discussion

Although many arthropods have evolved the ability to feed on blood, relatively little insight into the internal processing of blood meal heme and iron is available. Much of the available information regarding iron processing in arthropods, more specifically insects, is gleaned from *Drosophila melanogaster*. While certain life history traits make *D. melanogaster* a powerful model organism, they do not bloodfeed, highlighting the need to perform direct experimentation on the bloodfeeding arthropods.

Through this review, we provide a framework for future studies aimed at obtaining a better understanding as it relates to the fate of heme and iron processing in hematophagous arthropods (Fig. 4). With recent advancements in scientific tools such as high-throughput protein and RNA analysis, as well as CRISPR/Cas9, we are optimistic that many questions related to the

detoxification, acquisition, transport and ultimate fate of iron/heme in bloodfeeding arthropods can be effectively addressed. Below we have highlighted some key take away points and scientific knowledge gaps that await tackling.

- Given that catalase appears to be a key antioxidant in both midgut and ovarian oxidative stress avoidance for many hematophagous arthropods, further studies targeting this enzyme are needed to assess its potential for disrupting the midgut and ovarian oxidative balance on a larger scale when hematophagous arthropods take a blood meal.
- Heme aggregation/crystallization appears to be a common first line of defense in many hematophagous arthropods. Better understanding of this multifaceted protection playbook for each hematophagous arthropod can provide insight into key targets for breakdown of this system.
- In 2009, Dinglasan et al. set the stage for midgut PM protein composition exploration and discovery utilizing a highly sensitive MS-based approach. The success of this methodology was largely associated with the availability of an artificial protein-free meal. Such protein-free artificial meals for other hematophagous arthropods are needed to allow similar exploration of related and divergent PM structures.
- While peritrophic matrix peritrophins have been identified in many hematophagous arthropods, only two PM peritrophin has been knocked-down using RNAi (APER1 in *An. coluzzii* and peritrophin-1 in *I. scapularis)*. Further studies utilizing reverse genetic tools, such as RNAi and CRISPR/Cas9 are needed to determine the physiological function of PM peritrophins in medically important hematophagous arthropods.

- To date, only one quantitative analysis tracking the fate of blood meal iron in a hematophagous arthropod (*Ae. aegypti*) has been conducted [109]. A detailed road map for blood meal iron trafficking in other hematophagous arthropods is needed.
- Heme digestion and utilization regardless of its source, biosynthesis pathway or intake through diet, requires heme to pass across cell membranes. Despite, the characterization of membrane bound heme transport in vertebrates and nematodes, only one transporter has been characterized in a bloodfeeding arthropod to date indicating further work is needed to identify the heme import mechanisms utilized in these organisms.
- Heme catabolism by heme oxygenase 1 to biliverdin IX α, iron and CO is a conserved process in many organisms, however *Ae. aegypti* and *R. prolixus* deviate from this standard and produce alternate bilin pigments, thus there may be more deviations from the known standard yet to be discovered in other bloodfeeding arthropods.
- Heme oxygenase was shown to be essential to *D. melanogaster* tissue development as it regulates the DNA damage response and specific canonical clock gene expression. However, heme oxygenase's role in these two pathways has not been explored in bloodfeeding arthropods despite their diet consisting of a much more iron rich diet than flies.
- In *D. melanogaster*, three genes have been identified as membrane bound iron transporters or facilitators of this process, *mvl*, *zip13* and *mco1*. While orthologs of both *mvl* and *zip13* do exist in bloodfeeding arthropods, their involvement in iron transport has yet be examined in any to date, with the exception of *anaNramp*.

- The human poly(rC)-binding proteins (PCBP1-4) facilitate iron loading of ferritin. Homologues of these proteins in bloodfeeding arthropods could represent a missing link in iron homeostasis in these organisms.
- While ferritin or its substrate, dietary iron, has been localized in multiple tissues in both *D. melanogaster* and *Ae. aegypti* the mode of entry and recovery of iron from ferritin into cells and tissues remains uncharacterized.
- Transferrin, another conserved iron binding transport protein between vertebrates and arthropods, is found in many bloodfeeding arthropods. While transferrins have been shown to be upregulated after a blood meal or during pathogen infection, little is known about the biological role or specialization of these transferrin genes.
- Hemolymph heme-binding proteins (RHBP, HeLp and IrCP3) allow for proper transport of heme and iron to developing eggs. However, further studies are needed to determine if orthologs for these proteins exist in other hematophagous arthropods and their role in proper shuttling of heme to ovaries. Loss of any heme and iron shuttling processes can decrease egg viability, and ultimately be utilized in novel mosquito population control techniques.

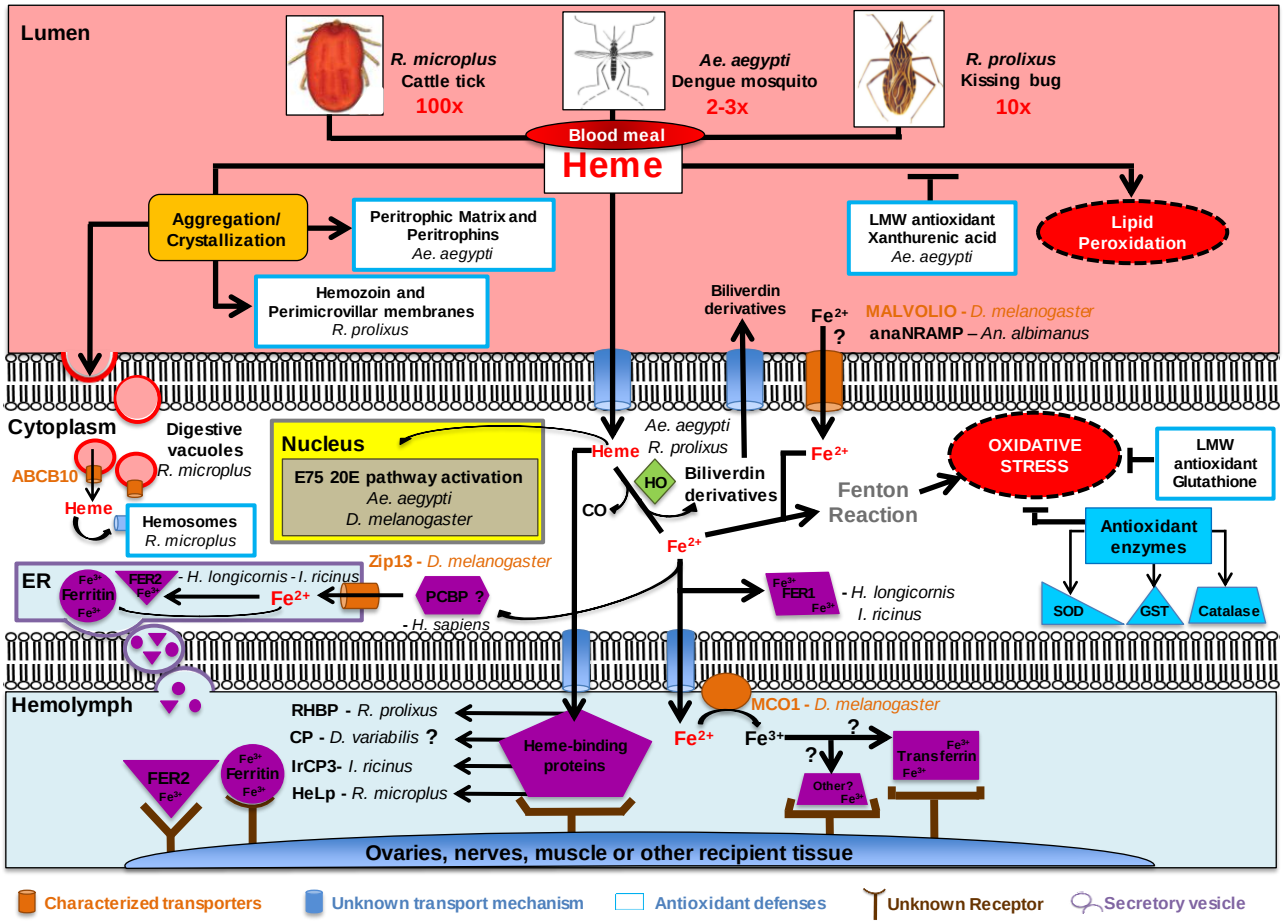

Figure 4. Fate of blood meal heme and iron in selected hematophagous arthropods. Hematophagous arthropods ingest a large amount of blood during a single meal (2-3x, 10x and 100x their normal body weight for *Ae. aegypti*, *R. prolixus* and *R. microplus*, respectively). Hematophagous arthropods deploy a multifactor mechanism to avoid oxidative stress after a blood meal. This multifactor mechanism includes: **1**) Aggregation/crystallization of heme for excretion; **2**) Transport of heme and iron across plasma membranes; **3**) Intracellular degradation of heme by Heme Oxygenase (HO); **4**) Enzymatic (shown in dark blue) and non-enzymatic low molecular weight (LMW) antioxidant molecules; and **5**) Heme and iron carrier proteins (shown in purple) which deposit these two molecules into ovaries, nerves, muscle or other recipient tissue. Abbreviations: *Anopheles albimanus* natural resistance-associated macrophage protein (anaNRAMP), ATP binding cassette subtype B10 (ABCB10), carrier protein (CP), endoplasmic reticulum (ER), ecdysone-induced protein 75 (E75), Ferritin (Fer), glutathione S-transferase (GST), heme lipoprotein (HeLp), *Ixodes ricinus* carrier protein 3 (IrCP3), multicopper oxidase 1 (MCO1), poly(rC)-binding protein (PCBP), *Rhodnius prolixus* heme binding protein (RHBP), superoxide dismutase (SOD), zinc iron permease 13 (Zip13), 20-hydroxyecdysone (20E) [66].

CHAPTER II

CHARACTERIZATION OF THE ADULT *AEDES AEGYPTI* EARLY MIDGUT PERITROPHIC MATRIX PROTEOME USING LC-MS*

2.1 Introduction

The *Aedes aegypti* mosquito is the principle vector of arboviruses throughout the tropics and subtropics worldwide [165]. In these regions, *Ae. aegypti* transmit dengue, chikungunya, yellow fever, and Zika viruses to humans, resulting in substantial morbidity and mortality worldwide [165-167]. Dengue is the most important mosquito-borne viral disease with more than 200 million reported cases per year [168]. Dengue has been reported in over 90 countries, and alarmingly, dengue incidences have increased more than 30-fold in the last 40 years [169]. Most importantly, dengue has recently been reported in nonendemic areas of the world such as the United States, Southern Europe, and Australia [169].

When adult female mosquitoes take a blood meal, they consume two to three times their normal body weight [170]. Digestion of the blood meal releases a large amount of free heme into the midgut lumen [51, 63]. Free heme can result in the oxidation of nucleic acids [11], lipids [12, 13], and proteins [14, 171]. Therefore, understanding the physiological mechanisms adult female mosquitoes use to process the potentially toxic blood meal and metabolites is needed. In particular, the midgut peritrophic matrix (PM) may serve as protective lining that separates the

* Reprinted with permission from "Characterization of the adult *Aedes aegypti* early midgut peritrophic matrix proteome using LC-MS" by Whiten, S.R., Ray, W.K., Helm, R., Adelman, Z.N., 2018. PLOS ONE, Vol. 13, Issue 3, p.e0194734, Copyright 2018 Adelman

single cell-layered midgut epithelium from pathogens, abrasion, and toxic compounds [51, 60, 61].

The type I PM of the adult mosquito is comprised of proteins, proteoglycans and chitin fibrils [50, 63]. PM proteins, commonly referred to as peritrophins are characterized by the presence of a secretory signal peptide, multiple chitin-binding domains containing cysteine-proline dipeptides and intervening mucin-like domains rich in proline, serine and threonine [58]. The multiple chitin-binding domains of PM peritrophins function as cross-linkers for chitin fibrils, thereby providing structure and support for the PM [47, 64]. Two-dimensional polyacrylamide gel electrophoresis and lectin-binding assays suggest the adult female *Ae. aegypti* PM may contain 20-40 major proteins [59]. However, only two proteins have been identified and characterized as adult *Ae. aegypti* peritrophins: intestinal mucin 1 (AeIMUC1) [67] and adult peritrophin 50 (AeAper50) [49]. Therefore, we conducted a mass spectrometry based proteomic analysis to obtain a comprehensive understanding of the adult female *Ae. aegypti* early PM, with particular interest in adult female PM proteins containing structural features characteristic of peritrophins. Our efforts resulted in the identification of more than 6000 peptides derived from the early PM, corresponding to 474 unique proteins, 115 of which are predicted to be secreted. We identified additional peritrophins and confirm that a substantial number of salivary proteins are delivered to the midgut and may potentially assist in blood meal detoxification and/or digestion.

2.2 Materials and methods

2.2.1 Mosquito rearing

Aedes aegypti (Liverpool strain) mosquitoes were reared under standard insectary conditions at 28 ^{o}C and 60-70% relative humidity with a 14:10 light:dark photoperiod. Adult mosquitoes were provided 10% sucrose solution and water. Mosquitoes were starved of 10% sucrose 12 hours prior to experiments.

2.2.2 Preparation of peritrophic matrix samples for analysis

PMs were dissected from 3-5 day old adult female *Ae. aegypti* that were fed a protein-free artificial meal (Fig. 5). The protein-free artificial meal consisted of 150 mM NaCl, 20 mM $NaHCO_3$, and 20 mM ATP as a phagostimulant [6, 59, 172, 173]. The protein-free artificial meal also contained 0.2% low melting agarose to provide bulk and induce distension of the midgut [6]. Six hours post-feeding [59], the mosquitoes were immobilized and PMs dissected in 50% EtOH and 50% PBS solution [6]. The dissected PMs were transferred to a 1.5 ml Eppendorf tube and snap-frozen with liquid nitrogen. All 1.5 ml Eppendorf tubes were stored at -80 ^{o}C until a total of 1,020 PMs were collected. The 1.5 ml Eppendorf tubes containing PMs were removed from -80^{o}C and placed in liquid nitrogen. Extraction buffer (50 mM Tris-HCl, pH 8.5) was added to the first tube and sample homogenized with a plastic pestle. The homogenized sample was transferred to the next tube and PM samples were homogenized. This was repeated for all subsequent tubes until all homogenized samples (800 μl) were combined in a single tube. The pipette tips and plastic pestle were also washed with the extraction buffer. This was referred to as the "Wash" sample. To each of the final tubes, 5 μl of Benzonase was added to remove excess DNA or RNA and then samples were vortexed. Proteins from the 1,020 PMs were sequentially

extracted in 200 μl buffer containing either Buffer A (50 mM Tris-HCl, pH 8.5), Buffer B (Buffer A+ 0.5% Triton X-100), or Buffer C (Buffer A+ 2% SDS). The initial Tris fraction and Tris "Wash" fraction were quantified by Bradford assay (0.25 μg/μl and 0.09 μg/μl, respectively). The samples were vortexed, incubated on ice for 1.5 hrs, and then centrifuged in a microcentrifuge at 12,000 x g for 15 minutes. The supernatant containing the extracted proteins was transferred to individual 1.5 Eppendorf tubes (tubes were washed with acetyl nitrile and pre-chilled). For sequential extractions, either Buffer B or Buffer C was added to the pellet fraction and the above extraction procedure was repeated.

2.2.3 Mass spectrometry based proteomic analysis

The adult female *Ae. aegypti* PM proteins were sequentially extracted with i) Buffer A ("Tris" fraction); ii) Buffer B ("Tris-Triton" fraction); iii) Buffer C ("Tris-SDS" fraction). The leftover pellets were washed twice with an excess of Buffer A to remove any excess detergent. This "Pellet" fraction was then analyzed, but no unique proteins were identified. Therefore, this fraction was not considered further. The fractions ("Tris", "Tris-Triton", and "Tris-SDS") were then prepared for digestion with trypsin.

The "Tris", "Tris-Triton", and "Tris-SDS" fractions and their respective "Wash" samples were TCA precipitated, and proteins solubilized in 30 μL of 100 mM Tris-HCl, pH 8.5, 8 M urea, reduced with 5 mM TCEP (Tris(2-carboxylethyl)phosphine hydrochloride, Pierce), alkylated with 10 mM IAM (iodoacetamide, Sigma), and deactivated with 10 mM dithiothreitol (DTT). Samples were diluted to 4 M urea with 100 mM Tris-HCl, pH 8.5. Endoproteinase Lys-C (Roche) was added to 0.5 μg [174], and samples were incubated overnight at 37 ^{o}C. The next morning, samples were diluted to 1.5 M urea with 100 mM Tris-HCl, pH 8.5. Calcium chloride

was added to 2 mM and samples digested with trypsin overnight at 37°C while shaking. The digestion was quenched by adding formic acid to a final concentration of 5 %.

The insoluble pellets ("pellet" fractions) from the PM sample and "wash" sample were dried under vacuum, solubilized in 100 μl cyanogen bromide at 500 mg/ml in 88% formic acid, and left in fume hood overnight in the dark [174]. The samples were neutralized by adding 30% ammonium hydroxide drop by drop. To adjust the pH to 8.5, 1M Tris-HCl was added to 100 mM. The samples were then denatured with 8 M urea, reduced with 5 mM TCEP, alkylated with 20 mM IAM, deactivated with 20 mM DTT (1,4-dithiothreitol). The samples were then digested with endoproteinase Lys-C and trypsin as described above. All peptides were cleaned-up using Agilent Bond Elute OMIX pipette tips.

Ten microliters of each resolubilized peptide sample was separated using an Acquity I-class UPLC system (Waters). The mobile phases were solvent A (0.1% (v/v) formic acid (Sigma) in LC/MS grade water (Spectrum Chemicals) and solvent B (0.1% (v/v) formic acid (Sigma) in LC/MS grade acetonitrile (Spectrum Chemicals). The separation was performed using a CSH130 C18 1.7 µm, 1.0 x 150 mm column (Waters) at 50 µL/min using a 110-minute gradient from 3-40% solvent B. The column temperature was maintained at 45°C.

Column effluent was analyzed using a Synapt G2-S mass spectrometer (Waters) using an $HDMS^E$ (high-definition mass spectrometry with alternating scans utilizing low and elevated collision energies) acquisition method in continuum positive ion "resolution" MS mode. Source conditions were as follows: capillary voltage, 2.9 kV; source temperature, 125°C; sampling cone, 40 V; desolvation temperature, 350°C; cone gas flow, 50 l/hr; desolvation gas flow, 500 l/hr; and nebulizer gas, 6 bar. Both low energy (no collision energy in either the trap or transfer region) and elevated energy (no collision energy in the trap region and the collision energy ramped based

on the bin number exiting the ion mobility cell in the transfer region, see below and Ref. 1) scans were 0.8 seconds each for the m/z range of 100 to 1800. For ion mobility separation, the IMS wave velocity was ramped from 800 to 500 m/sec over the full IMS cycle and the IMS wave height was 40 V. Wave velocity and height in the trap region were 313 m/s and 8 V. Wave velocity and height in the transfer region were 190 m/sec and 4 V. Mobility trapping utilized auto release and mobility separation was delayed 450 µs after trapping.

Collision energy in the transfer region was dependent upon the drift time (bin) within the ion mobility cell as described by Distler et al. (2014) [175]. The CE was ramped from 16-23 V for bins 1 to 40, from 24-47 V for bins 41 to 120, and from 48-60 V for bins 121 to 200.

For lock-mass correction, a 1.2 second low energy scan was acquired every 30 seconds of a 100 fmol/µl [Glu1]-fibrinopeptide B (Waters) solution (50:50 acetonitrile: water supplemented with 0.1 % formic acid) infused at 5 µl/min introduced into the mass spectrometer through a different source which was maintained at a capillary voltage of 3.0 kV. The data for lock-mass correction was collected but not applied to sample data until data processing.

Mass spectrometric data from each chromatographic run were processed and analyzed utilizing ProteinLynx Global Server version 3.0.2 (Waters). The software automatically determined average chromatographic and mass spectrometric peak width resolution. Mass values were lock-mass corrected based on the exact m/z value of the +2 charge state of [Glu1]-fibrinopeptide B (785.842). Peaks were defined based on the low energy, elevated energy and bin intensity thresholds of 100, 15 and 750 counts, respectively. The MS and MSMS tolerances for the peptide searches were 24 ppm and 24 ppm, respectively (automatically determined by the Waters PLGS search engine). The final peak list for each sample was then searched against a protein database containing the complete *Ae. aegypti* proteome downloaded from VectorBase

and 3 randomized decoy entries for each real entry appended using PLGS. Workflow parameters for the protein identification searches were 2 possible missed cleavages utilizing Lys-C and trypsin as the protease combination, a fixed modification of carbamidomethylation of cysteine, possible modifications of glutamine to pyroglutamate when glutamine is present at the N-terminus of a peptide and oxidation of methionine. The software automatically determined peptide and peptide fragment mass tolerances. Protein identification searches using PLGS had a false discovery rate of no more than 5%.

Results for all runs were tabulated utilizing IsoQuant [176]. The final data summary lists only proteins identified by at least 2 unique peptides at a false discovery rate (FDR) less than 3% in both replicates. Proteins were quantified using the Top3 method. Peptides with a minimum replication rate of 2 and a minimum score of 2 per EMRT (exact mass and retention time) cluster, including in-source fragments and those exhibiting a neutral loss of either water or ammonia, were considered valid for protein identification. Only peptides identified as either unique or razor were used for protein quantitation. The mass spectrometry proteomics data have been deposited to the ProteomeXchange Consortium via the PRIDE [177] partner repository with the dataset identifier PXD007627.

2.2.4 Bioinformatic analyses

The VectorBase Biomart tool was used to obtain predicted structural features for the 474 unique proteins that resulted from our proteomic analysis (AaegL3.3). Previously published RNA-seq transcriptomics data comparing sugarfed and bloodfed adult female *Ae. aegypti* [178] was accessed and downloaded to determine proteins isolated in our proteomic analysis with transcripts upregulated five hours after a blood meal. We compared our list of 474 VectorBase

Gene Stable IDs for the proteins identified by LC-MS to transcripts found in blood fed females only and transcripts upregulated in bloodfed or sugarfed females.

g: GOSt--gene group functional profiling (version: r1709_e87_eg34) was used to conduct a hypergeometric enrichment analysis for the 115 secreted proteins isolated in our LC-MS based proteomic analysis with a predicted secretory signal peptide [179, 180]. The unordered list of VectorBase Gene Stable IDs was entered in the g: GOSt user interface. Parameters used for the enrichment analysis included: 1) significant values only and 2) hierarchical sorting. The enriched data was output in an Excel spreadsheet (XLSX), and further custom sorted based on p-value. Only results with p-value <0.001 were considered significant.

Secreted midgut proteins were searched for repetitive cysteine-proline dipeptides which are a hallmark characteristic of PM peritophins [51]. The results were then entered into UniProt database and Center for Biological Sequence Analysis (CBS) prediction services database to determine secreted midgut proteins with: 1) two or more chitin-binding domains and 2) *O*-glycosylation and *N*-glycosylation status.

The adult female *Anopheles gambiae* PM proteome list was accesses and downloaded [53] and the VectorBase Gene Stable IDs for the 209 *Anopheles gambiae* PM proteins were entered in VectorBase Biomart. The data was output as a comma separated value (csv) file. We then compared this data with our list of 474 VectorBase Gene Stable IDs. Only one to one orthologs for the two species were kept for further analyses.

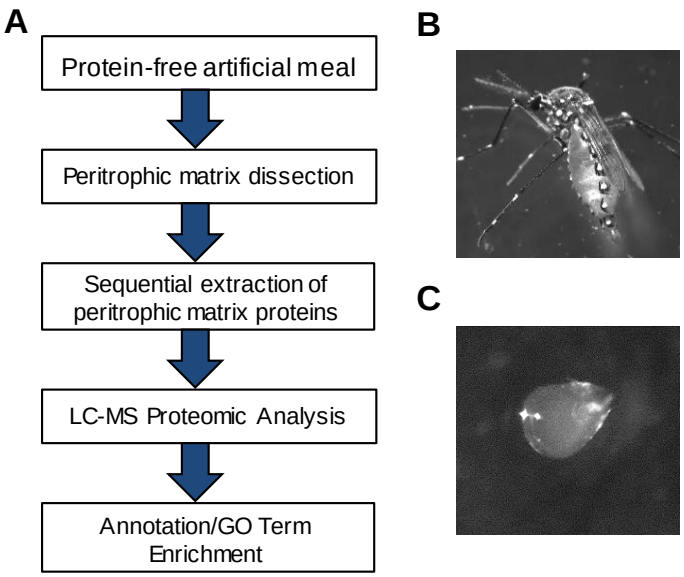

Figure 5. Analysis of *Aedes aegypti* peritrophic matrix proteins.
(**A**) Experimental flowchart detailing the feeding of 3-5 day old adult female *Ae. aegypti* with protein-free artificial meal containing low melting agarose to produce a rigid PM. Proteomic analysis was conducted (LC-MS). (**B**) Adult female post feeding with protein-free artificial meal containing low melting agarose. (**C**) Six hours post feeding with protein-free artificial meal containing low melting agarose, PMs were dissected in 50% PBS and 50% ethanol solution [181].

2.3 Results

2.3.1 Proteomic analysis

Following a protein-free artificial bloodmeal, *Ae. aegypti* peritrophic matrices were dissected and proteins were sequentially extracted according to solubility in buffers and detergents (Fig. 5). The extracted proteins were then prepared for LC-MS analysis, resulting in the identification of 6292 peptide sequences (4300 unique peptides) corresponding to 474 unique proteins identified with two or more peptides. Given the parent database searched was annotated to encode 15,796 possible proteins, this amounts to exactly 3% of the known protein-coding capacity of *Ae. aegypti* being potentially associated with the PM. Recovered peptides ranged from 6-52 amino acids in length, with a mean of 14.4 and a mode of 12 (Fig. A-1). Each protein

was identified with between 2-61 unique peptides (defined as having distinct coordinates on the matched protein), with a mean/median of 9.1/6.0 peptides per identified protein (Fig. 6A). As we observed a weak but significant (and unsurprising) correlation between predicted protein length and the number of unique peptides obtained (Fig. 6B), we also calculated the number of peptides obtained per 100 amino acids of protein (Fig. 6C). When normalized for protein length, we recovered an average of 3.1 total peptides and 2.3 unique peptides per protein per 100 amino acids (Fig. 6D).

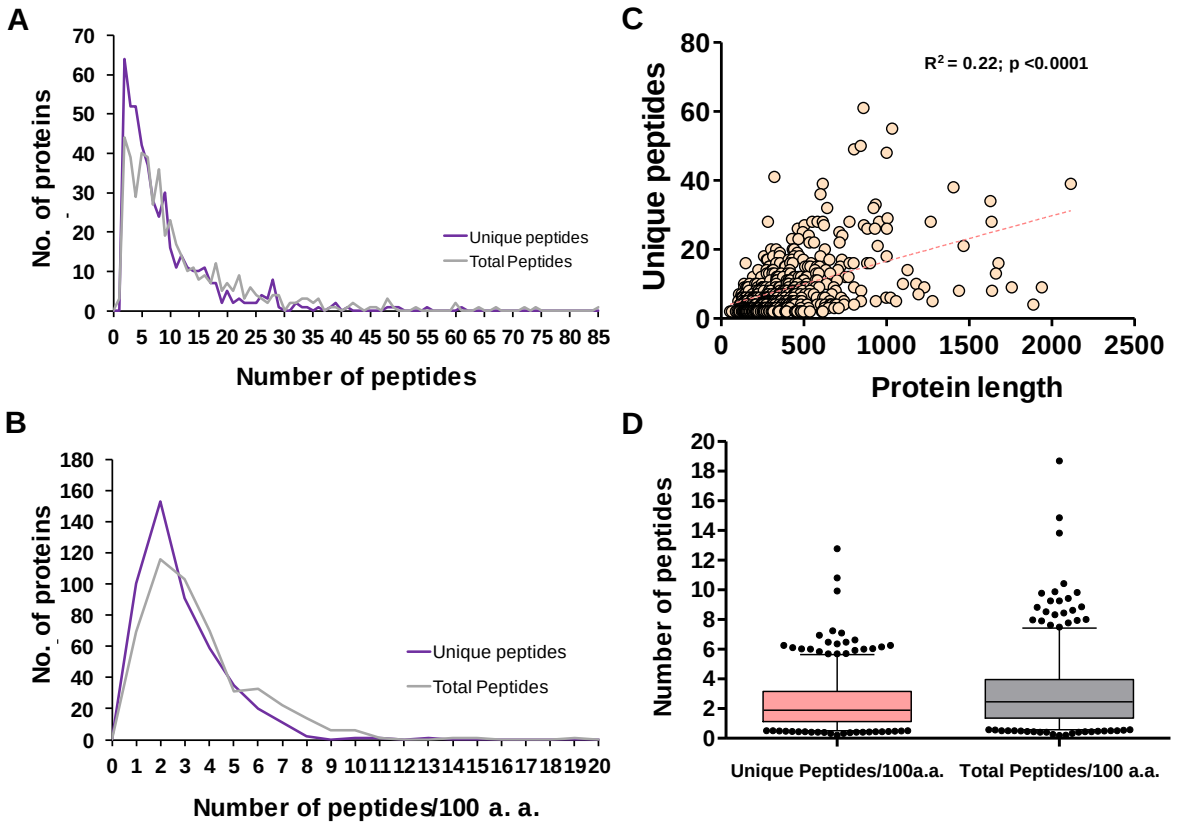

Figure 6. Frequency distribution of the number of peptides recovered per protein. Frequency distribution of the number (No.) of recovered peptides per protein (**A**) or normalized for protein length (**B**). (**C**) Relationship between the predicted length of each protein (Vectorbase AaegL3.3) and the number of unique peptides recovered; dotted line represents the linear regression. (**D**) Box and whisker plot of the number of peptides recovered per protein. Boxes represent the middle quartiles, errors bars the 95% confidence intervals [181].

To assess the completeness of our dataset, we computationally re-sampled an increasing number of random peptides from the full dataset and calculated how many unique proteins were represented. As shown in Fig. 7A, the number of unique proteins identified in our dataset is essentially at saturation for unique proteins identified by 1 or more, or 2 or more peptides. Based on these curves, the number of unique proteins that could be identified with 2+ peptides is expected to plateau between 483-491 (95% confidence intervals), indicating we have recovered 96.5-98.1% of the proteins present in the adult PM ~6 hrs after an artificial meal. In contrast, the number of unique peptides per protein had a strong linear relationship with the total number of peptides per protein, indicating our dataset did not reach saturation at the level of coverage of individual proteins (Fig. 7B). Taken together, we conclude that identifying more peptides using this methodology is very unlikely to uncover new proteins, but very likely to uncover additional unique peptides from proteins already identified.

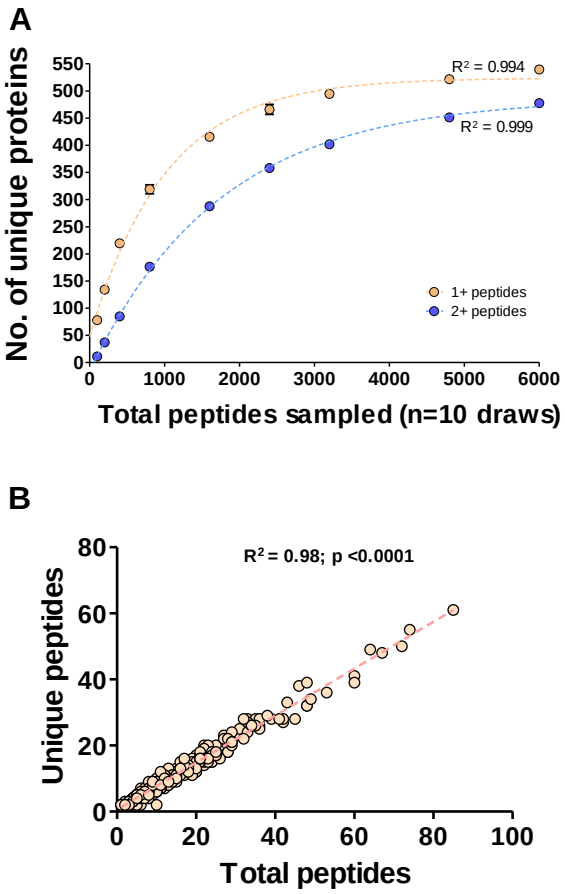

Figure 7. Proteomic analysis of the *Aedes aegypti* peritrophic matrix and contents. (**A**) Each point represents the mean number (No.) of unique proteins identified (with 1+ or 2+ peptides) after 10 random draws from the total dataset of the indicated magnitude. Curves were fit to a one-phase association curve using Graphpad Prism v5.04. (**B**) Linear regression between the total number of peptides recovered and the number of unique peptides [181].

Despite the stepwise extraction method, eighty-eight percent (n = 421) of the unique proteins identified were present in all three fractions (Fig. 8A). Thirteen proteins were present in both fractions A and B. Eight proteins were present in both fractions A and C. Thirteen proteins were present in fractions A and B. Fourteen proteins were present in both fractions B and C. While 19 proteins were found only in fraction C, none were unique to fraction B, and only one protein was unique to fraction A (Fig. 8A). Predicted structural features were used to categorize the 474 unique proteins identified by LC-MS based proteomic analysis. Of the 474 unique

proteins, thirty-two percent (n=152 proteins) contained predicted secretory signal peptides. Thirty-seven of the 152 proteins containing predicted signal peptides also contained predicted transmembrane domains (Fig. 8B), and thus are potential midgut surface proteins as opposed to candidate PM proteins (33). Of most interest were the remaining 115 proteins that contained predicted signal peptides without predicted transmembrane domains (Fig. 8B).

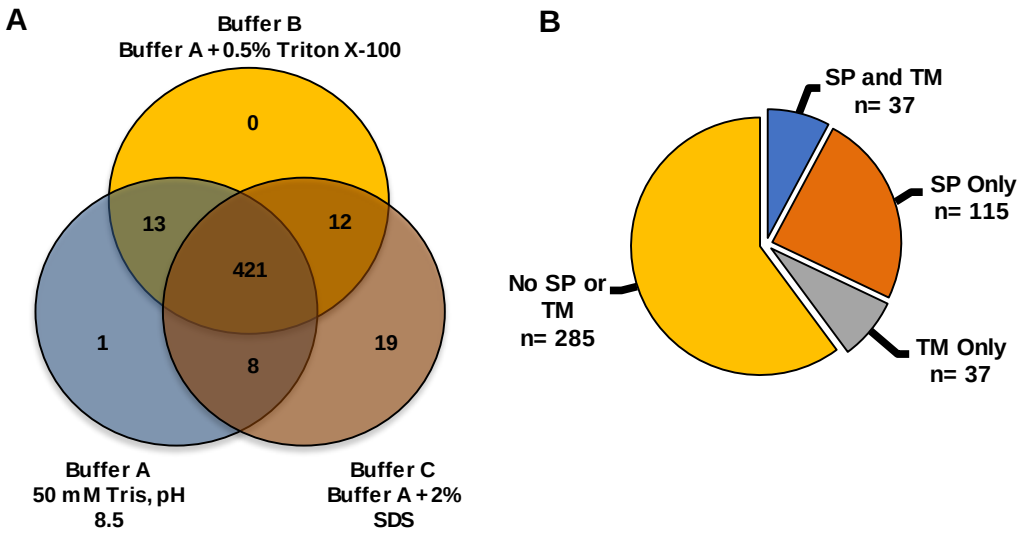

Figure 8. *Ae. aegypti* peritrophic matrix proteins by fraction and predicted localization. (**A**) Protein solubility in buffers and detergents; a total of 474 unique proteins were identified by mass spectrometry. (**B**) Categorization of peritrophic matrix proteins identified by mass spectrometry based on predicted structural features; signal peptide without transmembrane domain (SP), transmembrane domain without SP (TM), those that contain both SP and TM, and the remaining isolated proteins (No SP or TM) [181].

2.3.2 *Aedes aegypti* salivary gland proteins

One of the most striking findings was the presence of many of the best-characterized *Ae. aegypti* salivary proteins, including D7 (AAEL006424), which was the most abundant protein in our dataset (S1 Table). In total, 415 unique peptides were identified corresponding to salivary-specific or salivary-enriched gene products by comparing our protein list with previously

described salivary gland transcriptomics data, saliva and salivary gland proteomics data [182-184]. Potentially, these proteins were transferred to the midgut during ingestion of the protein-free artificial meal and were trapped by the low-melt agarose. In addition to the D7 protein listed above, we recovered *aegyptin* (AAEL010235), D7 long1 (AAEL006417), two C-type lectins (AAEL000533 and AAEL000556), antigen-5 (AAEL003053), two apyrases (AAEL006347 and AAEL006333), and the three serpins (AAEL007420, AAEL003182, AAEL002704).

2.3.3 *Aedes aegypti* blood meal-regulated genes

Several RNAseq studies have been performed to identify transcripts that are differentially regulated following a blood meal in *Ae. aegypti* [178]. To determine whether transcripts that are differentially regulated at 5 h following a blood meal were more or less likely to result in proteins detected in our dataset, we compared the $\log_2$ ratio of transcript abundance between bloodfed vs. sugarfed mosquitoes from Bonizzoni et al. (2011) with the length-normalized number of peptides recovered per protein for all 474 proteins in our dataset. Interestingly, there appeared to be no global relationship between the direction (up or down-regulated) or magnitude of gene expression change following a blood meal and the number of peptides that we subsequently recovered from the early PM (Fig. 9A). This lack of predictive power held when considering only predicted secreted proteins (Fig. 9B), peptidases or salivary proteins (Fig. 9C). Likewise, the absolute abundance of transcripts from sugarfed or bloodfed mosquitoes had little to no relationship with our ability to recover the corresponding proteins (Fig. A-2).

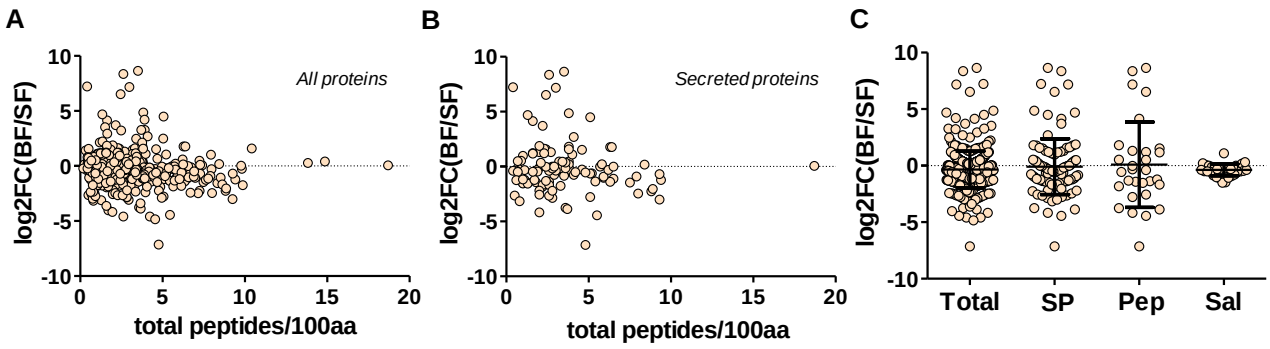

Figure 9. Peptide recovery from peritrophic matrix is independent of whether transcripts are regulated by a blood meal.
Relationship between the size-normalized number of peptides recovered and the regulation of the corresponding transcript at 5 hours post-blood meal (Bonizzoni et al 2011) for all identified proteins (**A**) or predicted secreted proteins (**B**). (**C**) Transcript regulation for all recovered proteins (Total), predicted secreted proteins (SP), peptidases (Pep) and salivary-enriched proteins (Sal). Error bars indicate the standard deviation from the mean [181].

2.3.4 GO term enrichment of predicted secreted proteins

A gene ontology enrichment analysis for the secreted proteins [179, 180] revealed that the largest number (n=57) were associated with catalytic activity (GO:0003824) (Fig. 10 A and B). As expected, the serine-type peptidases involved in blood protein digestion were the largest group of secreted midgut proteins isolated in our proteomic analysis [5]. In particular, we isolated early trypsin (AaET, AAEL007818), late trypsin (AaLT, AAEL013284), serine collagenase (AAEL007432, AaSP1), and AAEL013628 (AaSP4) along with 19 other serine-type peptidases [185-187]**.**

The mosquito midgut is the first site of contact for pathogens ingested during bloodfeeding. Correspondingly, we identified a number of secreted immune-related proteins, including four fibrinogen and fibronectin proteins (AAEL004156, AAEL000726, AAEL006704, AAEL007942), two transferrins (AAEL015458, AAEL011641), five serpins (AAEL002704, AAEL002720, AAEL003182, AAEL003686 and AAEL007420), two Niemann-pick type C-2

proteins (AAEL015136 and AAEL009760), four clip-domain serine proteases (AAEL000028, AAEL006674, AAEL003625, AAEL006576), cathepsin B and L (AAEL009637 and AAEL002833), three galectins (AAEL012135, AAEL005293, AAEL009842), prophenoloxidase (AAEL013498), and lysosomal aspartic protease (AAEL006169) [178, 188-191]. Finally, six of the 115 secreted proteins without transmembrane domains isolated in our proteomic analysis were novel proteins with unknown function.

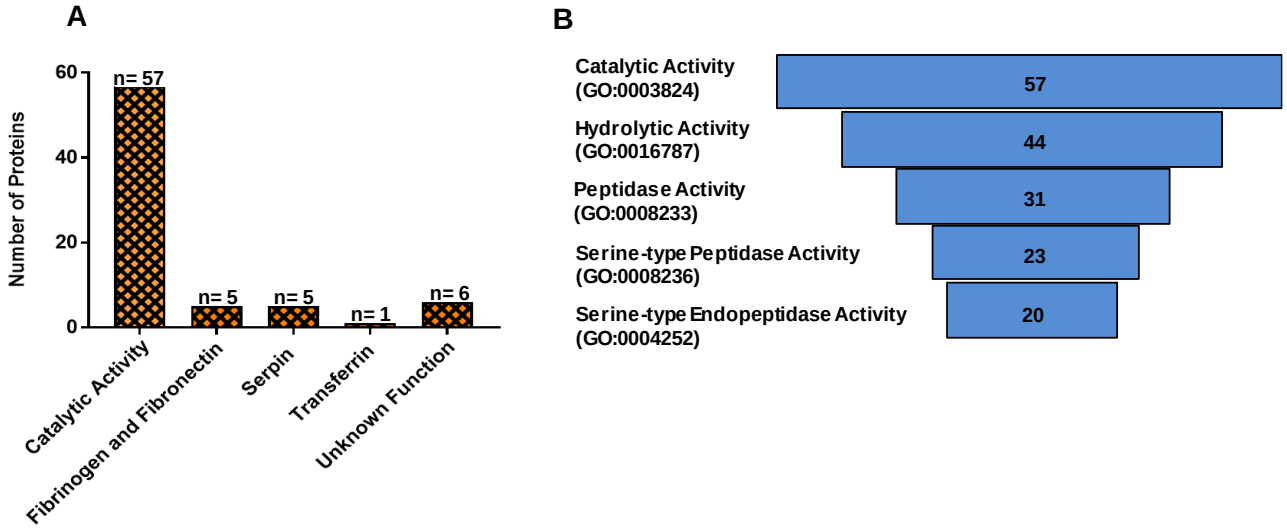

Figure 10. Adult *Aedes aegypti* secreted proteins isolated in this female peritrophic matric LC-MS proteomic analysis.
(**A**) Bar graph detailing different groupings of the secreted proteins isolated in our proteomic analysis. (**B**) Secreted proteins with catalytic activity, hydrolase activity, peptidase activity, serine-type peptidase activity, and serine-type endopeptidase activity. Hierarchical sorting based on gProfiler g: GOSt--gene group functional profiling ($p<0.001$) [181].

2.3.5 Chitin-binding proteins

Only two adult female *Ae. aegypti* peritrophic matrix proteins have been identified and characterized previously, *Aedes aegypti* intestinal mucin 1 (AeIMUC1) [67] and *Aedes aegypti* adult peritrophin 50 (Ae-Aper50) [49]. We identified both Ae-Aper50 (AAEL002467) and AeIMUC1 (AAEL002495), as well as a closely related gene (AAEL004798) and a fourth unrelated peritrophin gene AAEL006953 (Table 1).

Table 1. **Known and putative adult *Ae. aegypti* peritrophic matrix proteins identified by LC-MS with predicted chitin-binding domains.** The mass is based on the primary amino acid sequence and does not account for glycosylation [181].

Gene Stable ID [a]	Gene Name	Predicted MW [b]	Annotation/Comments [b,c,d]
AAEL002495	AeIMUC1	30.6	3 CBD; Peritrophin-A domain; Mucin domain; O-glycosylated; SP; UF
AAEL002467	AeAper50	54.2	5 CBD; Peritrophin-A domain; N- and O-glycosylated; SP; UF
AAEL006953	-	31.3	2 CBD; Peritrophin-A domain; N-glycosylated; SP; UF
AAEL004798	-	39.6	3 CBD; Peritrophin-A domain; Mucin domain; O-glycosylated; SP; TM; UF

[a]VectorBase, *Ae. aegypti* mosquito database, August 2017.
[b] The Universal Protein Resource (UniProt), August 2017.
[c] Center for Biological Sequence Analysis (CBS) prediction services used to determine O-glycosylation and N-glycosylation status, August 2017.
[d] CBD, chitin-binding domain; SP, signal peptide; TM, transmembrane domain; UF, unknown function.

2.3.6 Orthologs to *Anopheles gambiae* PM proteomic analysis

A similar adult female peritrophic matrix proteomic analysis was conducted for *Anopheles gambiae* [53]. Therefore, we compared our midgut peritrophic matrix proteomic results to determine conserved proteins present in both Aedes and Anopheles PMs. Of the 209 unique *An. gambiae* peritrophic matrix proteins identified by Dinglasan et al. (2009) [53], 49 have one to

one orthologs present in our *Ae. aegypti* peritrophic matrix proteomic analysis (Fig. 11). More specifically, just ten were classified as 1:1 orthologs and were predicted secreted proteins without transmembrane domains (Table 2). Overall, this suggests a potentially important physiological role for these proteins, as they have been conserved in two species that diverged more than 150 million years ago [181].

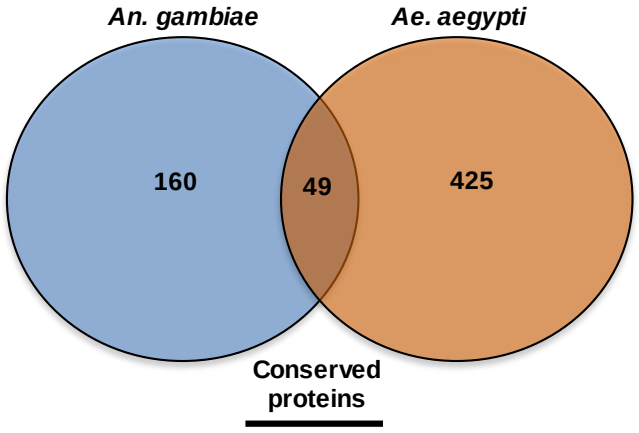

Figure 11. Adult *Ae. aegypti* peritrophic matrix proteins with *An. gambiae* orthologs isolated in Dinglasan et al. (2009) midgut peritrophic matrix proteomic analysis [181].

Table 2. Adult female *Ae. aegypti* secreted proteins and one to one orthologs isolated in Dinglasan et al. (2009) *An. gambiae* adult female LC-MS peritrophic matrix proteomic analysis [181].

***Ae. aegypti* Gene ID[a]**	***An. gambiae* Gene ID[a]**	**Description[a]**	**% Identity**
AAEL006347	AGAP011026	Apyrase Precursor	55.8
AAEL003066	AGAP006414	Brain chitinase and chia protein	56.6
AAEL008485	AGAP007663	DUF1397	62.0
AAEL010338	AGAP009313	DUF725	29.6
AAEL013775	AGAP007745	-	37.0
AAEL015136	AGAP002851	Niemann-Pick Type C-2, putative protein	50.3
AAEL012359	AGAP007120	Nucleoside-diphosphate kinase NBR-A, putative protein	87.5
AAEL007926	AGAP011442	Retinoid-inducible serine carboxypeptidase (serine carboxypeptidase protein	71.1
AAEL003046	AGAP001082	Saposin protein	62.1
AAEL008784	AGAP004900	Serine-type enodpeptidase, protein	60.8

[a]VectorBase, *Ae. aegypti* mosquito database, August 2017.

2.4 Discussion

Ae. aegypti feed on blood multiple times during their lifespan. While critical for adult reproduction, this leaves the midgut, a tissue not protected by chitinous cuticle, exposed to potential toxins, pathogens, and other abrasive compounds during blood digestion [36, 50, 61]. It has been hypothesized that the peritrophic matrix (PM)- an acellular sheath comprised of proteins, proteoglycans and chitin fibrils, may serve as a protective lining that separates the single cell-layered midgut epithelium from these hazards [51, 60, 61, 63]. However, little was known about the protein composition of this structure in *Ae. aegypti*. Therefore, we conducted a mass spectrometry based proteomic analysis to obtain a comprehensive understanding of the adult female *Ae. aegypti* PM. A protein-based analysis of a tissue such as the PM, which is

normally induced following a blood meal, is complicated by the large excess of protein present in the blood. Dinglasan et al. (2009) overcame this in *An. gambiae* by performing an artificial feed using a protein-free solution containing latex beads to aid in midgut distension. Our substitution of low-melt agarose into the protein-free solution simplified the dissection procedure, as once solidified the agarose provided internal rigidity to an otherwise fragile structure. Fortuitously, this also allowed the capture of both structural components of the PM as well as soluble proteins secreted and trapped in the lumen of the midgut. Based on two-dimensional polyacrylamide gel electrophoresis, Moskalyk et al. (1996) determined that the adult female *Ae. aegypti* peritrophic matrix may contain 20-40 major proteins [59]. In contrast, our LC-MS based proteomic analysis resulted in the identification of 474 unique proteins. Computational resampling indicated this is very close to saturation, suggesting we have achieved a substantially complete (96-98%) view of the early PM. At the same time, it is possible that some proteins were missed due to extensive glycosylation or other post-translational modifications that no peptides could be recognized. In addition, we cannot rule out that some components of the PM are selectively produced only following an authentic blood meal, but not from our protein-free meal. However, we consider this unlikely to substantially reduce the completeness of our dataset for several reasons. First, the PM is known to form rapidly based solely on distension of the midgut [61, 62] ; Second, we identified a large number of digestive enzymes including early trypsin known to be secreted into the midgut lumen and responsible for a preliminary tasting of the meal [2-5, 185-187]. Third, we identified both previously characterized *Ae. aegypti* PM peritrophins, AeIMUC1 [67] and AeAper50 [49].

In addition to chitin, peritrophins have also been shown to bind blood meal derived heme [63]. Pascoa et al. (2002) demonstrated the heme binding capacity of the adult *Ae. aegypti* PM.

They found that by the end of digestion the adult *Ae. aegypti* PM could bind 18 nmol of heme, which is an equivalent to the amount of heme present in a normal blood meal. AeIMUC1 is a 275-amino acid glycoprotein with a 19-amino acid secretory signal peptide sequence [51, 67] and contains three chitin-binding domains and a mucin domain between CBD 1 and CBD 2. Rayms-Keller et al. (2000) first reported AeIMUC1 RNA expression in metal exposed *Ae. aegypti* mosquito larvae, metal fed adult females and blood-fed adult females [67]. Devenport et al. (2006), found that AeIMUC1 could bind chitin and heme, suggesting a role in blood meal detoxification. Through deletion analysis, Devenport et al (2006) also determined that the heme-binding activity of AaIMUC1 was associated with its 3 CBDs. Finally, AeIMUC1 was confirmed as an integral PM peritrophin associated with the PM 12 to 24 hours post bloodfeeding, and that this protein is translationally regulated by bloodfeeding [51].

AeAper50 is a 486-amino acid protein that contains 18-amino acid secretory signal peptide [49]. AeAper50 is localized in the midgut of blood-fed adult females, and the protein is present within just one hour of adult female feeding [49]. In contrast to AeIMUC1 [51], mRNA for AeAper50 was not shown to be present prior to adult female bloodfeeding, but rapidly accumulated after the blood meal [49]. Shao et al. (2005) also confirmed chitin-binding for AeAper50. More specifically, through site-directed mutagenesis (cysteine to alanine) of AeAper50 CBD 5, Shao et al. (2005) demonstrated the importance of peritrophin-A domain (PAD) (six cysteine residues) conserved cysteine residues for disulfide bridge formation. These results suggest that the disulfide bridges position AeAper50 for chitin fibril binding [49, 58, 65].

We identified two additional putative PM peritrophins with structural features similar to known peritrophins: AAEL006953 is predicted to encode a 31.4 kDa protein with two predicted chitin-binding domains and N-glycosylation, while AAEL004798 is predicted to encode a 39.6

kDa protein with three predicted chitin-binding domains, a mucin domain and O-glycosylation. Additional work is needed to confirm if these *Ae. aegypti* PM peritrophins also bind chitin and/or heme, as RNAi mediated knockdown of *Anopheles gambiae* adult peritrophin 1 (AgAper1) resulted in bacterial proliferation and a corresponding immune response suggesting the heme-binding function of the PM may both protect the midgut from toxicity as well as sequester the heme to prevent microbial overproliferation [69]. The presence of multiple peritrophins in the PM complicates reverse genetic approaches such as RNAi, but ultimately such studies will be essential to clarifying the role of the four *Ae. aegypti* PM peritrophins in blood digestion, heme sequestration and immunity.

Although salivary proteins are primarily thought of in terms of blood meal acquisition, 10% of the PM protein content appears to be salivary-derived and we identified a substantial number of secreted salivary proteins associated with the PM, with the salivary D7 proteins being the most abundant protein when normalized by length (most peptides per 100 amino acids of protein). The simplest explanation is the ingestion of salivary proteins during feeding; Anopheline mosquitoes have been known to ingest malaria parasites originating from their salivary glands during the act of bloodfeeding [192, 193]. However, we cannot exclude the possibility that some of these proteins may also be produced to some extent by the midgut, as other PM proteomic studies have also isolated proteins traditionally ascribed to the salivary glands and saliva [37]. While several early studies found that severing of the salivary ducts of *Ae. aegypti* had little to no effect on blood meal digestion and subsequent egg production [194, 195], the difficulty and low survivorship associated with these microsurgeries resulted in extremely low sample sizes and thus limited the statistical power of these data. Genetic lesions in important salivary protein genes made possible now through Cas9-based gene editing will allow

further investigation as to the physiological importance of salivary proteins and their relationship to the PM, blood digestion and mosquito reproduction.

Similar to our findings, Dinglasan et al. (2009) also isolated salivary-associated proteins [53]. Interestingly, the authors isolated *An gambiae* apyrase (Table 2), an enzyme known to inhibit ADP-dependent platelet aggregation [196] and whose expression is specific to secretory cells of the distal-lateral lobes of adult female *Ae. aegypti* [197]. Given, that previous studies have also shown large amounts of saliva are ingested during feeding in hematophagous insects [195, 198], these salivary-associated proteins may have been trapped in the lumen when ingested, as our artificial meal included low melting agarose. However, further studies are needed to determine if apyrase is also functional in midgut blood meal digestion across hematophagous arthropods as it was one of just ten proteins found associated with the PM in both *An. gambiae* and *Ae. aegypti*.

As the first comprehensive proteomic analysis for the adult female *Ae. aegypti* midgut peritrophic matrix, our findings provide a foundation for future studies which are needed to better understand the physiological role of the PM after adult female bloodfeeding. While further strides have been taken to determine physiological function and importance of the PM in other hematophagous arthropods [37, 66, 69], reverse genetic analyses (RNAi mediated knockdown) are needed to confirm physiological function for known and putative *Ae. aegypti* PM proteins [66]. Likewise, *in vitro* heme-binding assays are needed to confirm heme-binding for known and putative PM proteins. Furthermore, an enrichment proteomic analysis comparing our current artificial meal to that of an artificial meal enriched with heme provides the ideal avenue for identifying additional PM heme-binding proteins, which were not isolated in our current proteomic analysis. Overall, understanding the PM and its components has the potential to

provide novel targets for molecular based vector and vector-borne disease control, as well as understanding the adaptations required for efficient blood digestion/detoxification.

CHAPTER III

AN INVESTIGATION INTO ADULT *AEDES AEGYPTI* HEME-ENRICHED MIDGUT PERITROPHIC MATRIX PROTEINS USING LC-MS/MS BASED PROTEOMIC ANALYSIS

3.1 Introduction

The bloodmeal feeding process is a high risk, high reward event in which adult female mosquitoes consume two to three times their normal body weight in blood [170]. Over the next 24 - 48 hours, digestion of the blood meal releases large amounts of the pro-oxidant molecule heme into the midgut lumen [51, 63]. The large amount of free heme can facilitate the oxidation of nucleic acids [11], lipids [12, 13], and proteins [14, 171]. Therefore, detailed understanding of the physiological adaptations adult female mosquitoes have evolved to process the potentially toxic blood meal and metabolites is needed. One such adaptation is the mosquito midgut peritrophic matrix (PM), which serves as a protective barrier separating the single cell-layered midgut epithelium from pathogens, abrasion, and toxic compounds [51, 60, 61, 69].

Mosquitoes contain a type I PM that is comprised of proteins, proteoglycans and chitin fibrils [50, 63]. PM proteins are commonly referred to as peritrophins and are characterized by the presence of a secretory signal peptide, multiple chitin-binding domains containing cysteine-proline dipeptides and intervening mucin-like domains rich in proline, serine and threonine [58]. The peritrophins contain multiple-chitin binding domains that serve as attachment points for chitin fibrils, and thereby produce an architectural support system for the PM [47, 64]. Through two-dimensional polyacrylamide gel electrophoresis and lectin-binding assays, Moskalyk et al. (1996) suggested the adult female *Ae. aegypti* PM may contain 20-40 major proteins [59]; only

two such proteins have been characterized in detail: intestinal mucin 1 (AeIMUC1) [67] and adult peritrophin 50 (AeAper50) [49].

To capture a snapshot of the *Ae. aegypti* early midgut PM protein composition we previously conducted an LC-MS based proteomic analysis, and identified a total of 474 unique proteins [181]. While the most abundant protein was of salivary origin, we did identify the two known peritrophins and two additional peritrophins, AAEL004798 and AAEL006953 (based on structural similarity to know PM peritrophins). However, in the time since this analysis was conducted a radically new and improved genome assembly (AaegL5) became available. In the new assembly, gene AAEL004798 was considered an allelic form of the known *Ae. aegypti* PM peritrophin AeIMUC1 (AAEL002495) and therefore the results of our previous analysis can be considered to have resulted in two known (AAEL002495/AAEL004798 and AAEL002467) and one putative (AAEL006953) PM peritrophin.

Although we confirmed the presence of the two known peritrophins and identified a novel putative PM peritrophin in Chapter 2, we further sought to conduct an unbiased forward genetic analysis aimed at identifying potential heme-binding proteins associated with the PM at a physiologically relevant time point. Consequently, in this study we conducted a second midgut PM proteomic analysis enriching for heme-binding proteins present 12 hrs post adult female *Ae. aegypti* artificial meal feeding. We successfully isolated 160 proteins in this midgut PM proteomic analysis, including 23 proteins enriched in our heme-agarose (T2) treatment.

3.2 Materials and methods

3.2.1 Mosquito rearing

Aedes aegypti (Rockefeller/ROCK strain) mosquitoes were reared under standard insectary conditions at 28 ^{o}C and 60-70% relative humidity with a 14:10 light:dark photoperiod. Adult mosquitoes were provided 10% sucrose solution and water. Mosquitoes were starved of 10% sucrose 24 hours prior to experiments.

3.2.2 Preparation of peritrophic matrix samples for analysis

PMs were dissected from 3-5 day old adult female *Ae. aegypti* that were fed a protein-free artificial meal (Fig. 12). The protein-free artificial meal consisted of 150 mM NaCl, 20 mM $NaHCO_3$, and 20 mM ATP as a phagostimulant [6, 59, 172, 173]. The protein-free artificial meal also contained 0.5% low melting agarose to provide bulk and induce distension of the midgut [6]. Twelve hours post-feeding [59], the mosquitoes were immobilized and PMs dissected in 1x Phosphate Buffered Saline (PBS) (Sigma; St. Louis, MO) solution. The dissected PMs were transferred to 1.5 ml Eppendorf tubes and snap-frozen with liquid nitrogen. All 1.5 ml Eppendorf tubes were stored at -80 ^{o}C until a total of 300 PMs were collected for Treatment 1 (non-hemin enriched) and Treatment 2 (hemin enriched), respectively (Fig. 12). The 1.5 ml Eppendorf tubes containing PMs were removed from -80^{o}C and placed in liquid nitrogen. For each treatment, extraction buffer (50 mM Tris-HCl, pH 8.5) was added to the first tube and the sample homogenized with a plastic pestle. The homogenized sample was transferred to the next tube and PM samples were homogenized. This was repeated for all subsequent tubes until all homogenized samples were combined in a single 1.5 ml tube (Sarstedt AG &Co.; D-51588 Nümbrecht) for each treatment (T1 and T2, respectively). The pipette tips and plastic pestle were

also washed with the extraction buffer and pooled with samples. To each of the final tubes, 5 μl of Benzonase (Sigma; Saint Louis, MO) was added to remove excess DNA or RNA. The samples were vortexed, incubated on ice for 1.5 hrs, and centrifuged at 12,000 x g for 15 min. The supernatant containing the extracted proteins was transferred to individual 1.5 ml tubes (tubes were pre-chilled). Given the large volume of T1, the sample was spin concentrated (70 µl final volume), and subsequently boiled in sample buffer (2% SDS and 5% β-mercaptoethanol) at 65^{o}C for 15 min.

3.2.3 Heme-agarose binding assay (Treatment 2)

Prior to heme-agarose binding assays, hemin-agarose beads (Sigma; St. Louis, MO) were washed 3x with high ionic strength buffer (0.5 M NaCl, 10 mM sodium phosphate and 0.1% Triton X-100 at pH 7.5) [199, 200]. Hemin-agarose beads resuspended in high ionic strength buffer (167 µl) were added to 1 ml of T2 sample and incubated overnight at 4^{o}C with constant mixing. The T2 sample containing hemin-agarose beads was centrifuged at 13 000 x g for 2 min. The unbound supernatant fraction was stored, but not used further. The bound fraction "pellet" was washed 6x with 1 ml of high ionic strength buffer, and bound proteins were eluted by boiling the protein bound bead "pellet" in sample buffer (2%SDS and 5% β-mercaptoethanol) at 65^{o}C for 15 min. An additional 25 µl of sample buffer was added to the protein-bound bead "pellet" and boiling step repeated. The T2 samples were pooled (75 µl).

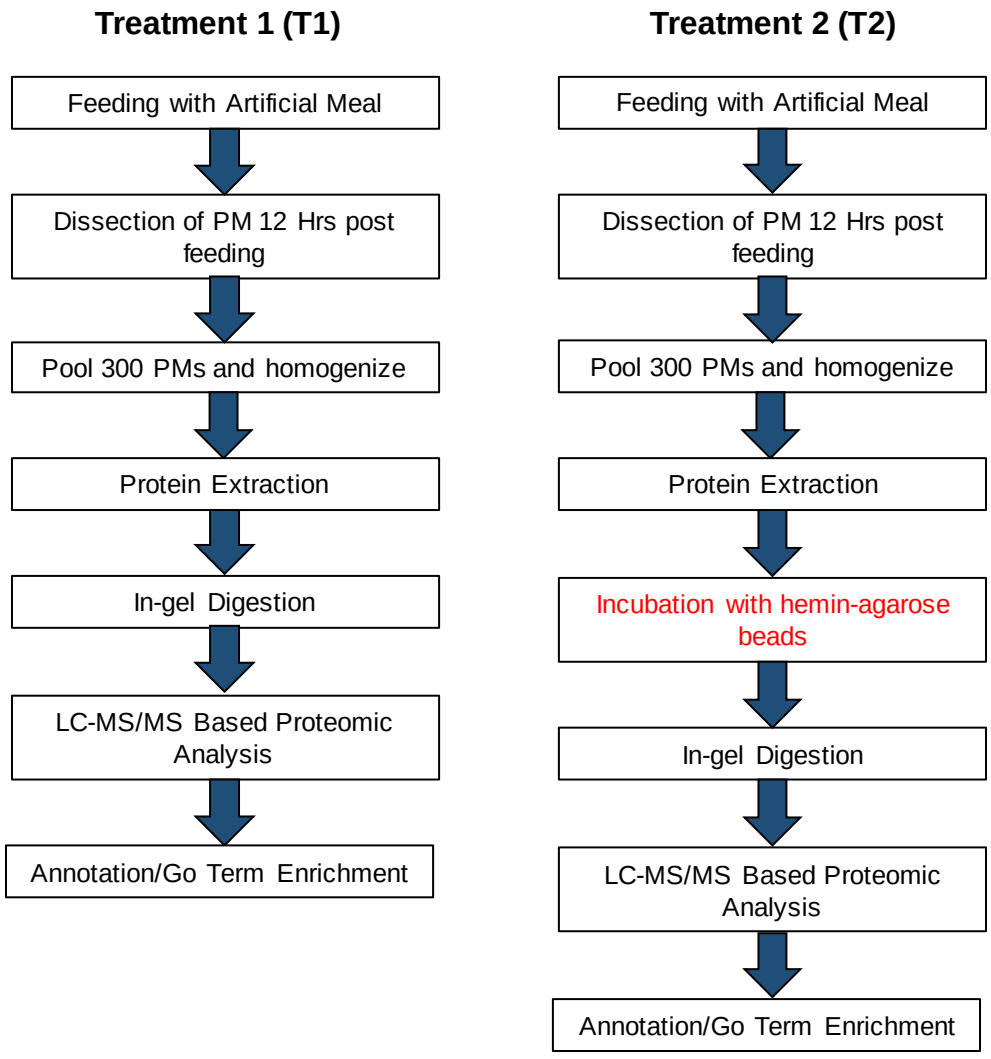

Figure 12. *Aedes aegypti* peritrophic matrix LC-MS/MS proteomic analysis flowchart. Experimental flowchart detailing the feeding of 3-5 day old adult female *Ae. aegypti* with protein-free artificial meal containing low melting agarose and subsequent sample processing of Treatment 1 (T1) and hemin-enriched Treatment 2 (T2) in preparation for LC-MS/MS based proteomic analysis .

3.2.4 SDS polyacrylamide gel electrophoresis

To further concentrate T1 and T2 samples, each was individually loaded into a hand-casted SDS polyacrylamide gel (10% Tris-Bis gel). Both samples were run at 30 mA for 30 min, until samples reached the stacking and separating interphase of the gel. The gel was stained

overnight with InstantBlue Coomassie protein stain (Expedeon, Inc.; San Diego, CA). The next morning, the gel was soaked in water for 30 min, and gel bands excised (T1 and T2 band).

3.2.5 Reduction, alkylation and digestion

Each excised gel plug (T1 and T2) was cut into small bits and placed in 150 µl of 100 mM ammonium bicarbonate. An additional 10 µl of 100 mM ammonium bicarbonate (ABC) was added to each sample. The samples were reduced with 45 mM dithiothreitol (DTT) (Sigma; Saint Louis, MO) and alkylated with 100 mM iodoacetamide (IAM) (Sigma; Saint Louis, MO). Gel plugs were dehydrated in 50% acetonitrile: 50% 50 mM ABC for 30 min. To completely dehydrate each sample, 50% acetonitrile:50% 50 mM ABC was replaced with 500 µl of acetonitrile and incubated for 30 min. Acetonitrile was removed and samples dried on a Speed Vac for 5 min (no heat). Samples were rehydrated with Endoproteinase Lys-C (Roche) (1mg/1ml protease) solution and incubated at 37^{o}C overnight. The next morning, trypsin (400 μg/1ml) solution was added and samples incubated at 37^{o}C overnight. The supernatant for each treatment (T1 and T2) was removed and saved for downstream LC-MS/MS analysis. An 80% acetonitrile: 1% formic acid solution was added to the remaining gel bits and incubated for 10 min. The subsequent supernatants for T1 and T2 samples, respectively, were removed and pooled with above-mentioned supernatant samples. Samples were dried down via Speed Vac and submitted for LC-MS/MS analysis.

3.2.6 Mass spectrometry based proteomic analysis

Digested samples were analyzed by capillary HPLC-electrospray ionization tandem mass spectrometry (HPLC-ESI-MS/MS) on an Orbitrap Velos Pro mass spectrometer (Thermo Fisher)

fitted with a New Objective Digital PicoView 550 NanoESI source. On-line HPLC separation was accomplished with an Eksigent/AB Sciex NanoLC-Ultra 2-D HPLC system: column, PicoFrit™ (New Objective; 75 μm i.d.) packed to 15 cm with C18 adsorbent (Vydac; 218MS 5 μm, 300 Å); mobile phase A, 0.5% acetic acid (HAc)/0.005% trifluoroacetic acid (TFA); mobile phase B, 90% acetonitrile/0.5% HAc/0.005% TFA; gradient 2 to 42% B in 30 min; flow rate, 0.4 μl/min. MS conditions were: ESI voltage, 2.75 kV; MS1 scan range, m/z 300 - 2000; isolation window for MS/MS, 3; normalized collision energy, 30%; scan strategy, survey scan followed by acquisition of data dependent collision-induced dissociation (CID) spectra of the six most intense ions in the survey scan above a threshold of 3000; dynamic exclusion, 30 sec; no charge state screening; reject list of background ions (± 10 ppm).

Mascot version 2.6.0 (Matrix Science; Boston, MA) was used to search the spectra against a combination of the following databases: Aedes-aegypti-LVP_AGWG_PEPTIDES_AaegL5.1 (28,316 sequences; 20,202,750 residues); SwissProt 2017_02 (553,655 sequences; 198,177,566 residues). Peptide tolerance was 20 ppm, fragment tolerance, 0.8 Da. Cysteine carbamidomethylation was set as a fixed modification and methionine oxidation, deamidation of glutamine and asparagine and protein N-terminal acetylation were considered as variable modifications; trypsin was specified as the proteolytic enzyme, with one missed cleavage allowed. Subset searches of the identified proteins by X! Tandem, cross-correlation with the Mascot results and determination of protein and peptide identity probabilities were accomplished by Scaffold version 4.8.7 (Proteome Software Inc.; Portland, OR). The thresholds for acceptance of peptide and protein assignments in Scaffold were 95% and 99%, respectively with a minimum of two peptides required.

3.2.7 Bioinformatic analyses

The VectorBase Biomart tool was used to obtain predicted structural features for the 160 unique proteins that resulted from our proteomic analysis (AaegL5.1). Likewise, we compared our list of 160 VectorBase Gene Stable IDs for the proteins identified by LC-MS to the list of 474 unique PM proteins identified as part of our Chapter 2 early midgut PM proteomic analysis [181]. This analysis took into account VectorBase genome assembly/annotation changes associated with AaegL3.3 to AaegL5.

g: GOSt--gene group functional profiling (version: r1750_e91_eg38) was used to conduct a hypergeometric enrichment analysis for T1 and T2 proteins isolated in our LC-MS based proteomic analysis [179, 180]. For each treatment (T1, T2 or shared proteins), the unordered list of VectorBase Gene Stable IDs were entered in the g: GOSt user interface. Parameters used for the enrichment analysis included: 1) significant values only and 2) hierarchical sorting. The enriched data was output in an Excel spreadsheet (XLSX), and further custom sorted based on p-value. Only results with p-value <0.001 were considered significant.

Secreted midgut proteins from T2 and T1/T2 were searched for repetitive cysteine-proline dipeptides which are a hallmark characteristic of PM peritophins [51]. The results were then entered into UniProt database and Center for Biological Sequence Analysis (CBS) prediction services database to determine secreted midgut proteins with: 1) two or more chitin-binding domains and 2) *O*-glycosylation and *N*-glycosylation status.

The adult female *Anopheles gambiae* PM proteome list was downloaded [53] and the VectorBase Gene Stable IDs for the 209 *Anopheles gambiae* PM proteins were entered in VectorBase Biomart. The data was output as a comma separated value (csv) file. We then

compared this data with our list of 160 VectorBase Gene Stable IDs. Only one to one orthologs for the two species were kept for further analyses with respect to T1, T2 or shared proteins.

3.3 Results

3.3.1 Proteomic analysis of midgut PM heme-enriched proteins

Through this study, we sought to identify potential heme-binding proteins present in the adult female *Ae. aegypti* midgut PM 12 hrs post artificial meal feeding. Therefore, twelve hours following a protein-free artificial bloodmeal, *Ae. aegypti* peritrophic matrices were dissected and proteins extracted for Treatment 1 (300 PMs). For Treatment 2 (300 PMs), heme-binding proteins were isolated via a hemin-agarose bead pull-down procedure. The extracted proteins for the respective samples, T1 and T2, were then run on an SDS PAGE gel and prepared for LC-MS/MS analysis. This resulted in the identification of 160 unique proteins identified with two or more peptides. Of these, 137 were present in the T1 sample and not in the T2 sample, consistent with the assumption that most proteins present in the 12 hr PM are not heme-binding proteins. Of the 23 proteins identified in the T2 sample, 11 were not found in T1 and 12 were shared between T1 and T2, respectively (Fig. 13; Table 3). The number of unique peptides for the eleven T2 heme-enriched portions ranged from 2-21 peptides (Fig. 14).

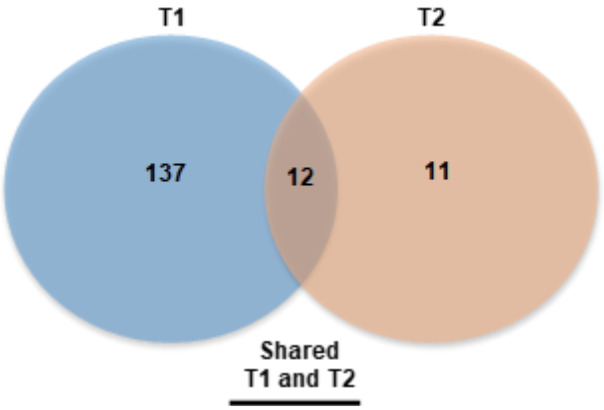

Figure 13. Distribution of *Aedes aegypti* midgut peritrophic matrix proteins identified in each treatment via LC-MS/MS proteomic analysis.
Breakdown for the160 unique proteins identified by LC-MS/MS proteomic analysis for *Ae. aegypti*.

We considered the possibility that proteins present in the T2 sample represented insufficient washing of the heme-agarose beads, rather than specific binding of proteins to this substrate. In this case, we would expect a direct, positive relationship between the number of peptides identified in the T1 sample and the corresponding T2 sample. However, regression analysis indicated no relationship between the number of peptides recovered in T1 and T2 (Fig. 14).

Table 3. Adult female *Ae. aegypti* heme-enriched (treatment 2) peritrophic matrix proteins isolated in this LC-MS/MS proteomic analysis.

***Ae. aegypti* Gene ID[a]**	**Description[a,b]**	**Treatment**	**# Peptides T1**	**# Peptides T2**
AAEL009244	serine-type endopeptidase[a]	T2	--	5
AAEL006971	|protein_coding	T2	--	2
AAEL012351	prolylcarboxypeptidase, putative[a]	T2	--	2
AAEL025567	peroxiredoxin-2 [b]	T2	--	4
AAEL009993	SGS1[b]	T2	--	21
AAEL012702	ATP-binding cassette sub-family A member 3, putative[a]	T2	--	3
AAEL018219	basement membrane-specific heparan sulfate proteoglycan core protein isoform X2[b]	T2	--	2
AAEL026582	probable cytochrome P450[b]	T2	--	2
AAEL010464	glutamate dehydrogenase[a]	T2	--	12
AAEL012135	GALE2: Galectin[a]	T2	--	6
AAEL022304	voltage-dependent anion-selective channel-like protein[b]	T2	--	2
AAEL007765	SRPN10: Serine Protease Inhibitor[a]	T1/T2	19	2
AAEL013885	|protein_coding[a]	T1/T2	5	11
AAEL000726	fibrinogen and fibronectin[a]	T1/T2	7	3
AAEL000749	Angiopoietin-like protein variant (Fragment) [a]	T1/T2	6	2
AAEL003056	brain chitinase and chia[a]	T1/T2	3	7
AAEL003066	brain chitinase and chia[a]	T1/T2	19	19
AAEL008607	tep3[a]	T1/T2	30	2
AAEL009955	Lipophorin[b]	T1/T2	152	98
AAEL013775	|protein_coding[a]	T1/T2	156	9
AAEL003318	oligopeptide transporter[a]	T1/T2	8	5
AAEL009432	SCRBQ3: Class B Scavenger Receptor (CD36 domain) [a]	T1/T2	8	6
AAEL011197	actin[a]	T1/T2	8	2

[a]VectorBase, *Ae. aegypti* mosquito database, August 2018.
[b]National Center for Biotechnology Information (NCBI), August 2018.

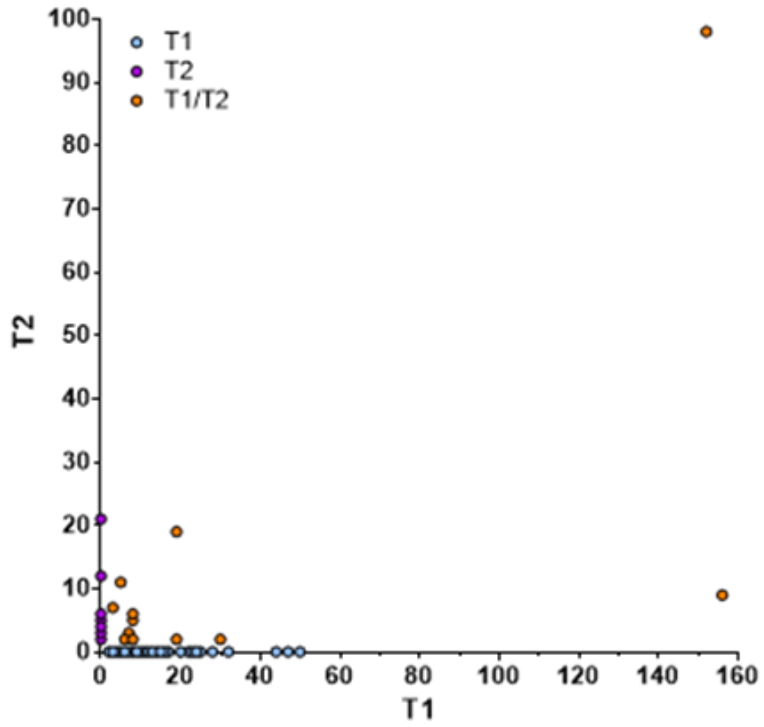

Figure 14. Number of unique peptides identified for each recovered protein in this adult *Aedes aegypti* heme-binding enrichment proteomic analysis.
Each dot represents a protein recovered in T1 (blue), T2 (purple) or T1/T2 shared (orange) 12 hours post artificial meal feeding. Data analyzed via regression analysis; two-tailed p=0.0513, Spearman r= -0.1543.

In an effort to delineate between midgut membrane or cytoplasmic proteins released as a result of the dissection procedure and secreted midgut PM proteins, we used VectorBase Biomart Tool to access the predicted localization information (signal peptide, transmembrane domains) for all proteins identified in T1 (Fig 15A), T2 (Fig 15B) or T1/T2 (Fig 15C). Three of the eleven proteins found only in T2 contained a secretory signal peptide without transmembrane domains, including a thioredoxin peroxidase (TPx)- AAEL025567 (identified four unique peptides). This protein has two highly conserved cysteine residues in the form of a Val-Cys-Pro (VCP) motif, and is a known hemoprotein [201, 202]. Four of the eleven proteins recovered in T2 contained predicted transmembrane domains, and no secretory signal peptide. Of the 13 unique proteins

identified in both T1 and T2, nine contained predicted secretory signal peptides. Interestingly, the secreted protein *Ae. aegypti* lipophorin (AAEL009955), was the second most abundant protein in T1 (152 peptides) and most abundant protein in T2 (98 peptides). Two of the nine T1/T2 proteins containing predicted signal peptides also contained predicted transmembrane domains (Fig. 14C). In contrast, we report the presence of two predicted transmembrane only proteins in T1/T2 shared, one of which is a Class B scavenger receptor (AAEL009432).

In our Chapter 2 study, we found many of the best-characterized *Ae. aegypti* salivary proteins [181, 182], including D7 (AAEL006424), which was the most abundant protein. In our current study, we again isolated D7 (AAEL006424) in the 12 hr PM. However, while D7 was present in T1, it was not the most abundant protein (2 peptides). Likewise, we again recovered several other salivary proteins such as alpha-amylase (AAEL009524), apyrase (AAEL006347), carboxylic ester hydrolase (AAEL008757), venom allergen (AAEL000793) and an unknown protein (AAEL007776) in T1 [182]. We also recovered a salivary gland surface protein (SGS1) (AAEL009993) in T2 [182].

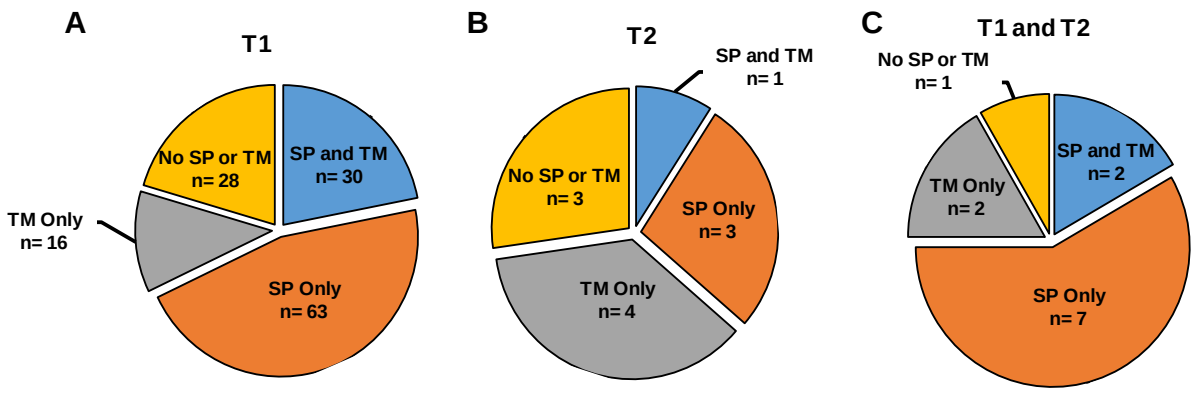

Figure 15. *Ae. aegypti* peritrophic matrix proteins by predicted localization for each treatment.
A total of 160 unique peritrophic matrix proteins were identified by mass spectrometry, and categorized based on predicted structural features; signal peptide without transmembrane domain (SP), transmembrane domain without SP (TM), those that contain both SP and TM, and the remaining isolated proteins (No SP or TM) for T1 (**A**), T2 (**B**) or shared T1 and T2 (**C**).

3.3.2 Comparison of RNAseq transcriptional profile data

With the understanding that proteins identified in this proteomic analysis could have come from the saliva (during feeding), the midgut (during PM formation) or the hemolymph (during dissection), published transcriptional profiles for different tissues were compared to obtain the likely source of each protein [203];(Fig. 16). *Ae. aegypti* lipophorin (AAEL009955), the second most abundant protein in T1 (152 peptides) and most abundant protein in T2 (98 peptides) showed elevated mRNA levels in the female *Ae. aegypti* carcass 12-24 hrs PBM [203]. Similarly, the T1/T2 shared Class B scavenger receptor (AAEL009432), which to our knowledge has not been shown to bind heme, shows highest expression in bloodfed females 1 day post injection with or without dengue virus. This protein has been shown to be involved in immunity in *Anopheles gambiae* [204], however given that this protein only shows pronounced expression in bloodfed *Ae. aegypti* mosquitoes 1 day post injection with or without dengue virus , we

hypothesize this scavenger may bind heme (at its peak period in the midgut lumen) and allow a safe port of entry into the intracellular space. In accordance, the T2 recovered ATP-binding cassette sub-family A member- AAEL012702 (3 peptides) may transport heme across the cell without degradation by heme oxygenases. This proposed mechanism would be similar to the heme transport mechanism seen in the midgut cells of R. *microplus* ticks [83]. We also report constitutive expression for the unknown gene product AAEL022340 that was isolated in T2. Based on conserved sequence, this protein is predicted to be a voltage-dependent anion-selective channel-like protein. Of most interest, the unknown function protein AAEL013885 which was recovered in both T1 (5 peptides) and T2 (11 peptides), has elevated mRNA transcript levels 1-14 days post injection with dengue virus (Fig. 16 A) [205].

With regards to salivary proteins, while we isolated SGS1 in our midgut PM proteomic T2 analysis, as detailed in Figure 16B, this protein has increased mRNA expression 14 days post injection (dpi) with and without dengue virus (original transcript data from Bonizzoni et al (2012) [205]. As detailed in Figure 16A (transcriptomic comparison data), fibrinogen and fibronectin (AAEL000726) showed high expression in the salivary glands 14 days post injection with and without dengue virus. However, this protein has lower expression levels in the *Ae. aegypti* carcass up to 72 hrs post bloodmeal feeding [203]. Similarly, the angiopoietin-like protein (AAEL000749) showed high salivary gland expression 14 days post injection with and without dengue virus, and lower carcass expression up to 72 hours post bloodmeal feeding [203]. With regards to both of these salivary proteins (AAEL000726 and AAEL000749) [183], transcriptomics data provide no evidence of midgut expression (Fig. 16A). Therefore, these salivary proteins were likely ingested during the artificial meal feeding process and deposited into the midgut.

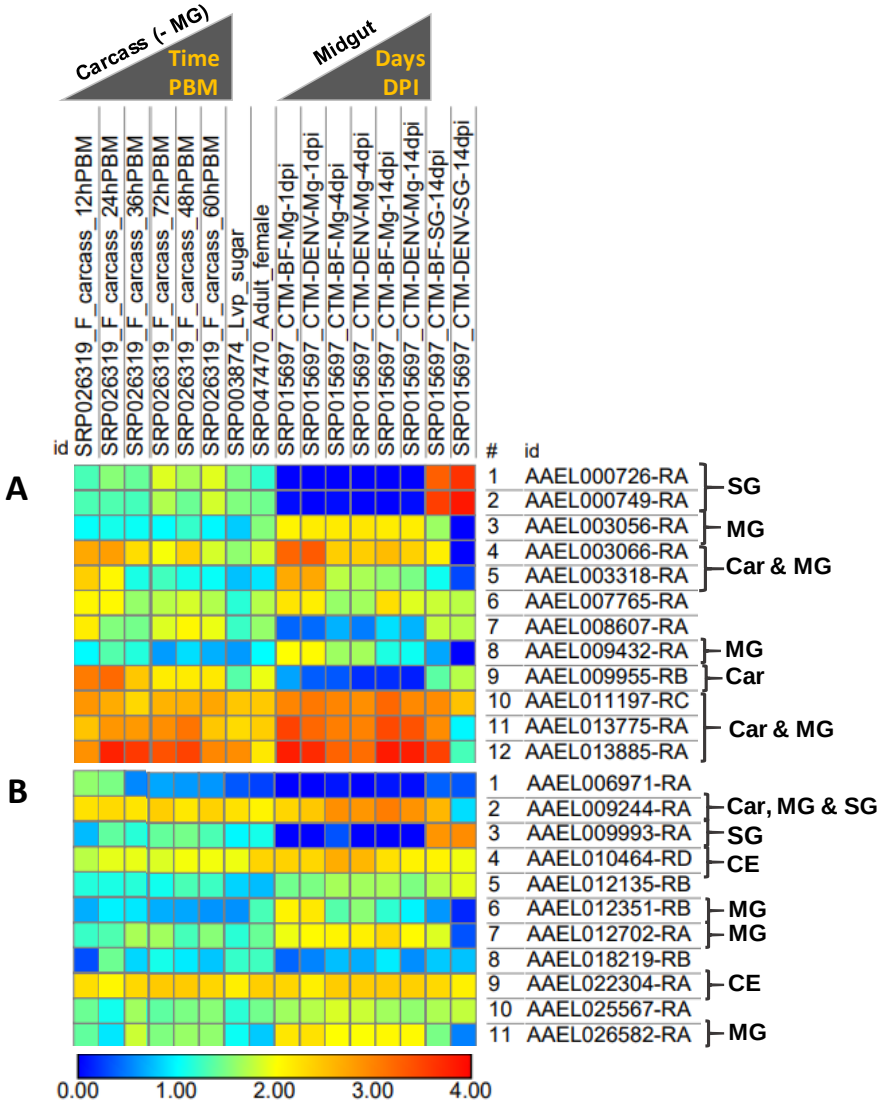

Figure 16. Comparison of transcriptomic data for heme-enriched proteins isolated in T1/T2 or T1 for this adult female *Ae. aegypti* peritrophic matrix proteomic analysis.
Transcriptomics data from Bonizzoni et al. (2012) and Akbari et al. (2013) was compiled for the (**A**) T1/T2 shared proteins and (**B**) T2 hemin-enriched proteins to explore mRNA expression under various physiological conditions and time points. All raw transcript expression data were log10 transformed. Morpheus, https://software.broadinstitute.org/morpheus, was used to generate heat maps for transformed transcriptomics data. Constitutively Expressed (CE), Salivary Gland (SG), Midgut (MG), Carcass (Car), Post Bloodmeal (PBM) and Days Post Injection (DPI).

3.3.3 Comparison of early and mature PM protein composition

As previously mentioned, in our Chapter 2 early midgut PM proteomic analysis, we identified 474 unique proteins by two or more peptides [181]. These proteins are representative of the early (6 hrs post artificial meal feeding) PM composition. However, given that our current PM analysis was conducted with PMs dissected from Rockefeller (ROCK) strain (different strain) female mosquitoes 12 hrs post artificial meal feeding, we compared the midgut PM protein composition at the two time points. Fifty-six percent (n=90) of the 160 PM proteins isolated in the 12 hr post artificial meal PM were also present in the early PM. However, we note that gene identifiers corresponding to 49 PM proteins isolated in our Chapter 2 early PM proteomic analysis were deprecated during the transition from AaeL3.1 to AaeL5 assemblies due to merging of gene predictions, suggesting prior redundancy overinflated the number of proteins identified in our earlier work.

3.3.4 GO term enrichment of predicted secreted proteins

To gain insight into the molecular function groupings for the proteins isolated in this proteomic analysis, we conducted a gene ontology (GO) term enrichment analysis (T1, T2 or T1/T2). The largest number (n=38) of T1 secreted proteins were associated with catalytic activity (GO:0003824) [179, 180]. As detailed in Figure 17, fourteen (n=14) T1 secreted proteins were further grouped as serine-type peptidases (GO:0004252) involved in blood protein digestion [5]. In particular, we isolated late trypsin (AaLT, AAEL013284), serine collagenase (AAEL007432, AaSP1), and AAEL013628 (AaSP4) along with 11 other serine-type peptidases [185-187]**.** Due to the later time point of PM dissections (12 hrs post artificial meal feeding), we were not

surprised that early trypsin (AaET, AAEL007818), which we previously recovered in our Chapter 2 early midgut PM proteomic analysis was not present in our current PM analysis [181].

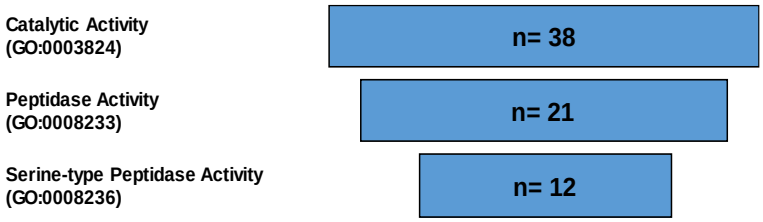

Figure 17. Adult *Aedes aegypti* Treatment 1 secreted proteins with catalytic activity isolated in this female peritrophic matric LC-MS/MS proteomic analysis.
Secreted proteins with catalytic activity, peptidase activity and serine-type peptidase activity. Hierarchical sorting based on gProfiler g: GOSt--gene group functional profiling ($p<0.001$).

The mosquito midgut is the first site of contact for pathogens ingested during bloodfeeding. Correspondingly, we again identified a number of secreted immune-related proteins in the midgut PM 12 hrs post artificial meal feeding. More specifically, in T1 we recovered a fibrinogen and fibronectin protein (AAEL006704), thioester–containing protein- (AAEL001794), prophenoloxidase (AAEL015116), two transferrins (AAEL015458 and AAEL011641), six serpins (AAEL002720, AAEL005665, AAEL008364, AAEL011777, AAEL013936 and AAEL014078) and Niemann-pick type C-2 protein (AAEL009760) [178, 188-191, 206]. Finally, twelve of the 63 T1 secreted proteins without transmembrane domains isolated in our proteomic analysis were novel proteins with unknown function (AAEL022931, AAEL015247, AAEL018249, AAEL026458, AAEL026165, AAEL010338, AAEL023112, AAEL007703, AAEL000500, AAEL023729, AAEL020823 and AAEL019828). For T2 we isolated one secreted immune-related protein- galectin AAEL012135 and one secreted protein without transmembrane domains that was a novel protein with unknown function (AAEL006971). Concerning our T1/T2 shared proteins, we report three secreted immune-related

proteins- fibrinogen and fibronectin (AAEL000726), a serpin (AAEL007765) and a thioester–containing protein- tep3 (AAEL008607), which we previously isolated in our Chapter 2 early midgut PM proteomic analysis [181]. Lastly, in our T1/T2 shared proteins, we report a secreted protein without transmembrane domains that is novel a protein with no putative conserved domains (AAEL013775).

3.3.5 Orthologs to *Anopheles gambiae* PM proteomic analysis

As described in Chapter 2, we compared our 12 hr post artificial meal feeding midgut peritrophic matrix proteomic results to those obtained by Dinglasan et al. (2009) to determine conserved proteins present in both Aedes and Anopheles PMs. Of the 209 unique *An. gambiae* peritrophic matrix proteins identified by Dinglasan et al. (2009) [53], 35 had one to one orthologs present in our 12 hr *Ae. aegypti* peritrophic matrix proteomic analysis (Fig. 18). Thirteen (n=13) of the one to one orthologs present in our current *Ae. aegypti* peritrophic matrix proteomic analysis were predicted secreted proteins without transmembrane domains (Table 4). More specifically, eleven (n=11) of these proteins were isolated in T1 and two (n=2) were isolated in T1/T2 shared (Table 4). Interestingly, Dinglasan et al. (2009) also isolated the major hemolymph lipid transport protein, lipophorin, in their PM proteomic analysis [53]. In our current study, the major hemolymph lipid transport protein- *Ae. aegypti* lipophorin (AAEL009955) was the second most abundant protein in T1 (152 peptides) and most abundant protein in T2 (98 peptides) [207, 208].

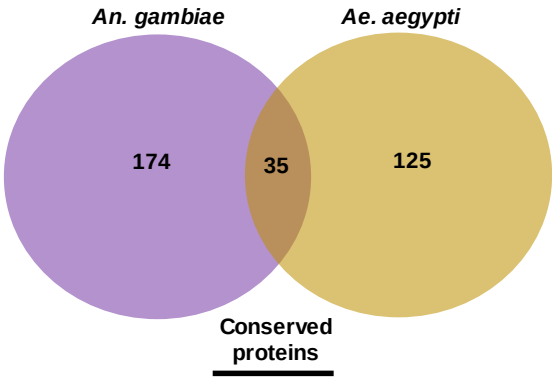

Figure 18. Adult *Ae. aegypti* peritrophic matrix proteins with *An. gambiae* orthologs isolated in Dinglasan et al. (2009) midgut peritrophic matrix proteomic analysis.

Table 4. Adult female *Ae. aegypti* secreted proteins and one to one orthologs isolated in Dinglasan et al. (2009) *An. gambiae* adult female LC-MS peritrophic matrix proteomic analysis.

***Ae. aegypti* Gene ID[a]**	***An. gambiae* Gene ID[a]**	**Description[a]**	**% Identity**	**Treatment**
AAEL003066	AGAP006414	brain chitinase and chia	63.1	T1/T2
AAEL004532	AGAP009610	glyoxylate/hydroxypyruvate reductase	68.5	T1
AAEL004931	AGAP010056	beta-hexosaminidase b	70.3	T1
AAEL006381	AGAP008487	sphingomyelin phosphodiesterase	57.2	T1
AAEL006902	AGAP010240	serine-type enodpeptidase	59.2	T1
AAEL007926	AGAP011442	retinoid-inducible serine carboxypeptidase	70.4	T1
AAEL009955	AGAP001826	unknown function|protein_coding	62.2	T1/T2
AAEL010338	AGAP009313	unknown function|protein_coding	28.7402	T1
AAEL015070	AGAP006400	mALP: alkaline phosphatase	64.3	T1
AAEL015110	AGAP008176	dipeptidyl-peptidase	58.8	T1
AAEL018249	AGAP002508	|protein_coding	48.6	T1
AAEL019828	AGAP001881	|protein_coding	56.4	T1
AAEL022931	AGAP000862	|protein_coding	70.6	T1

[a]VectorBase, *Ae. aegypti* mosquito database, August 2018.

3.4 Discussion

Pascoa et al. (2002) demonstrated that the adult female *Ae. egypti* PM can bind an equivalent amount of heme as found in a normal bloodmeal. This suggests that there are multiple heme-binding proteins present in the adult female *Ae. aegypti* PM after blood feeding. It has been shown that interactions between heme and various proteins can be coordinated by: 1) a histidine-methionine pair, 2) bihistidine, or 3) a cysteine-proline dipeptide [209, 210]. More specifically, cysteine-proline dipeptides are central amino acids in the Heme Regulatory Motifs (HRM) of certain heme-binding proteins. In a study conducted by Zhang and Guarente (1995), the HRM cysteine was found to be essential for heme binding, and HRM proline increased binding affinity [209]. The only known *Ae. aegypti* PM heme-binding protein, AeIMUC1, has been shown to *in vitro* coordinate binding through the above mentioned conserved cysteine-proline dipeptide motifs (HRMs) which also overlap the known chitin-binding domains present in AeIMUC1 [51]. With only one *in vitro* study demonstrating recombinant AeIMUC1 heme-binding [51], our current study serves as the first to investigate adult female *Ae. aegypti* midgut PM heme-binding proteins in an unbiased manner via an *in vitro* heme-enrichment proteomic analysis.

In keeping with our Chapter 2 artificial meal feeding methodology, we initially attempted *in vivo* heme-binding experiments through artificial meal feeding enriched with heme. However, we were unable to keep the largely hydrophobic heme in solution at solvent (DMSO) concentrations that were non-toxic or non-attractive to the mosquitoes. The lack of successful feeding rates on an artificial heme-enriched protein-free meal resulted in our utilization of an *in vitro* heme-enrichment proteomic analysis. Similarly, based on our Chapter 2 results, we hypothesized heme-binding proteins enriched in this proteomic analysis would only represent a

small subset of the isolated PM proteins. Therefore, we utilized a modified in-gel digestion procedure whereby T1 and T2 samples were allowed to run until reaching the interphase of the stacking and separating portions of the SDS PAGE gel. This modified procedure resulted in the recovery of 160 *Ae. aegypti* PM proteins identified by two or more unique peptides 12 hrs post artificial meal feeding. More specifically, we recovered eleven proteins in T2 and twelve proteins in T1/T2 shared. We were surprised that neither of the two known *Ae. aegypti* PM proteins (AeIMUC1 or AeAper50) were isolated in T1 or T2 of this proteomic analysis. Our lack of recovery of the two known PM peritrophins may be associated with the digestion methodology modification (Chapter 2 in-solution digestion vs. Chapter 3 in-gel digestion) or PM sample size for T1 (300 PMs) and T2 (300 PMs) in this proteomic analysis. This provides a plausible explanation, as for our Chapter 2 proteomic analysis we dissected and in-solution digested 1,020 PMs, but only 2 peptides were recovered for each of the known PM proteins [181]. Therefore, it was very likely that even if these proteins were present in our T1 or T2 enriched treatment, they may not have been detected. Furthermore, the six-hour difference in PM dissections for our Chapter 2 and Chapter 3 studies provide an extensive amount of time for which many physiological changes in the PM protein composition to could occur. More specifically, the lack of heme signaling by 12 hrs (due to the artificial meal feed) potentially could have resulted in decreased gene expression and ultimately protein product. However, the lack of gene expression profiling data for these gene targets after artificial meal feeding makes drawing this conclusion impossible at the current time.

We were very surprised not to recover AeIMUC1 in T2, given that this protein has previously been shown to *in vitro* bind heme [199]. However, specific to T2 we recovered one of five known *Ae. aegypti* thioredoxin peroxidases (AAEL025567). This peroxidase contains

conserved cysteine residues which are present as a Val-Cys-Pro (VCP) motif [202], and contains the cysteine proline dipeptide, which facilitates binding in the heme regulatory motifs (HRM) of certain heme-binding proteins [209]. Likewsie, specific to T2 we recovered the putative *Ae. aegypti* cytochrome P450 monooxygenase (AAEL026582), which is a heme-thiolate-containing enzyme involved in metabolism of xenobiotics and endogenous molecules [211, 212]. Finally, it is possible that AeIMUC1 or other heme-binding proteins may have indeed been present in our sample, but were unable to properly bind the heme moiety due to steric hindrance caused by the cross-linkage with agarose beads.

Interestingly, the most abundant protein found in T2 and second most abundant protein found in T1 was the major hemolymph lipophorin- AAEL009955 [207, 208]. Synthesized primarily in the fat body, lipophorin is known to transport lipids to the developing ovaries following a bloodmeal [207]. The fact that this protein was highly abundant in our T1 dataset suggests our results are a mixture of hemolymph proteins and true PM components, though we cannot rule out the potential for this lipophorin to scavenge lipids directly from the diet. However, the abundance of lipophorin in the T2 sample (almost 50% of all mosquito peptides recovered) suggests that in addition to transporting lipids, lipophorin may directly bind and shuttle heme from the gut to the developing ovaries. This is reminiscent of the heme lipoprotein (HeLp), which serves as the major hemolymph heme-binding protein which transports heme to the ovaries in *R. microplus* [163]. While ticks are unable to synthesize their own heme, mosquitoes can, though direct heme-shuttling from the gut to the developing ovaries in this mosquito may be more expedient. Reverse genetic analysis of the role if lipophorin in heme transport is complicated by its critical role in shuttling lipids (REFs). The generation of recombinant proteins lacking heme-binding residues could be used in tandem with full length

recombinant protein to *in vitro* determine heme binding. Subsequently, *in vivo* heme-binding assays can be utilized to determine if this known lipid transport protein in *Ae. aegypti* has derived additional functionality as a heme-shuttling protein, and thereby transporting heme directly to the ovaries.

Our current study only provides a snapshot of the *Ae. aegypti* PM protein composition at 12 hrs post artificial meal feeding. A more in-depth heme-enrichment PM proteomic analysis which spans several physiologically relevant time points will allow for more robust conclusions regarding heme-binding proteins present in the adult female mosquito PM. However, taken together, our current forward genetics study provides new insight into heme-enriched proteins represented in the adult female PM 12 hrs post artificial meal feeding. We now turn our focus to reverse genetic analyses (RNAi and CRISPR/Cas9) to determine the physiological role of AeIMUC1, AeAper50 and the novel PM protein (AAEL006953) isolated in our Chapter 2 early *Ae. aegypti* PM proteomic analysis.

CHAPTER IV

GENE EXPRESSION PROFILING AND REVERSE GENETIC ANALYSIS FOR ADULT *AEDES AEGYPTI* MIDGUT PERITROPHIC MATRIX HEME-BINDING PROTEINS

4.1 Introduction

During a blood meal, adult female mosquitoes ingest two to three times their normal body weight [170]. Digestion of this blood meal releases large amounts of heme in the mosquito midgut lumen [51, 63]. If not properly chaperoned, this free heme can facilitate oxidation of nucleic acids [11], lipids [12, 13], and proteins [14, 171]. Therefore, understanding the physiological mechanisms adult female mosquitoes have evolved to process the potentially toxic blood meal and associated metabolites is needed. One such mechanism is the mosquito midgut peritrophic matrix (PM), an acellular protective lining which separates the single cell-layered midgut epithelium from pathogens, abrasion, and toxic compounds [51, 60, 61].

In adult female mosquitoes, the type I PM is comprised of proteins, proteoglycans and chitin fibrils [50, 63]. PM proteins are commonly referred to as peritrophins and hallmark characteristics of peritrophins include: 1) the presence of a secretory signal peptide, 2) multiple chitin-binding domains containing cysteine-proline dipeptides and 3) intervening mucin-like domains rich in proline, serine and threonine [58]. More specifically, PM peritrophin chitin-binding domains function as cross-linkers for chitin fibrils, consequently providing structural support for the PM [47, 64]. Initially, two-dimensional polyacrylamide gel electrophoresis and lectin-binding assays suggested the adult female *Ae. aegypti* PM may contain 20-40 major proteins [59]. However, only two proteins have been identified and characterized as adult *Ae. aegypti* midgut PM peritrophins: intestinal mucin 1 (AeIMUC1) [67] and adult peritrophin 50

(AeAper50) [49]. Our recent LC-MS based *Ae. aegypti* midgut PM proteomic analysis (Chapter 2) identified 474 unique proteins with two or more peptides, and 115of these proteins contained a predicted secretory signal peptide without transmembrane domain. Likewise, we isolated the two known PM peritrophins (AeIMUC1 and AeAper50) and two novel PM proteins with characteristics similar to the known PM peritrophins [181]. However, based on the new VectorBase genome assembly (AaegL5), the known *Ae. aegypti* PM peritrophin AeIMUC1 (AAEL002495) was collapsed with AAEL004798, and therefore, resulted in two known (AAEL002495/AAEL004798 and AAEL002467) and one putative (AAEL006953) PM peritrophin.

Although our Chapter 3 midgut PM heme-enriched proteomic analysis resulted in 160 PM proteins, ten of which were hemin-enriched secreted proteins without transmembrane domain, we did not isolate either of the known PM peritrophins (AeIMUC1 and AeAper50). Therefore, in this study, we conducted comprehensive gene expression profiling via quantitative PCR to understand the expression patterns for the known and putative PM peritrophins identified via mass spectrometry in Chapter 2 [181]. We also conducted reverse genetic analyses for adult *Ae. aegypti* midgut peritrophic matrix heme-binding proteins to determine any resulting physiological defects (fecundity, larval counts and fertility). We found that RNAi-mediated knockdown of the known and putative PM peritrophins did not substantially decrease adult survivorship or reproduction. Therefore, our results suggest that the adult female *Ae. aegypti* defense response in the gut lumen (extracellular) as well as in the cytoplasm of midgut epithelial cells (intracellular) is sufficiently robust as to avoid a milieu prone to oxidative stress [66] after acquiring a blood meal despite a reduction in some components.

4.2 Materials and methods

4.2.1 Mosquitoes

For all experiments, *Aedes aegypti* (Liverpool strain) were maintained in environmental growth chambers (Thermo Fisher) at 28 ^{o}C, 70% RH and 14H:10H light:dark photoperiod. The mosquito colony was maintained on defibrillated sheep blood (Colorado Serum Company; Denver, Colorado or Hemostat Laboratories; Dixon, California) using an artificial feeding system.

4.2.2 Midgut expression profiling

4.2.2.1 Midgut dissections and RNA extraction

Midguts (MGs) were dissected from adult 3-5 day old female *Aedes aegypti* Liverpool (LVP) strain in 1x Phosphate Buffered Saline (PBS) (Sigma; St. Louis, MO) under a Leica M60 microscope (Leica Microsystems Inc.; Buffalo Grove, IL) and immediately transferred to 1.5 mL Eppendorf tubes containing TRIzol reagent (Thermo Fisher). Total RNA was isolated using the manufacturer's protocol (Thermo Fisher) and quantified using SoftMAX Pro 6.5.1 software on a SpectraMax i3x spectrophotometer (Molecular Devices; Sunnyvale, California). See Figure 19 for midgut expression profiling flowchart.

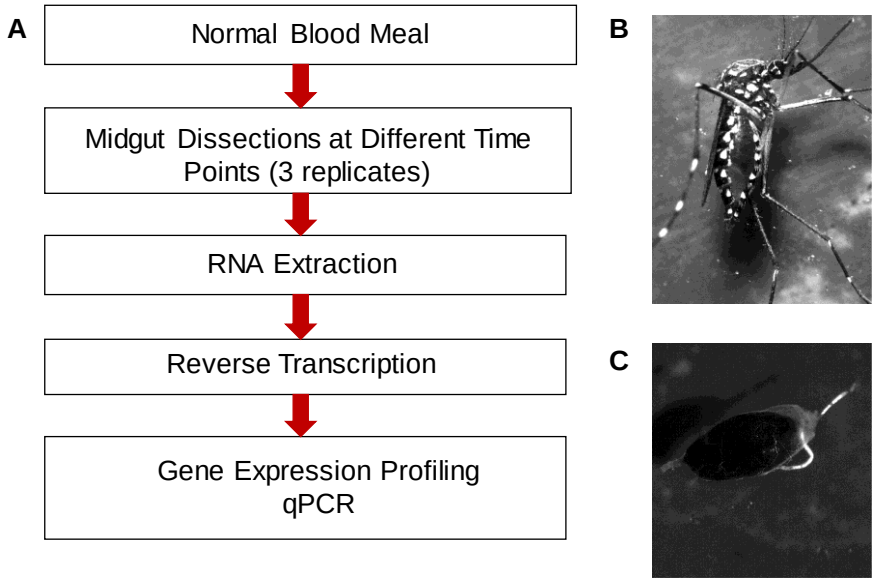

Figure 19. Gene expression profiling for *Aedes aegypti* peritrophic matrix proteins. (**A**) Experimental flowchart detailing the feeding of 3-5 day old adult female *Ae. aegypti* with normal bloodmeal, midgut dissections in 1xPBS (Non-blood fed (NBF), 2, 4, 8, 12, 18, 24 and 48 hr post bloodfeeding), RNA extraction, reverse transcription (cDNA generation), and analysis of gene expression for known and putative PM peritrophins. (**B**) Adult female post feeding with normal bloodmeal. (**C**) Dissected midgut post adult female feeding.

4.2.2.2 cDNA synthesis

The Invitrogen SuperScript IV VILO ezDNase enzyme (Thermo Fisher) was used to remove residual genomic DNA contamination from each total RNA sample prior to cDNA synthesis. Following inactivation of the ezDNase, cDNA was synthesized using the Invitrogen SuperScript IV VILO 5X Master Mix which includes SuperScript IV Reverse Transcriptase, RNase inhibitor, helper proteins, stabilizer proteins, oligo (dT)18, random hexamer primers, $MgCl_2$ and dNTPs (Thermo Fisher). For primer annealing, reactions were incubated at 25^{o}C for 10 min and subject to reverse transcription for 10 min at 50 ^{o}C. The reverse transcriptase was inactivated at 85^{o}C for 5 minutes. The cDNA was diluted 1/50 in DEPC H_2O, and used for downstream qRT-PCR analyses.

4.2.2.3 Quantitative real-time PCR (qRT-PCR)

Quantitative real-time PCR (qRT-PCR) was performed on a CFX69 Touch Real-Time PCR Detection System (Bio Rad) using SsoAdvanced Universal SYBR Green Supermix (Bio Rad). Primers as listed in Table 5 (adapted from Tsujimoto et al. [215]) were designed using Primer3 server (version 4.0.0) or PrimerSelect (DNASTAR) [213]. Primer amplification efficiency was determined for all primer pairs. Each reaction was performed following the Sso Advanced Universal SYBR Green Supermix manufacture's protocol for a 10 μL total volume reaction with 0.5 μL 250 nM primers and 1 μL of 1/50 diluted cDNA in triplicates. All reactions were conducted as follows: 30s at 95^{o}C (polymerase activation and DNA denaturation), then 45 cycles of 15 s at 95^{o}C, 30s at 57^{o}C (2495 and 6953) or 60^{o}C (2467, CAT, FER, S7) and melt curve analysis 65-95^{o}C with 0.5^{o}C increments for 5 sec/step. Expression was calculated relative to the reference housekeeping gene ribosomal protein S7 (rpS7) following the dCt method [214]. The C_q values for all primer sets/samples are detailed in Appendix B (Table B-1 and B-2).

Table 5. **Primers used in this study.** The bolded letters represent T7 promoter sequence; FrLCH: Ferritin light chain; rpS7: ribosomal protein S7. Adapted from Tsujimoto et al. [215].

Gene ID/Accession #	Direction	Primers	Class	Purpose
AAEL002467	Forward	**TAATACGACTCACTATAGGG**TTTGCAATTGAATC GAAATCAT	Peritrophin	dsRNA temp
	Reverse	**TAATACGACTCACTATAGGG**CGTGAGGAAGGTAC ACCTGG	Peritrophin	dsRNA temp
AAEL002495	Forward	**TAATACGACTCACTATAGGG**ATGAAGGGCAATTT GTTCATTTCG	Peritrophin	dsRNA temp
	Reverse	**TAATACGACTCACTATAGGG**CCAGATGGACAGCT CTTTTCAAC	Peritrophin	dsRNA temp
AAEL006953	Forward	**TAATACGACTCACTATAGGG**ATGTTGGCGCTCAT CGTTTTGC	Putative Peritrophin	dsRNA temp
	Reverse	**TAATACGACTCACTATAGGG**ACCCTGTCCGTTCC GTCGCAC	Putative Peritrophin	dsRNA temp
AAEL027249[a]	Forward	**TAATACGACTCACTATAGGG**CCCTTCACAAACCT GGAGAA	Positive control	dsRNA temp
	Reverse	**TAATACGACTCACTATAGGG**CCAATCCATGATAC TGCACCAT	Positive control	dsRNA temp
AST15063.1 (EGFP)[b]	Forward	**TAATACGACTCACTATAGGG**ATGGTGAGCAAGG GCGAGGAGC	Negative control	dsRNA temp
	Reverse	**TAATACGACTCACTATAGGG**ATCTTGAAGTTCAC CTTGATGCCGTT	Negative control	dsRNA temp
AAEL009496[b]	Forward	ACCGCCGTCTACGATGCCA	RpS7	qRT-PCR
	Reverse	ATGGTGGTCTGCTGGTTCTT	RpS7	qRT-PCR
AAEL002467	Forward	GGAGCCTGCAACTACTACCG	Peritrophin	qRT-PCR
	Reverse	GCTTGCTGCGGGTAATCAC	Peritrophin	qRT-PCR
AAEL002495	Forward	CGATCCCGAGAATGAAGTTT	Peritrophin	qRT-PCR
	Reverse	CAGTTCAGCAGTACCGGGAT	Peritrophin	qRT-PCR
AAEL006953	Forward	GTGGTTCGAGTGGAAGTGGT	Putative Peritrophin	qRT-PCR
	Reverse	GGACTGAGCTGTGTTCCCAT	Putative Peritrophin	qRT-PCR
AAEL007383[b]	Forward	CGGATTTGAGAAGCTGTACCGC	FrLCH	qRT-PCR
	Reverse	AGGCCACGTTTGCTCTGATACT	FrLCH	qRT-PCR
AAEL013407[c]	Forward	CAATGAACTGCACCGACAAC	CAT	qRT-PCR
	Reverse	AGCCTCATCCAGAACACGAC	CAT	qRT-PCR

[a] Primers (F/R) from Isoe et al. [216]
[b] Primers (F/R) from Tsujimoto et al. [215]
[c] Primers (F/R) from Oliveira et al. [19]

4.2.3 Mosquito RNAi

4.2.3.1 dsRNA synthesis

Gene-specific double stranded RNAs (dsRNAs) were generated using Phusion polymerase (New England Biolabs; Ipswich, MA), primers listed in Table 5 and cDNA generated from Liverpool (LVP) strain mosquito genomic DNA as template [19, 215, 216]. PCR amplicons with T7 RNA polymerase promoter sequence on the 5' end (See Table 5) were used as templates for the MEGASCRIPT T7 RNAi kit (Life Technologies; Carlsbad, CA). dsRNAs were synthesized according to the MEGASCRIPT T7 RNAi kit manufacturer's instructions. Synthesized dsRNAs were treated with TURBO DNase to remove template DNA. dsRNAs were purified using the MEGAClear kit (Life Technologies; Carlsbad, CA).

4.2.3.2 Double-stranded RNA (dsRNA) thoracic microinjections

RNAi experiments were conducted with cold-anesthetized 5-day-old mated/non-blood fed (NBF) LVP strain females starved of sucrose for 24 hr prior to injections. For all RNAi experiments, 500 ng of a specific dsRNA (ds2467, ds2495, ds6953) was injected into the thoracic cavity of an individual female mosquito using a Nanoject II Auto-Nanoliter Injector (Drummond Scientific Company; Broomall, PA) with needle drawn from a glass capillary. EGFP and γ-coatomer protein I (COPI) were used as negative and positive controls, respectively, for all single injection replicates. All RNA injections were conducted in triplicate. In addition, cold-anesthetized 5-day-old mated/non-blood fed (NBF) LVP strain females starved of sucrose for 24 hr prior to injections were used for multiplex (ds2467, ds2495, ds6953) dsRNA injections. For all multiplex dsRNA injections, a mixture containing 500 ng of each dsRNA was injected

into a single female mosquito. EGFP served as negative control, and multiplex dsRNA injection experiments were conducted in triplicate.

4.2.3.3 Post-injection bloodfeeding, mortality and fecundity counts

Seventy-two hours (3 days) after dsRNA injection, adult female mosquitoes were fed on defibrinated sheep blood (Colorado Serum Company; Denver, Colorado or Hemostat Laboratories; Dixon, California) using an artificial feeding system and mortality was recorded at 24, 48 and 72 hr post blood meal (PBM) (Fig. 20)(adapted from Isoe et al. [216]). To determine knockdown efficiency at 24 hr PBM (4 days post dsRNA injection), a subset of midguts (MGs) from dsRNA injected mosquitoes were dissected in 1x Phosphate Buffered Saline (PBS) (Sigma; St. Louis, MO) under a Leica M60 microscope (Leica Microsystems Inc.; Buffalo Grove, IL) and immediately transferred to 1.5 mL Eppendorf tubes containing TRIzol reagent (Thermo Fisher). RNA isolation, cDNA synthesis and qRT-PCR quantification were conducted as detailed in sections 4.2.2.2 and 4.2.2.3.

To measure the effect of gene-specific or multiplex RNAi-mediated knockdown on fecundity and hatch-rate, surviving adult females were individually placed in a well of a 24-well plate containing 2% agarose, which served as wet surface for egg laying [215]. At forty-eight hours after egg laying, each well containing embryos was photographed using a Leica M165 FC microscope (Leica Microsystems Inc.; Buffalo Grove, IL) and AmScope 3MP Microscope Digital Camera (AmScope; Irvine, CA). Subsequently, embryos were counted via ImageJ Fiji software [217]. After photographing embryos, water was added to each well to the point of embryo submergence. After an additional six days, wells containing hatched larvae were photographed using a Leica M165 FC microscope (Leica Microsystems Inc.; Buffalo Grove, IL)

and AmScope 3MP Microscope Digital Camera (AmScope; Irvine, CA). Hatched larvae were counted via ImageJ Fiji software [217].

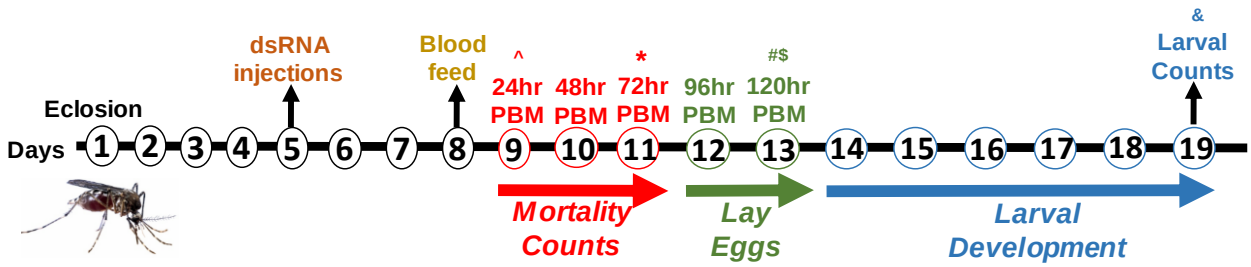

Figure 20. RNAi-mediated knockdown and phenotypic effect (mortality and fecundity) timeline for *Aedes aegypti* putative peritrophic matrix proteins.
At 24 hr PBM a subset of midguts (MGs) were dissected, RNA extracted, cDNA synthesized and used for qPCR analysis (^). On Day11, surviving mosquitoes were placed in individual well of a 24-well plate contain 500 µL of 2% agarose (*****) and allowed to lay eggs for two days (Day 12 and 13). On Day 13, adult females were removed from the individual wells and embryos were photographed (#). On Day 13 H_20 was added to point of embryo submergence in each well ($). Embryos were allowed to hatch and larvae develop for six days (Days 14-19). On Day 19, larvae were photographed and counted (&). Adapted from Isoe et al. [216].

4.2.3.5 Statistical analysis

All experiments were conducted independently three times, and the appropriate statistical analyses performed using GraphPad Prism software version 7.01 (GraphPad Software; La Jolla, CA). The Mantel-Cox (logrank) test was used to compare survival distributions. The Kruskal-Wallis (non-parametric) test and post hoc Dunn's multiple comparison test were used to analyze/compare fecundity and hatch percent for each gene-specific RNAi-mediated knockdown replicate. The Mann-Whitney-Wilcoxon (MWW) test was used to analyze/compare fecundity and hatch percent for multiplex RNAi-mediated knockdown replicates.

4.3 Results

4.3.1 Midgut expression profiling

We first sought to investigate the expression profile for known and putative adult peritrophic matrix (PM) proteins (AAEL002467, AAEL002495, AAEL006953) by quantitative real-time PCR (qRT-PCR) at various time points [non-blood fed (NBF), 2, 4, 8, 12, 18, 24, 48 hrs] post blood meal (PBM). Strikingly, expression of AAEL002467 increased more than 10-fold within 2 hrs of bloodfeeding and continued to increase reaching a maximum expression almost 300 times greater than the ribosomal RNA comparator by 4 hrs PBM across all three replicates (Fig. 21). As detailed in Figure 21, the expression of AAEL002467 remained elevated (approximately 100X relative to S7 ribosomal protein) through 48 hrs PBM. This robust expression pattern suggests the potential for a physiologically important role for Ae-Aper 50 (AAEL002467)- a known peritrophic matrix peritrophin [49], throughout the blood meal digestion processes.

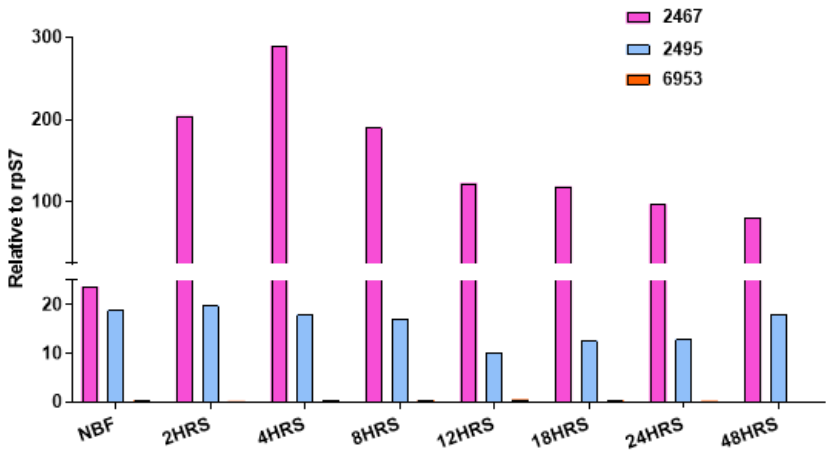

Figure 21. Average gene expression patterns for known and putative adult *Ae. aegypti* peritrophic matrix peritrophins determined by quantitative PCR using primer sets. Figure is average of 3 independent experiments for each gene target (AAEL002467, AAEL002495, AAEL006953).

Devenport et al. (2006) previously determined *in vitro* heme-binding for AeIMUC1 (AAEL002495), and we found transcripts for this gene to be approximately 10-20X more abundant than S7 ribosomal protein (Fig. 21). In contrast, the expression for AAEL006953 (putative PM peritrophin) was much more variable across experimental replicates, and substantially lower than the two known peritrophins (Fig. 21 and 22C). Taken together, these results suggest both confirmed PM peritrophins (AAEL002467 and AAEL002495) may make the largest contribution with the bloodmeal detoxification process, with a potential lesser role for AAEL006953. We therefore sought to determine the physiological role of these PM peritrophins via RNAi mediated knockdown experiments.

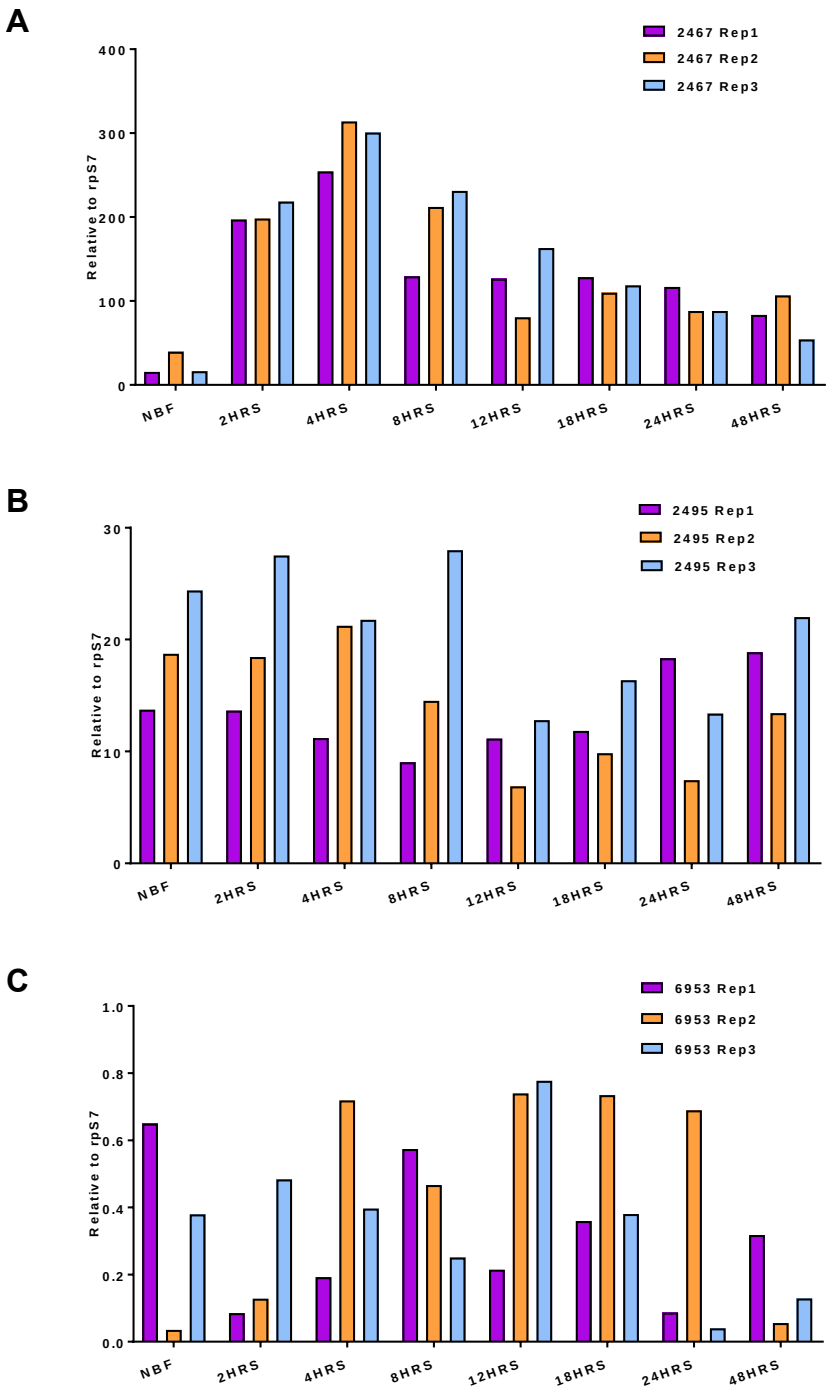

Figure 22. Gene expression patterns for known and putative adult *Ae. aegypti* peritrophic matrix peritrophins determined by quantitative PCR using primer sets.
Analysis shows the three different replicates for each gene-target (**A**) AAEL002467, (**B**) AAEL002495 and (**C**) AAEL006953.

4.3.2 Mosquito RNAi

4.3.2.1 RNAi mediated knockdown efficiency

To determine the physiological role of known and putative PM peritrophins, we injected single dsRNAs against AAEL002467, AAEL002495, and AAEL006953 and evaluated the corresponding mRNA levels four days later (24 hr PBM). As detailed in Figure 23, we observed an average knockdown efficiency of 30.11%, 87.94%, and 97.51% for AAEL002467, AAEL002495 and AAEL006953, respectively for single-gene target injection experiments. More specifically, for AAEL002467 we observed no knockdown, 93% and 28% knockdown efficiency for replicates 1, 2 and 3, respectively. For AAEL002495, we observed 71%, 93% and 74% knockdown efficiency for replicates 1, 2 and 3, respectively. For AAEL006953, we observed 91% and 97% knockdown efficiency for replicates 1 and 2, respectively. However, we note the absence of knockdown efficiency data for replicate 3, as all injected mosquitoes were allocated to phenotypic effect experiments (high post blood meal feeding mortality). See Appendix B (Table B-3 and B-4) for Cq and relative expression values.

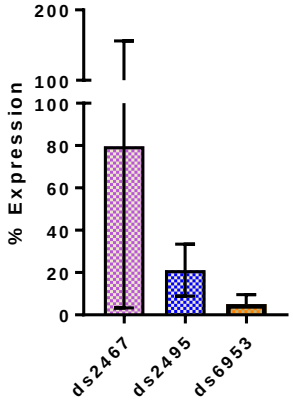

Figure 23. Gene expression for single-injection RNAi-mediated knockdown midguts determined by quantitative PCR.
Percent expression determined 96 hr post dsRNA injection/24 hr post bloodmeal (PBM) for each single-injection gene-target relative to expression in GFP negative control. Error bars indicate mean ± standard deviation and figures are representative of minimum of 2 independent experiments.

As these three peritrophins may exhibit functional redundancy, we conducted multiplex (AAEL002467, AAEL002495, AAEL006953) knockdown experiments and evaluated the mRNA levels of each corresponding gene 24 hr PBM. As detailed in Figure 24, we observed an average knockdown efficiency of 86%, 78% and 76% for AAEL002467, AAEL002495 and AAEL006953, respectively for multiplex injection experiments. More specifically, for AAEL002467 dsRNA knockdown replicates, we report 88%, 76% and 94% knockdown efficiency for multiplex replicates 1, 2 and 3, respectively. For AAEL002495, we report 96%, 67% and 68% knockdown efficiency for multiplex replicates 1, 2 and 3, respectively. For AAEL006953, we report 79%, 79% and 69% knockdown efficiency for multiplex replicates 1, 2 and 3, respectively. See Appendix B (Table B-5 and B-6) for Cq and relative expression values. We note that a more consistent level of knockdown was observed for multiplex-injection RNAi-

mediated knockdown experiments when compared to our single gene-target injection experiments.

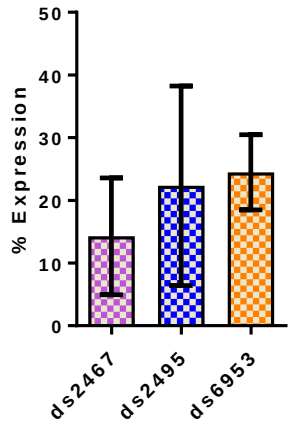

Figure 24. Gene expression for multiplex-injection RNAi-mediated knockdown midguts determined by quantitative PCR.
Expression determined 96 hr post dsRNA injection/24 hr PBM for multiplex-injections relative to expression in GFP negative control. Error bars indicate mean ± standard deviation.

4.3.2.2 Mortality, fecundity and fertility counts

As detailed in Figure 25, we determined survivorship (24, 48 and 72 hr PBM) for all single gene-target and multiplex RNAi-mediated knockdown experiments. Based on the Log-rank (Mantel-Cox) test, we report a significant difference in survival curves for single gene-target replicates 1, 2, 3 and pooled replicates **(**$p<0.0001$ for all replicates and pooled**)** (Fig. 25). As expected, for all replicates we observed the greatest mortality for the COPI (gamma subunit) positive control.

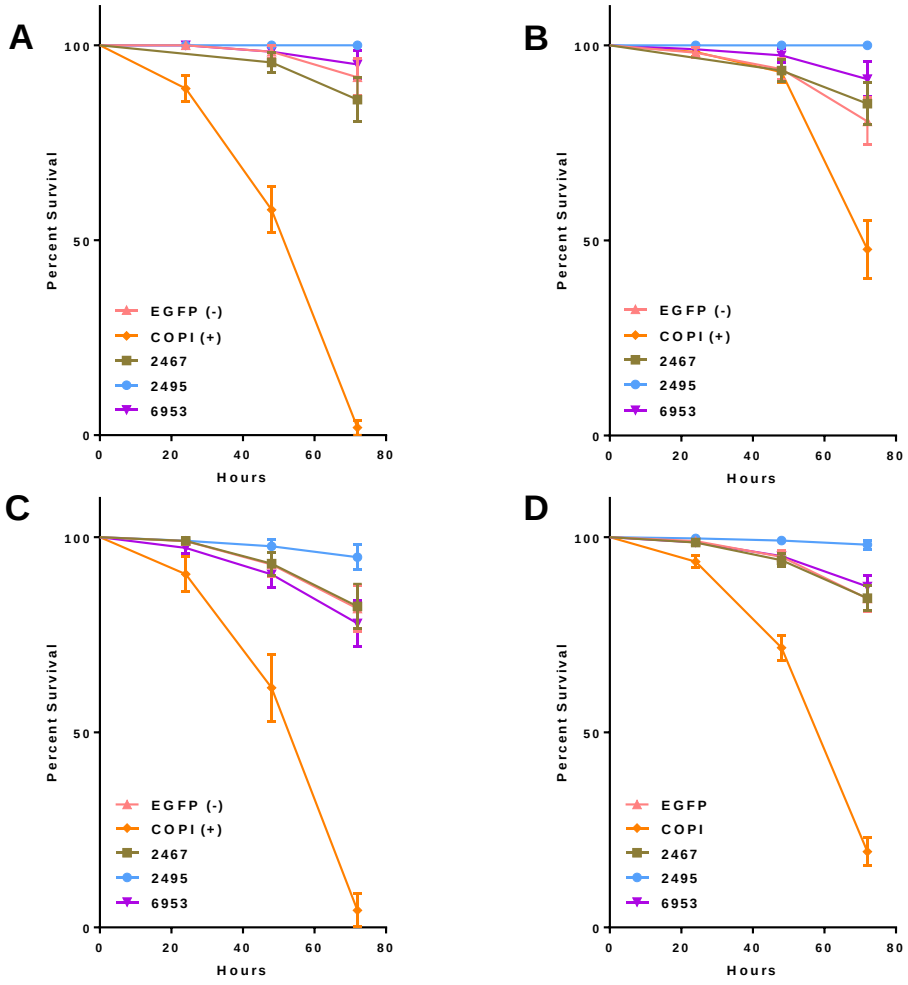

Figure 25. Survivorship curves for single gene-target RNAi-mediated knockdown in *Aedes aegypti* post blood meal.
Survivorship was recorded at 24, 48 and 72 hr PBM. EGFP and COPI (gamma subunit) were used as negative and positive controls, respectively. Based on the Log-rank (Mantel-Cox) test, we report a significant difference in survival curves for single gene-target replicates 1, 2, 3 and when all three replicates were pooled together ($p<0.0001$ for all replicates and pooled). Error bars indicate mean ± standard deviation. (**A**), (**B**) and (**C**) are representative of replicates 1, 2 and 3, respectively while (**D**) represents pooled replicates.

Survivorship was also determined 24, 48 and 72 hr PBM for multiplex RNAi-mediated knockdown experiments. Based on the Log-rank (Mantel-Cox) test, we report a significant difference in survival curves for replicates 1 ($p = 0.0236$) and 2 ($p = 0.0223$) (Fig. 26 A and B).

We report no significant difference in survival curves for replicate 3, as this may be associated with the extensive mortality seen in our control group (Fig. 26C). Similarly, when all three replicates were pooled, we report no significant difference in survival curves (Fig. 26D). While for replicate 1 we reported 88%, 96% and 79% knockdown efficiency for multiplex injections (AAEL002467, AAEL002495, AAEL006953, respectively), survivorship remained greater than 80% through 72 hr PBM (Fig. 26A). Likewise, for replicate 2 we reported 76%, 67% and 79% knockdown efficiency for multiplex injections (AAEL002467, AAEL002495, AAEL006953, respectively), we again observed survivorship greater than 80% through 72 hr PBM (Fig. 26B). Taken together, our results suggest knockdown of these three PM proteins singularly or in tandem do not greatly affect adult *Aedes aegypti* female survivorship after a blood meal. Therefore, we sought to determine if transcript knockdown was associated with a physiological effect on reproduction (fecundity and fertility).

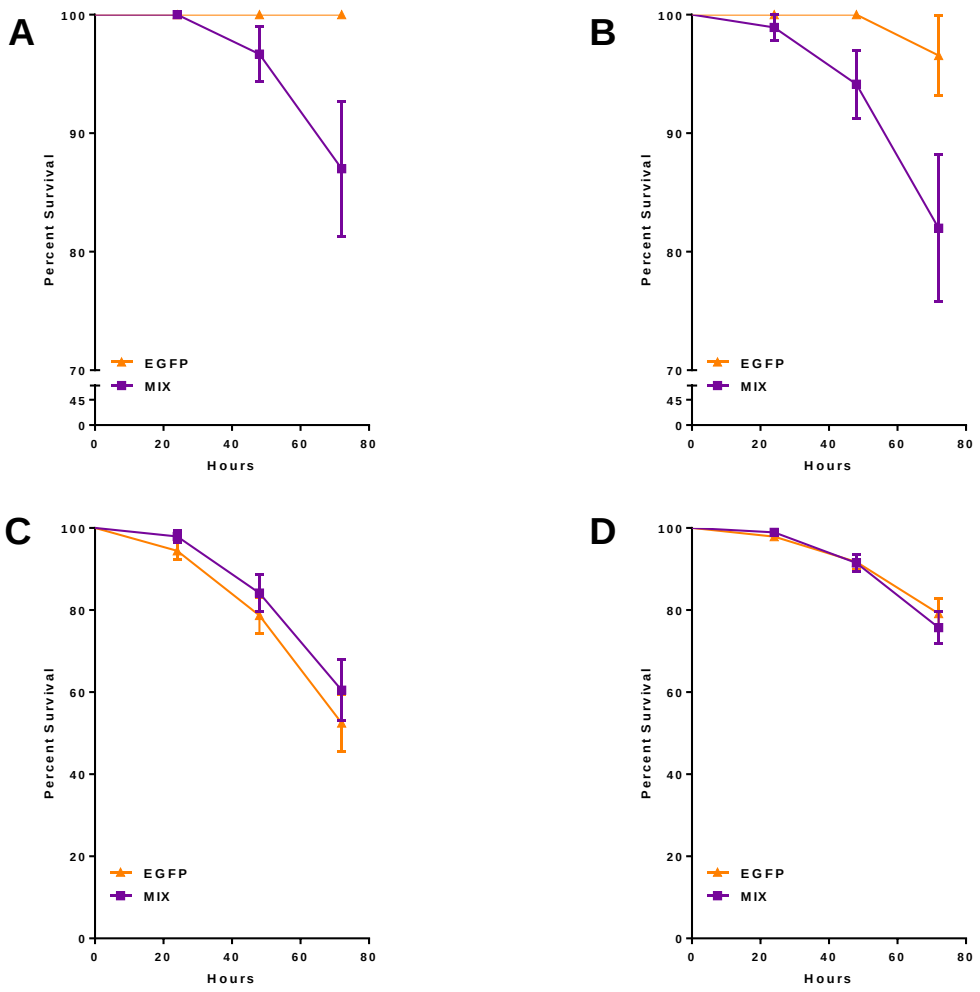

Figure 26. Survivorship curves for multiplex gene-target RNAi-mediated knockdown in *Aedes aegypti* post blood meal.
Survivorship was recorded at 24, 48 and 72 hr PBM. Only EGFP negative control was used for multiplex gene-target RNAi-mediated knockdown experiments. Based on the Log-rank (Mantel-Cox) test, we report a significant difference in survival curves for replicate 1 ($p = 0.0236$) and 2 ($p = 0.0223$). Error bars indicate mean ± standard deviation. (**A**), (**B**) and (**C**) are representative of replicates 1, 2 and 3, respectively while (**D**) represents pooled replicates.

As detailed in Figure 20, we determined the effect of knockdown on each peritrophin singularly (single gene-target dsRNA injections) and collectively (multiplex dsRNA injections) on the number of embryos deposited per female (Fig. 27 and 30, respectively), number of larvae per female (Fig. 28 and 31, respectively) and overall fertility [# larvae/ # embryos; hatch rate,

(Fig. 29 and 32, respectively)] for a single gonotrophic cycle. For single-gene knockdown experiments, we observed the lowest fecundity values for EGFP negative control (Fig. 27D). For pooled replicates (Fig 27D), fecundity was not significantly different when compared to EGFP following knockdown of AAEL002467. However, pooled fecundity for AAEL002495 and AAEL006953 knockdown mosquitoes were significantly different from EGFP, but not AAEL002467 (Fig. 27D). Concerning number of larvae hatched/female, only replicate 2 showed significant difference in medians between the treatments (Fig. 28B). However, when all replicated were pooled together, we report no significant difference in median number of larvae hatched/female, with median values being approximately 50 larvae hatched/female (Fig. 28D). Interestingly, hatch rates were higher for EGFP when compared to hatch rates for single-gene-target dsRNA injected females (Fig. 29D). These results suggest that while more embryos were laid for the respective gene-targets (AAEL002467, AAEL002495 and AAEL006953) when compared to EGFP negative control, the embryos may have not been viable (lacking proper nutrients for embryogenesis).

We next sought to determine the effect of multiplex RNAi-mediated knockdown of known and putative PM peritrophins on fecundity (embryos per female) (Fig. 30), larval counts (Fig. 31) and fertility (hatch rate) (Fig. 32). To our surprise, knockdown of all three gene-targets in tandem did not result in a significant difference with regards to fecundity (Fig. 30), larval counts (Fig. 31) or hatch rates (Fig. 32). This suggests that these genes either do not play a critical role in protecting the mosquito from toxicity associated with a blood meal, or that other pathways can compensate for their reduction during digestion [19, 66, 135, 136]. See Figure 4 (Chapter 1) for detailed information on various pathways at play after blood meal feeding.

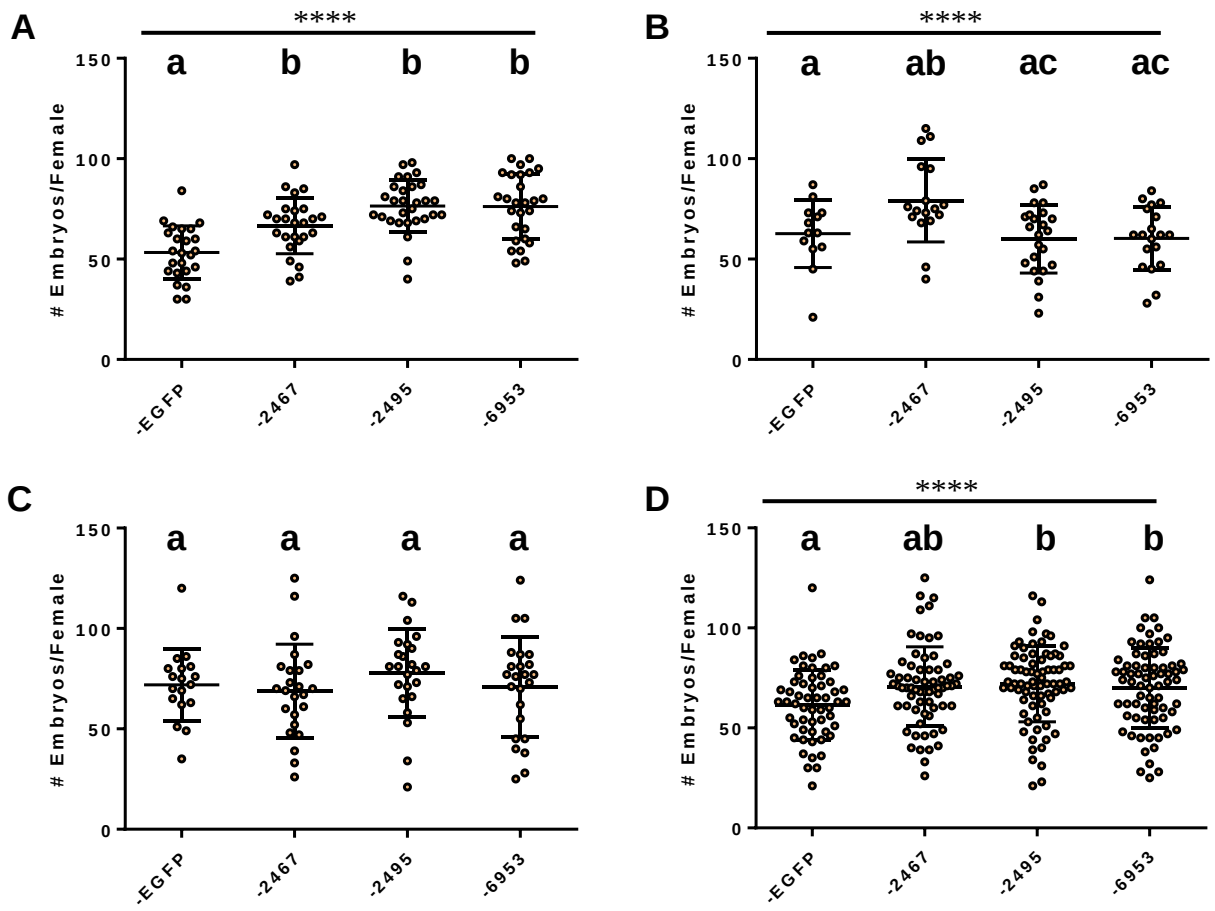

Figure 27. Fecundity (#embryos/female) for single gene-target RNAi-mediated knockdown in *Aedes aegypti* post blood meal.

Fecundity was determined for each gene-target **(A)** replicate 1, **(B)** replicate 2**, (C)** replicate 3 and **(D)** total from all 3 replicates. Each dot represents the number of embryos per female. Error bars indicate median ± standard deviation. Medians were significantly different for replicate 1, 2 and total fecundity analyses (Kruskal-Wallis test, **** indicates $p < 0.05$). Post hoc Dunn's multiple comparison test was conducted for each replicate and total embryo counts.

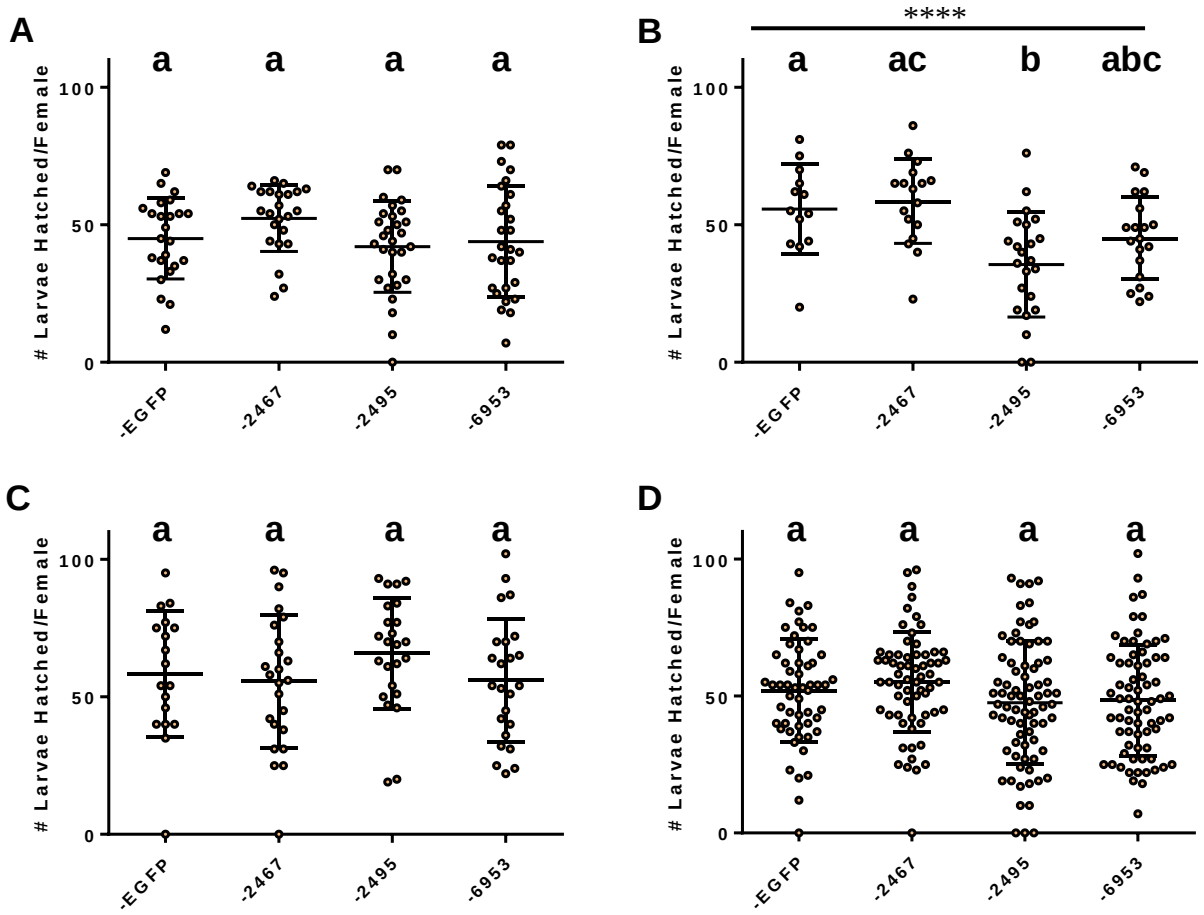

Figure 28. Number of larvae hatched per female for single gene-target RNAi-mediated knockdown in *Aedes aegypti* post blood meal.

Larval hatch counts were determined for each gene-target **(A)** replicate 1, **(B)** replicate 2, **(C)** replicate 3 and **(D)** total from all 3 replicates. Each dot represents the number of larvae hatched per female. Error bars indicate median ± standard deviation. Medians were significantly different for replicate 2 (Kruskal-Wallis test, **** indicates $p < 0.05$). Post hoc Dunn's multiple comparison test was conducted for each replicate and total larval hatch counts.

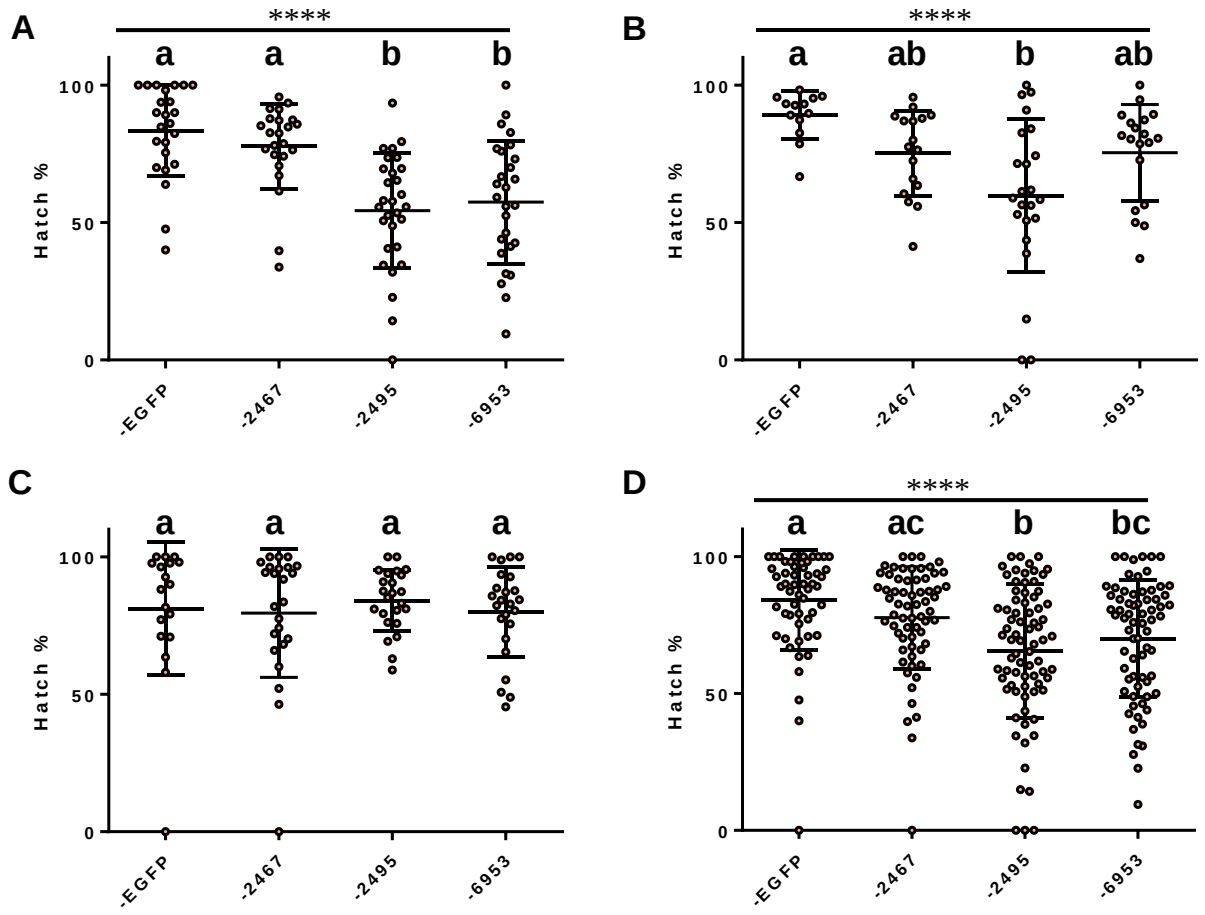

Figure 29. Fertility (hatch rate) for single gene-target RNAi-mediated knockdown in *Aedes aegypti* post blood meal.

Hatch rates were determined for each gene-target (**A**) replicate 1, (**B**) replicate 2, (**C**) replicate 3 and (**D**) total from all 3 replicates. Each dot represents the hatch percent per female. Error bars indicate median ± standard deviation. Medians were significantly different for replicates 1, 2 and total from all 3 replicates (Kruskal-Wallis test, **** indicates $p < 0.05$). Post hoc Dunn's multiple comparison test was conducted for each replicate and total hatch rate.

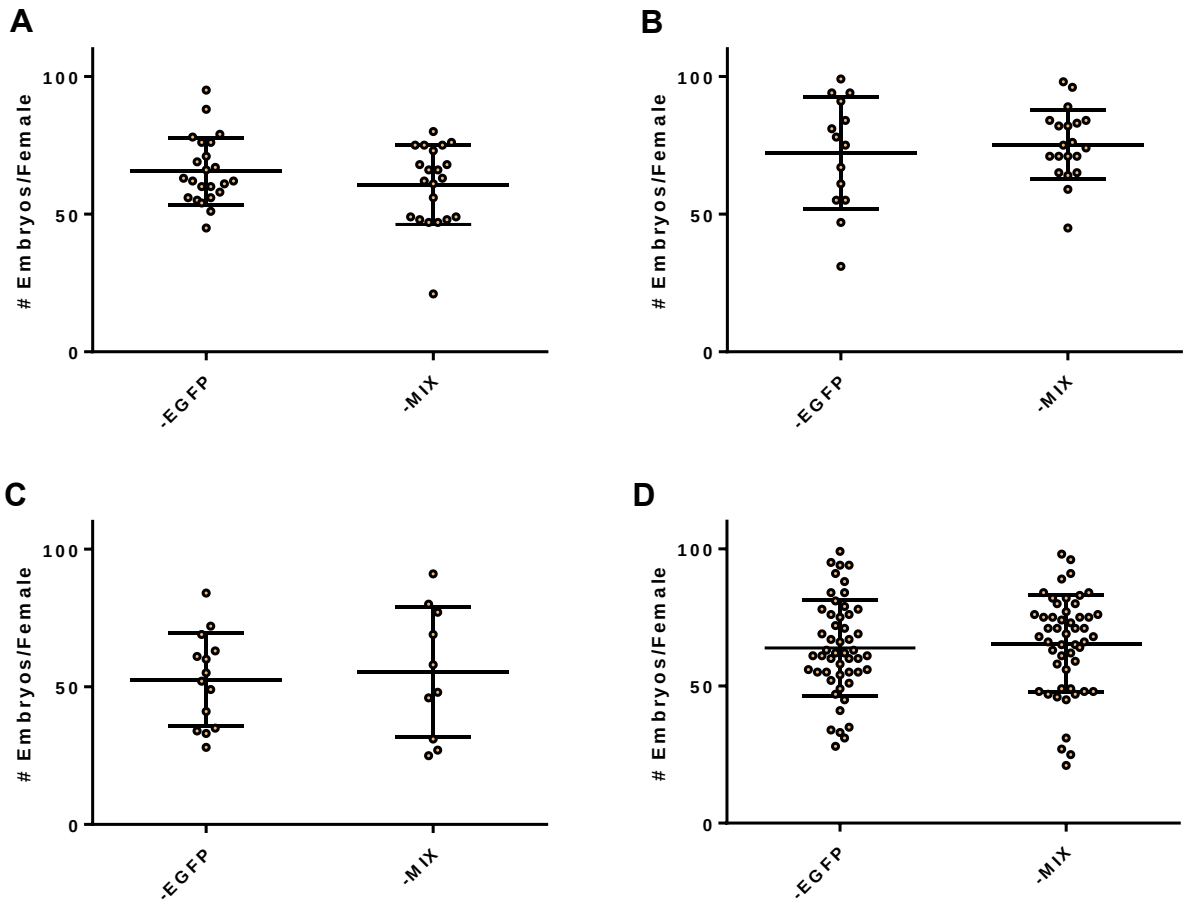

Figure 30. Fecundity (#embryos/female) for multiplex RNAi-mediated knockdown in *Aedes aegypti* post blood meal.
Fecundity was determined for multiplex (MIX) knockdown (**A**) replicate 1, (**B**) replicate 2, (**C**) replicate 3 and (**D**) total from all 3 replicates. Each dot represents the number of embryos per female. Error bars indicate median ± standard deviation. Number of embryos per female medians were not significantly different for EGFP (negative control) and MIX for each replicate or total for all 3 replicates (Mann–Whitney–Wilcoxon two-tailed test).

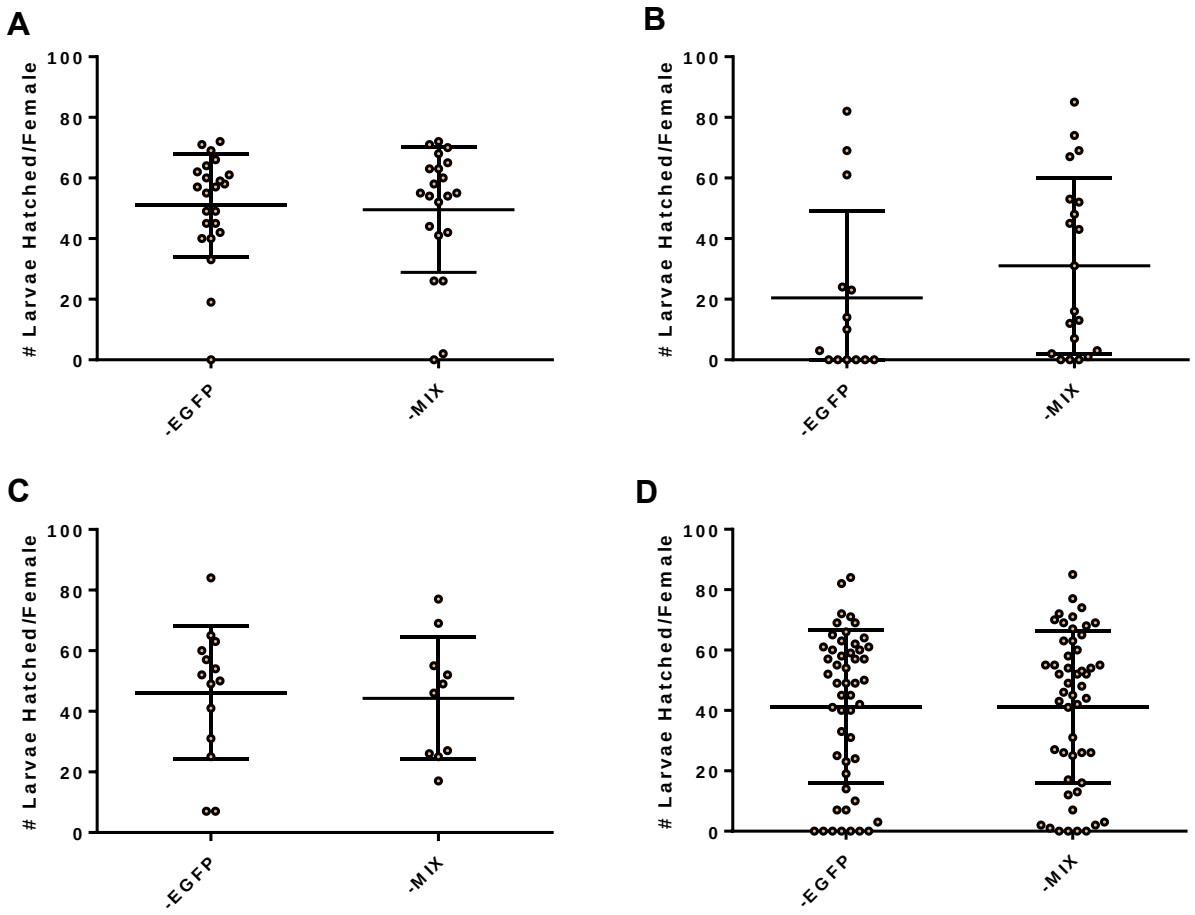

Figure 31. Number of larvae hatched per female for multiplex RNAi-mediated knockdown in *Aedes aegypti* post blood meal.
Larval hatch counts were determined for multiplex (MIX) knockdown (**A**) replicate 1, (**B**) replicate 2, (**C**) replicate 3 and (**D**) total from all 3 replicates. Each dot represents the number of larvae hatched per female. Error bars indicate median ± standard deviation. Number of larvae hatched per female medians were not significantly different for EGFP (negative control) and MIX for each replicate or total for all 3 replicates (Mann–Whitney–Wilcoxon two-tailed test).

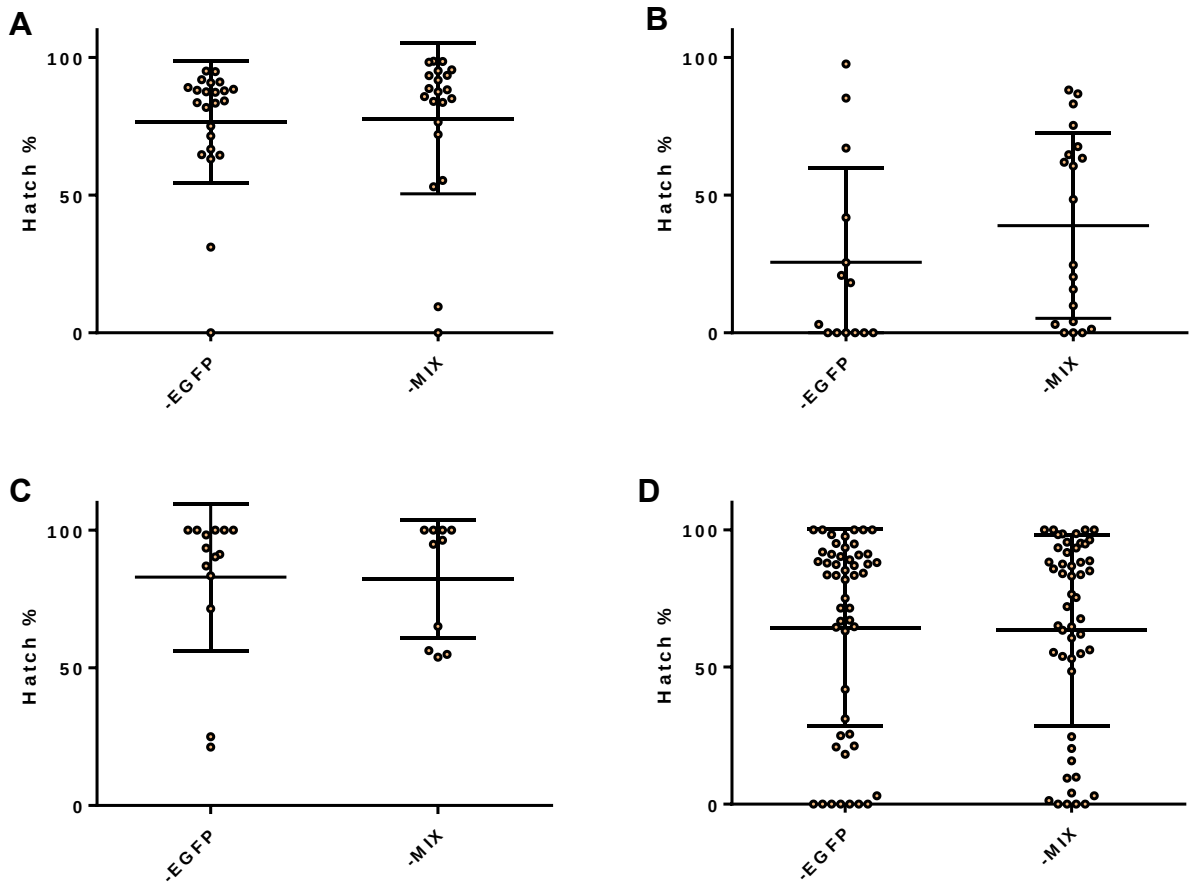

Figure 32. Fertility (hatch rate) for multiplex RNAi-mediated knockdown in *Aedes aegypti* post blood meal.
Hatch rates were determined for multiplex (MIX) knockdown (**A**) replicate 1, (**B**) replicate 2, (**C**) replicate 3 and (**D**) total from all 3 replicates. Each dot represents the hatch percent per female. Error bars indicate median ± standard deviation. Hatch rate per female medians were not significantly different for EGFP (negative control) and MIX for each replicate or total for all 3 replicates (Mann–Whitney–Wilcoxon two-tailed test).

4.3.2.3 Determination of midgut catalase and ferritin expression

Oliveira et al. (2017) previously determined that catalase mRNA expression reaches its maximum level (6-fold increase) at 24 hr through 48 hr PBM [19]. Therefore, we sought to determine if mRNA expression for the antioxidant catalase would be altered due to knockdown of single PM peritrophins AAEL002467, AAEL002495 or AAEL006953. However, we

observed no significant difference in catalase expression when each gene was silenced compared to EGFP (negative control) (Fig. 33). Likewise, we observed no significant difference in catalase expression following multiplex knockdown of PM peritrophins relative EGFP (Fig. 34A). These results suggest that changes in catalase mRNA expression is not compensating for the loss of functionality of known PM peritrophins individually (AAEL002467) or when all the PM proteins are silenced in tandem, suggesting that the overall free peroxide levels in the gut lumen may be unchanged.

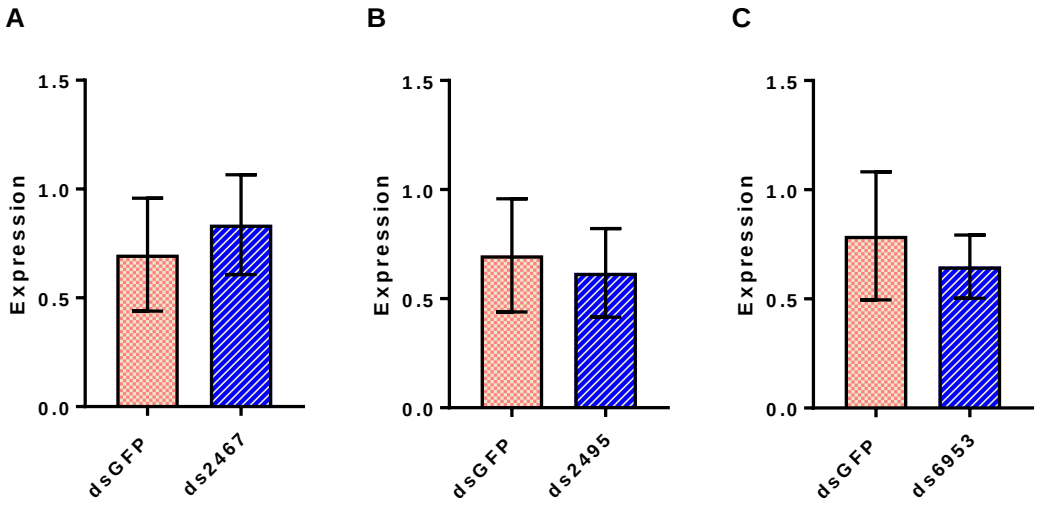

Figure 33. Catalase expression for single gene-target RNAi-mediated knockdown of known and putative PM peritrophins in *Aedes aegypti* post blood meal.
Catalase mRNA expression was determined 24 hr PBM for RNAi-mediated knockdown of (**A**) AAEL002467 (**B**) AAEL0024952 and (**C**) AAEL006953. Error bars indicate median ± standard deviation. Medians were not significantly different for EGFP (negative control) and each gene-target based on Mann–Whitney–Wilcoxon two-tailed test.

We reasoned that an increase in heme importation and catabolism might also prevent the accumulation of reactive oxygen species and hence the need for additional catalase activity. A byproduct of heme catabolism is free iron that can result in intracellular oxidative stress. Previous literature has shown that in mosquitoes and other bloodfeeding arthropods, ferritin is particularly important due to the large influx of iron obtained during a blood meal [135-137]. More specifically, in *Ae. aegypti*, both ferritin subunits, HCH and LCH, increase in expression after an iron overload or a blood meal, indicating that ferritin may serve as a cytotoxic protector [135, 136]. Therefore, we also sought to determine if mRNA expression for ferritin would be altered due to loss of single or multiplex RNA-mediated knockdown of the known and putative PM peritrophins AAEL002467, AAEL002495 or AAEL006953. However, we observed no significant difference in ferritin expression when each gene target was silenced individually (Fig. 35) or multiplexed (Fig. 34) as compared to dsEGFP (negative control) (Fig. 34 and 35). Overall, these results suggest no evidence of physiological compensation following knockdown of these integral PM proteins.

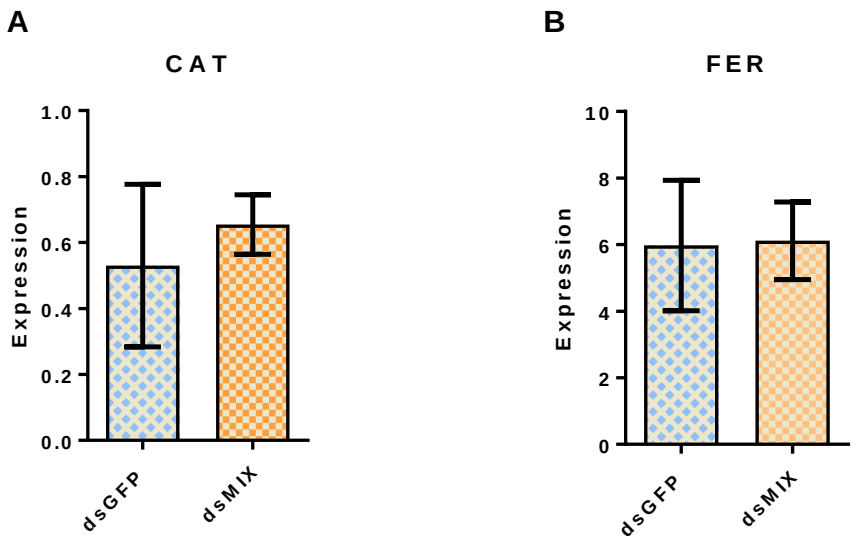

Figure 34. Catalase and Ferritin expression for multiplex RNAi-mediated knockdown of known and putative PM peritrophins in *Aedes aegypti* post blood meal.
Catalase (**A**) and ferritin (**B**) mRNA expression was determined 24 hr PBM for multiplex (MIX) RNAi-mediated knockdown of AAEL002467, AAEL0024952 and AAEL006953. Error bars indicate median ± standard deviation. Median was not significantly different for EGFP (negative control) and multiplex RNAi-mediated knockdown experiments based on Mann–Whitney–Wilcoxon two-tailed test.

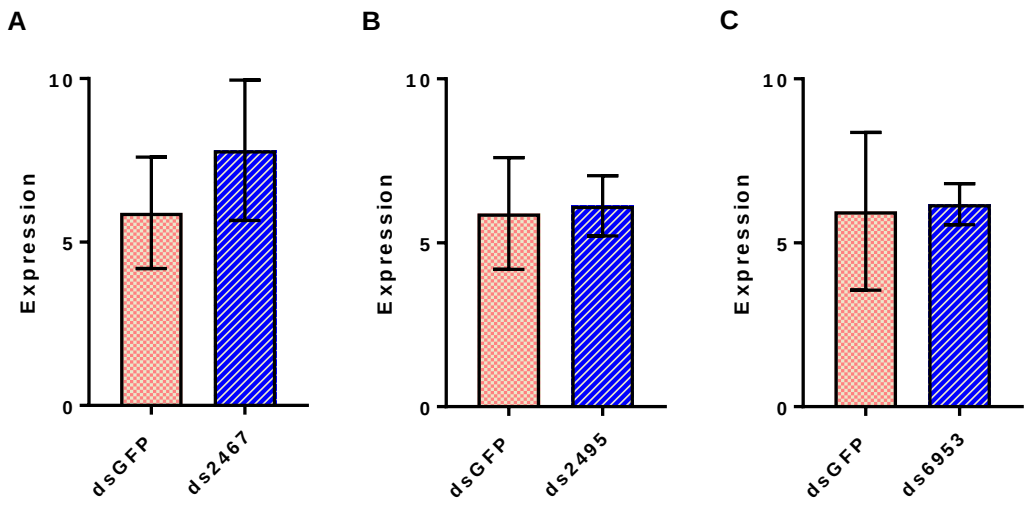

Figure 35. Ferritin expression for single gene-target RNAi-mediated knockdown of known and putative PM peritrophins in *Aedes aegypti* post blood meal.
Ferritin mRNA expression was determined 24 hr PBM for RNAi-mediated knockdown of (**A**) AAEL002467 (**B**) AAEL0024952 and (**C**) AAEL006953. Error bars indicate median ± standard deviation. Medians were not significantly different for EGFP (negative control) and each gene-target based on Mann–Whitney–Wilcoxon two-tailed test.

4.4 Discussion

Previous literature suggests that the *Aedes aegypti* female midgut PM- an acellular sheath comprised of proteins, proteoglycans and chitin fibrils, may contain 20-40 major proteins [59]. As part of our Chapter 2 adult female early midgut PM proteomic analysis, we identified 474 unique proteins, three of which were the two known (AeIMUC1 and AeAper50) and one novel (AAEL006953) PM peritrophins [49, 67, 181, 199]. Subsequently, in our adult female *Ae. aegypti* midgut PM heme-enriched proteomic analysis, we recovered 23 heme-enriched proteins. However, up until this point, no *in vivo* studies have determined the physiological role of any PM peritrophin in adult female *Ae. aegypti*. In accordance, we conducted gene expression profiling and RNAi-mediated knockdown experiments for the known and putative PM peritrophins.

Our gene expression profiling data confirm the findings of Rayms-Keller et al. (2000), as the known PM peritrophin AeIMUC1 is expressed prior to bloodmeal feeding. However, in contrast to Shao et al. (2005), we found AeAper50 (AAEL002467) expression prior to bloodmeal feeding (Fig. 21 and 22A). It is important to note that these authors used Northern blot analysis, while we used a more sensitive approach- quantitative PCR [218]. We also found that the putative PM peritrophin- AAEL006953 is expressed prior to bloodfeeding. Strikingly, AAEL002467 (AeAper50) mRNA expression rapidly increases PBM and reaches maximum (300X compared to rpS7) expression by 4 hours PBM (Fig. 21). Interestingly, this protein is orthologous (1 to many) to the *Anopheles gambiae* Adult Peritrophin 1 (AgAper1), which was the most abundant chitin-binding domain (CBD) protein identified in the *An. gambiae* midgut PM proteome [53]. More recently, RNAi-mediated knockdown of *An. gambiae* AgAper1 was used to determine its role in midgut epithelium response to microbiota in adult *Anopheles coluzzii* [69]. Interestingly, knockdown of AgAper1 resulted in an increased immune response and translocation of bacteria from family *Enterobacteriaceae* from the gut lumen into the body cavity. These recent findings suggest that while no phenotypic effects (fecundity, larval counts and fertility) were observed for AAEL002467 (AeAper50) knockdown mosquitoes, further studies are needed to determine if there are changes in the microbiome and/or immune response in adult *Ae. aegypti* associated with loss of function for AAEL002467 via RNAi-mediated knockdown. The possibility of a mounted immune response would further provide evidence to explain the high survivorship seen for AAEL002467 (>80% survivorship) after single gene-target knockdown (Fig. 25).

Previously, Oliveira et al. (2011) showed an inverse relationship between the abundance of adult *Ae. aegypti* gut microbes (microbiota) and reactive oxygen species (ROSs) after a blood

meal [15]. Through does-dependent experiments with heme (diluted in sucrose), the authors found a decrease in ROSs levels in the midgut of adult *Ae. aegypti* and increased intestinal microbiota [15]. This would suggest that if PM heme-binding proteins are not present to properly bind heme, this provides an advantageous environment for gut microbes to sequester the free heme. Given that Oliveira et al. (2011) found the highest levels of cultivable bacteria 24 - 36 hr PBM, which is also the peak of blood meal digestion, further studies using bacterial 16*S* ribosomal RNA sequencing are needed to determine if RNAi-mediated knockdown of PM peritrophins are associated with increased gut microbiome or changes in its composition. Ultimately, this would suggest decreased opportunities for blood meal heme associated toxicity among dsRNA knockdown mosquitoes and potentially higher survivorship (as we reported in this study). Likewise, in mosquitoes and other bloodfeeding arthropods, ferritin is particularly important to sequester the large influx of iron obtained during a blood meal. In *Ae. aegypti*, both ferritin subunits, HCH and LCH, increase in expression after an iron overload or a blood meal, indicating that ferritin may serve as a cytotoxic protector [135, 136]. However, as part of our study, we did not observe a significant increase in ferritin mRNA expression following knockdown of the three peritrophin genes. This is consistent with an interpretation where an increase in free blood meal heme may be sequestered by midgut bacteria and never transported to the midgut for degradation by heme oxygenase (Fig. 4). Likewise, while the PM serves as a protective barrier separating the blood bolus components from midgut epithelium [219], the antioxidant enzyme catalase also plays a role in avoidance of oxidative stress after a blood meal [19]. Oliveira et al. (2017) found catalase mRNA expression maximum levels at 24 hours PBM, when blood meal digestion is also at its maximum. This led us to question and hypothesize that increased catalase levels seen 24 hr PBM for AAEL00246 (Fig. 33A) and multiplex knockdown

(Fig. 34A) mosquitoes, may potentially be a compensation mechanism to avoid oxidative stress. However, additional biological replicates containing more gene-specific or multiplex RNAi-mediated knockdown midgets are needed to accurately determine if catalase is compensating for the loss of functionality of AAEL00246 (AeAper50) singularly or when multiplexed with known (AAEL002495) and putative (AAEL006953) PM peritrophins.

As detailed in our Chapter 1 literature review, *Ae. aegypti* and other hematophagous arthropods have deployed a number of defenses into the gut lumen (extracellular) as well as in the cytoplasm of midgut epithelial cells (intracellular) to avoid a milieu prone to oxidative stress [66]. This study is the first to provide a detailed gene expression profile for AAEL002467, AAEL002495 and AAEL006953. While we did not observe a robust phenotypic consequence following RNAi-mediated knockdown of the known and putative PM peritrophins, we provide foundational evidence that many players have evolutionarily evolved to ensure a favorable environment for adult *Ae. aegypti* after bloodfeeding. We note in particular that while we achieved knockdown rates of 60-90%, the remaining transcripts for AAEL002467 and AAE002495 were still more abundant that the comparator ribosomal RNA, indicating that sufficient functional protein may still be produced. The generation of CRISPER/Cas9 knockout mosquitoes with complete loss-of-function genotypes of the known or putative PM peritrophins may be required to more firmly establish any phenotypic consequences concerning catalase compensation, midgut bacteria sequestration of free blood meal heme and potential effects. Overall, understanding the PM and its components has the potential to provide novel targets for molecular based vector and vector-borne disease control, as well as understanding the adaptations required for efficient blood digestion/detoxification.

CHAPTER V

CONCLUSION

The evolutionary adaptation of feeding on vertebrate blood has independently arisen in more than 14,000 insect and arachnid species [1], however this potentiates a toxic environment in hematophagous arthropods. *Aedes aegypti* have evolved the midgut peritrophic matrix (PM), which serves as a protective barrier separating the single cell-layered midgut epithelium from pathogens, abrasion, and toxic compounds [51, 60, 61, 69]. The type I PM is comprised of proteins, proteoglycans and chitin fibrils [50, 63], with PM proteins commonly referred to as peritrophins. An initial discovery study that investigated the PM protein composition suggested the adult female *Ae. aegypti* PM may contain 20-40 integral proteins [59]. However, only two *Ae. aegypti* integral PM proteins have been characterized in detail: intestinal mucin 1 (AeIMUC1) [67] and adult peritrophin 50 (AeAper50) [49]. Pascoa et al. (2002) first demonstrated heme-binding capacity for the adult *Ae. aegypti* PM [63], and by 48 hr PBM (end of blood meal digestion), the authors provided evidence supporting the binding of the adult *Ae. aegypti* PM to 18 nmol of heme (amount of heme in a normal blood meal) [63]. Interestingly, Rayms-Keller et al. (2000) reported AeIMUC1 expression in metal fed adult females and blood-fed adult females [67]. Six year later, Devenport et al. (2006), demonstrated that: 1) AeIMUC1 could bind chitin and heme, 2) confirmed that the 3 CBDs of AeIMUC1 facilitated heme-binding through conserved heme regulatory motifs (cysteine-proline dipeptides), and 3) suggested that this PM peritrophin may be an important player in blood meal detoxification [199].

With the above knowledge, we sought to better investigate adult female *Ae. aegypti* midgut PM protein composition. We first conducted a LC-MS based proteomic analysis, and

identified a total of 474 unique proteins [181]. More specifically, we recovered 115 proteins containing predicted N-secretory signal peptide sequence [181]. As expected, the largest majority of the secreted proteins without transmembrane domains were associated with catalytic activity, and interestingly six proteins were of unknown function [181]. While we were surprised to isolate salivary proteins (most abundant protein being of salivary origin), we did recover the two known peritrophins- AeIMUC1 (2 peptides) and AeAper50 (2 peptides). Likewise, we identified two additional peritrophins, AAEL004798 and AAEL006953 (based on structural similarity to know PM peritrophins). However, the new genome assembly now considers AAEL004798 an allelic form of the known *Ae. aegypti* PM peritrophin AeIMUC1 (AAEL002495). Therefore, our Chapter 2 study resulted in two known (AAEL002495/AAEL004798 and AAEL002467) and one putative (AAEL006953) PM peritrophin for the early (6 hours) adult female *Ae. aegypti* midgut PM [181].

While our Chapter 2 study provided a snapshot into the adult female *Ae. aegypti* PM composition 6 hr post artificial meal feeding, we recognized the need for an unbiased forward genetics approach to investigate heme-binding proteins present in the adult female *Ae. aegypti* midgut PM at a physiologically relevant time point. While our initial strides attempted *in vivo* heme-binding experiments through artificial meal feeding enriched with heme, our inability to keep heme resuspended and lack of successful feeding rates, resulted in our utilization of an *in vitro* heme-enrichment proteomic analysis (Chapter 3). Through a modified in-gel digestion procedure to increase sample recovery, we isolated 160 *Ae. aegypti* PM proteins identified by two or more unique peptides 12 hr post artificial meal feeding. In total, we isolated 23 proteins in our heme-enriched treatment 2 (T2). While we were surprised that neither of the two known *Ae. aegypti* PM proteins (AeIMUC1 or AeAper50) were isolated in T1 or T2 of this proteomic

analysis, we were equally surprised that the most abundant protein found in T2 and second most abundant protein found in T1 was the major hemolymph lipophorin- AAEL009955 [207, 208]. The overwhelming abundance of this protein in our hemin-enriched T2 (98 peptides) led us to the possibility that lipophorin may directly bind and shuttle heme from the gut to the developing ovaries. This is similar to the heme shuttling process seen for the *R. microplus* cattle tick lipoprotein- heme lipoprotein (HeLp) [163]. Likewise, in both T1 and T2 samples, we isolated a Class B scavenger receptor (AAEL009432), which to our knowledge had not been shown to bind heme, and based on compiled transcriptomics data, showed highest expression in bloodfed females 1 day post bloodfeeding [205]. While the literature shows this protein to be involved in immunity in *Anopheles gambiae* [204], the pronounced expression in bloodfed *Ae. aegypti* mosquitoes only at 1 day post injection with or without dengue virus led us to speculate that this scavenger protein may bind heme (at its peak period in the midgut lumen) and assist in its import into the intracellular space. Similarly, for T2 we recovered an ATP-binding cassette sub-family A member- AAEL012702 (3 peptides). Working in concert, possibly, the scavenger protein could bind heme to be transported into the cell by the ATP-binding cassette protein. While highly speculative, this proposed novel mechanism of heme transport in adult female *Ae. aegypti* parallels the heme transport mechanism seen in the midgut cells of *R. microplus* ticks [83]. However further studies are needed to investigate this proposed heme transport mechanism in *Ae. aegypti*.

Although we did not successfully recover the two known *Ae. aegypti* PM proteins (AeIMUC1 or AeAper50) in our Chapter 3 heme-enrichment midgut PM proteomic analysis, comprehensive gene expression profiling as part of Chapter 4 confirmed that the two known and novel midgut PM proteins are expressed in non-bloodfed female mosquitoes (Fig. 21). We also

determined that AeAper50 expression reached 300x that of the reference gene within just 4 hr of blood feeding (Fig. 21). Expression profiling data suggested the two known PM peritrophins may in fact be important for blood meal digestion, and avoidance of heme-associated toxicity. However, RNAi-mediated knockdown experiments did not provide evidence to support significant adverse physiological effects (increased mortality and decreased hatch rate) with single or multiplex knockdown (Fig. 27-32). While unable to determine a phenotypic effect, we next investigated whether other known molecules involved in the avoidance of oxidative damage post blood meal feeding (catalase and ferritin) [19, 135, 136] might display altered expression due to knockdown of the known and putative PM proteins. However, lack of significant changes in expression for either of these proteins provide evidence supporting that hematophagous arthropods have evolved numerous sophisticated mechanisms (intracellularly and extracellularly) to avoid oxidative damage after a blood meal [66].

Overall, this body of work has shed light on additional studies that are needed to better connect the various players (known and unknown) which have successfully allowed *Ae. aegypti* and other mosquitoes to hone their respective bloodfeeding processes. More generally, we are optimistic that CRISPER/Cas9 knockout mosquitoes with complete loss-of-function genotypes have the potential to level the playing field and allow for more conclusive insight regarding this complex feeding and digestive process in the *Ae. aegypti* and other mosquitoes. In closing, further studies are needed to continue advancing this areas of vector biology, as understanding the PM and its components has the potential to provide novel targets for molecular based vector and vector-borne disease control, as well as understanding the adaptations required for efficient blood digestion/detoxification.

REFERENCES

1. Graça-Souza, A.V., et al., *Adaptations against heme toxicity in blood-feeding arthropods.* Insect Biochemistry and Molecular Biology, 2006. **36**(4): p. 322-335.
2. Barillas-Mury, C. and M.A. Wells, *Cloning and sequencing of the blood meal-induced late trypsin gene from the mosquito* Aedes aegypti *and characterization of the upstream regulatory region.* Insect Molecular Biology, 1993. **2**(1): p. 7-12.
3. Jiang, Q., et al., *cDNA cloning and pattern of expression of an adult, female-specific chymotrypsin from* Aedes aegypti *midgut.* Insect Biochemistry and Molecular Biology, 1997. **27**(4): p. 283-289.
4. Edwards, M.J., et al., *Characterization of a carboxypeptidase A gene from the mosquito,* Aedes aegypti. Insect Molecular Biology, 2000. **9**(1): p. 33-38.
5. Brackney, D.E., et al., *Expression profiling and comparative analyses of seven midgut serine proteases from the yellow fever mosquito,* Aedes aegypti. Journal of Insect Physiology, 2010. **56**(7): p. 736-744.
6. Marquardt, W.C. and B.C. Kondratieff, *Biology of disease vectors*. 2nd ed. 2005, Burlington, MA: Elsevier Academic Press. xxiii, 785 p.
7. Felton, G.W. and C.B. Summers, *Antioxidant systems in insects.* Archives of Insect Biochemistry and Physiology, 1995. **29**(2): p. 187-197.
8. Champion, C.J. and J. Xu, *The impact of metagenomic interplay on the mosquito redox homeostasis.* Free Radical Biology and Medicine, 2017. **105**: p. 79-85.
9. Betteridge, D.J., *What is oxidative stress?* Metabolism, 2000. **49**(2, Supplement 1): p. 3-8.

10. Chaitanya, R.K., K. Shashank, and P. Sridevi, *Oxidative stress in invertebrate systems*. Free Radicals and Diseases, ed. R. Ahmad. 2016, Rijeka: Intech Europe. 19-36.

11. Ryter, S.W. and R.M. Tyrrell, *The heme synthesis and degradation pathways: role in oxidant sensitivity: Heme oxygenase has both pro- and antioxidant properties.* Free Radical Biology and Medicine, 2000. **28**(2): p. 289-309.

12. Tappel, A.L., *Unsaturated lipid oxidation catalyzed by hematin compounds.* Journal of Biological Chemistry, 1955. **217**: p. 721-733.

13. Vincent, S.H., et al., *The influence of heme-binding proteins in heme-catalyzed oxidations.* Archives of biochemistry and biophysics, 1988. **265**(2): p. 539-550.

14. Aft, R.L. and G.C. Mueller, *Hemin-mediated oxidative degradation of proteins.* Journal of Biological Chemistry, 1984. **259**(1): p. 301-305.

15. Oliveira, J.H., et al., *Blood meal-derived heme decreases ROS levels in the midgut of* Aedes aegypti *and allows proliferation of intestinal microbiota.* PLoS Pathog, 2011. **7**(3): p. e1001320.

16. Oliveira, P.L. and M.F. Oliveira, *Vampires, pasteur and reactive oxygen species.* FEBS Letters, 2002. **525**(1-3): p. 3-6.

17. Gonçalves, R.L.S., et al., *Blood-Feeding Induces Reversible Functional Changes in Flight Muscle Mitochondria of* Aedes aegypti *Mosquito.* PLOS ONE, 2009. **4**(11): p. e7854.

18. Paes, M.C., M.B. Oliveira, and P.L. Oliveira, *Hydrogen peroxide detoxification in the midgut of the blood-sucking insect,* Rhodnius prolixus. Archives of Insect Biochemistry and Physiology, 2001. **48**(2): p. 63-71.

19. Oliveira, J.H.M., et al., *Catalase protects* Aedes aegypti *from oxidative stress and increases midgut infection prevalence of Dengue but not Zika.* PLOS Neglected Tropical Diseases, 2017. **11**(4): p. e0005525.

20. DeJong, R.J., et al., *Reactive oxygen species detoxification by catalase is a major determinant of fecundity in the mosquito* Anopheles gambiae. Proceedings of the National Academy of Sciences of the United States of America, 2007. **104**(7): p. 2121-2126.

21. Diaz-Albiter, H., et al., *Reactive oxygen species scavenging by catalase is important for female* Lutzomyia longipalpis *fecundity and mortality.* PLOS ONE, 2011. **6**(3): p. e17486.

22. Freitas, D.R.J., et al., *Relationship between glutathione S-transferase, catalase, oxygen consumption, lipid peroxidation and oxidative stress in eggs and larvae of* Boophilus microplus *(Acarina: Ixodidae).* Comparative Biochemistry and Physiology Part A: Molecular & Integrative Physiology, 2007. **146**(4): p. 688-694.

23. Lumjuan, N., et al., *The* Aedes aegypti *glutathione transferase family.* Insect Biochemistry and Molecular Biology, 2007. **37**(10): p. 1026-1035.

24. Lima, V.L., et al., *The antioxidant role of xanthurenic acid in the* Aedes aegypti *midgut during digestion of a blood meal.* PLoS One, 2012. **7**(6): p. e38349.

25. Dansa-Petretski, M., et al., *Antioxidant role of* Rhodnius prolixus *heme-binding protein: protection against heme-induced lipid peroxidation.* Journal of Biological Chemistry, 1995. **270**(18): p. 10893-10896.

26. Gutiérrez-Cabrera, A.E., et al., *Origin, evolution and function of the hemipteran perimicrovillar membrane with emphasis on Reduviidae that transmit Chagas disease.* Bulletin of Entomological Research, 2015. **106**(3): p. 279-291.

27. Silva, C.P., et al., *Occurrence of midgut perimicrovillar membranes in paraneopteran insect orders with comments on their function and evolutionary significance.* Arthropod Structure & Development, 2004. **33**(2): p. 139-148.

28. Lane, N.J. and J.B. Harrison, *Unusual cell-surface modification - double plasma-membrane.* Journal of Cell Science, 1979. **39**(OCT): p. 355-372.

29. Oliveira, M.F., et al., *Haem detoxification by an insect.* Nature, 1999. **400**(6744): p. 517-518.

30. Oliveira, M.F., et al., *Haemozoin formation in the midgut of the blood-sucking insect* Rhodnius prolixus. FEBS Letters, 2000. **477**(1-2): p. 95-98.

31. Silva, J.R., et al., *Perimicrovillar membranes promote hemozoin formation into* Rhodnius prolixus *midgut.* Insect Biochemistry and Molecular Biology, 2007. **37**(6): p. 523-531.

32. Pagola, S., et al., *The structure of malaria pigment β-haematin.* Nature, 2000. **404**: p. 307.

33. Oliveira, M.F., et al., *Structural and morphological characterization of hemozoin produced by* Schistosoma mansoni *and* Rhodnius prolixus. FEBS Letters, 2005. **579**(27): p. 6010-6016.

34. Lara, F.A., et al., *A new intracellular pathway of haem detoxification in the midgut of the cattle tick* Boophilus microplus*: aggregation inside a specialized organelle, the hemosome.* Journal of Experimental Biology, 2003. **206**(10): p. 1707-1715.

35. Braz, G.R.C., et al., *A missing metabolic pathway in the cattle tick* Boophilus microplus. Current Biology, 1999. **9**(13): p. 703-706.

36. Peters, W., *Peritrophic Membranes*. Vol. 130. 1992, Berlin: Springer-Verlag.

37. Rose, C., et al., *An Investigation into the protein composition of the teneral* Glossina morsitans morsitans *peritrophic matrix.* PLoS Neglected Tropical Diseases, 2014. **8**(4): p. e2691.

38. Narasimhan, S., et al., *Gut microbiota of the tick vector* Ixodes scapularis *modulate colonization of the lyme disease spirochete.* Cell host & microbe, 2014. **15**(1): p. 58-71.

39. Oliveira, M.F., et al., *Heme crystallization in the midgut of triatomine insects.* Comparative Biochemistry and Physiology C-Toxicology & Pharmacology, 2007. **146**(1-2): p. 168-174.

40. Stiebler, R., et al., *On the physico-chemical and physiological requirements of hemozoin formation promoted by perimicrovillar membranes in* Rhodnius prolixus *midgut.* Insect Biochemistry and Molecular Biology, 2010. **40**(3): p. 284-292.

41. Stiebler, R., et al., *Unsaturated glycerophospholipids mediate heme crystallization: Biological implications for hemozoin formation in the kissing bug* Rhodnius prolixus. PLOS ONE, 2014. **9**(2): p. e88976.

42. Mury, F.B., et al., *Alpha-glucosidase promotes hemozoin formation in a blood-sucking bug: An evolutionary history.* PLOS ONE, 2009. **4**(9): p. e6966.

43. Bittencourt-Cunha, P.R., et al., *Perimicrovillar membrane assembly: the fate of phospholipids synthesised by the midgut of* Rhodnius prolixus. Memórias do Instituto Oswaldo Cruz, 2013. **108**(4): p. 494-500.

44. Soares, J.B.R., et al., *Extracellular lipid droplets promote hemozoin crystallization in the gut of the blood fluke* Schistosoma mansoni. Febs Letters, 2007. **581**(9): p. 1742-1750.

45. Oliveira, M.F., et al., *Inhibition of heme aggregation by chloroquine reduces* Schistosoma mansoni *infection.* The Journal of Infectious Diseases, 2004. **190**(4): p. 843-852.

46. Lara, F.A., et al., *ATP binding cassette transporter mediates both heme and pesticide detoxification in tick midgut cells.* PLOS ONE, 2015. **10**(8): p. e0134779.

47. Shen, Z. and M. Jacobs-Lorena, *A Type I peritrophic matrix protein from the malaria vector* Anopheles gambiae *binds to chitin: Cloning, expression, and characterization.* Journal of Biological Chemistry, 1998. **273**(28): p. 17665-17670.

48. Devenport, M., et al., *Storage and secretion of Ag-Aper14, a novel peritrophic matrix protein, and Ag-Muc1 from the mosquito* Anopheles gambiae. Cell and Tissue Research, 2005. **320**(1): p. 175-185.

49. Shao, L., et al., *Identification and characterization of a novel peritrophic matrix protein, Ae-Aper50, and the microvillar membrane protein, AEG12, from the mosquito,* Aedes aegypti. Insect Biochemistry and Molecular Biology, 2005. **35**(9): p. 947-959.

50. Shao, L., M. Devenport, and M. Jacobs-Lorena, *The peritrophic matrix of hematophagous insects.* Archives of Insect Biochemistry and Physiology, 2001. **47**(2): p. 119-125.

51. Devenport, M., et al., *Identification of the* Aedes aegypti *peritrophic matrix protein AeIMUCI as a heme-binding protein†.* Biochemistry, 2006. **45**(31): p. 9540-9549.

52. Morlais, I. and D.W. Severson, *Identification of a polymorphic mucin-like gene expressed in the midgut of the mosquito,* Aedes aegypti*, using an integrated bulked segregant and differential display analysis.* Genetics, 2001. **158**(3): p. 1125-1136.

53. Dinglasan, R.R., et al., *The* Anopheles gambiae *adult midgut peritrophic matrix proteome.* Insect Biochemistry and Molecular Biology, 2009. **39**(2): p. 125-134.

54. Dimopoulos, G., et al., *Malaria infection of the mosquito* Anopheles gambiae *activates immune-responsive genes during critical transition stages of the parasite life cycle.* The EMBO Journal, 1998. **17**(21): p. 6115-6123.

55. Hao, Z. and S. Aksoy, *Proventriculus-specific cDNAs characterized from the tsetse,* Glossina morsitans morsitans. Insect Biochemistry and Molecular Biology, 2002. **32**(12): p. 1663-1671.

56. Jochim, R.C., et al., *The midgut transcriptome of* Lutzomyia longipalpis*: comparative analysis of cDNA libraries from sugar-fed, blood-fed, post-digested and* Leishmania infantum chagasi-*infected sand flies.* BMC Genomics, 2008. **9**: p. 15-15.

57. Ramalho-Ortigão, M., et al., *Exploring the midgut transcriptome of* Phlebotomus papatasi*: comparative analysis of expression profiles of sugar-fed, blood-fed and Leishmania major-infected sandflies.* BMC Genomics, 2007. **8**: p. 300-300.

58. Tellam, R.L., G. Wijffels, and P. Willadsen, *Peritrophic matrix proteins.* Insect Biochemistry and Molecular Biology, 1999. **29**(2): p. 87-101.

59. Moskalyk, L.A., M.M. Oo, and M. Jacobs-Lorena, *Peritrophic matrix proteins of* Anopheles gambiae *and* Aedes aegypti. Insect Molecular Biology, 1996. **5**(4): p. 261-268.

60. Stohler, H., *The peritrophic membrane of blood-sucking Diptera in relation to their role as vectors of blood parasites.* Acta Tropica, 1961. **18**: p. 263-266.

61. Richards, A.G. and P.A. Richards, *The peritrophic membranes of insects.* Annual Review of Entomology, 1977. **22**(1): p. 219-240.

62. Freyvogel, T.A. and C. Jaquet, *The prerequisites for the formation of a peritrophic membrane in Culicidae females.* Acta Tropica, 1965. **22**: p. 148-154.

63. Pascoa, V., et al., Aedes aegypti *peritrophic matrix and its interaction with heme during blood digestion.* Insect Biochemistry and Molecular Biology, 2002. **32**(5): p. 517-523.

64. Schorderet, S., et al., *cDNA and deduced amino acid sequences of a peritrophic membrane glycoprotein, `Peritrophin-48', from the larvae of* Lucilia cuprina. Insect Biochemistry and Molecular Biology, 1998. **28(**2): p. 99-111.

65. Toprak, U., M. Erlandson, and D. Hegedus, *Peritrophic matrix proteins.* Trends in Entomology, 2010. **6**: p. 23-51.

66. Whiten, S.R., H. Eggleston, and Z.N. Adelman, *Ironing out the details: Exploring the role of iron and heme in blood-sucking arthropods.* Frontiers in Physiology, 2018. **8**(1134).

67. Rayms-Keller, A., et al., *Molecular cloning and characterization of a metal responsive* Aedes aegypti *intestinal mucin cDNA.* Insect Molecular Biology, 2000. **9**(4): p. 419-426.

68. Schirmer, E.C., J. Yates 3rd, and L. Gerace, *MudPIT: A powerful proteomics tool for discovery.* Discovery medicine, 2003. **3**(18): p. 38-39.

69. Rodgers, F.H., et al., *Microbiota-induced peritrophic matrix regulates midgut homeostasis and prevents systemic infection of malaria vector mosquitoes.* PLOS Pathogens, 2017. **13**(5): p. e1006391.

70. Bottino-Rojas, V., et al., *Heme signaling impacts global gene expression, immunity and dengue virus infectivity in* Aedes aegypti. PLoS ONE, 2015. **10**(8): p. e0135985.

71. Hooda, J., A. Shah, and L. Zhang, *Heme, an essential nutrient from dietary proteins, critically impacts diverse physiological and pathological processes.* Nutrients, 2014. **6**(3): p. 1080-102.

72. Byon, J.C., et al., *FLVCR is necessary for erythroid maturation, may contribute to platelet maturation, but is dispensable for normal hematopoietic stem cell function.* Blood, 2013. **122**(16): p. 2903-10.

73. Philip, M., et al., *Heme exporter FLVCR is required for T cell development and peripheral survival.* J Immunol, 2015. **194**(4): p. 1677-85.

74. Quigley, J.G., et al., *Identification of a human heme exporter that is essential for erythropoiesis.* Cell, 2004. **118**(6): p. 757-66.

75. Vinchi, F., et al., *Heme exporter FLVCR1a regulates heme synthesis and degradation and controls activity of cytochromes P450.* Gastroenterology, 2014. **146**(5): p. 1325-38.

76. Mercurio, S., et al., *The heme exporter Flvcr1 regulates expansion and differentiation of committed erythroid progenitors by controlling intracellular heme accumulation.* Haematologica, 2015. **100**(6): p. 720-729.

77. Tahara, T., et al., *Heme-dependent up-regulation of the alpha-globin gene expression by transcriptional repressor Bach1 in erythroid cells.* Biochem Biophys Res Commun, 2004. **324**(1): p. 77-85.

78. Tahara, T., et al., *Heme positively regulates the expression of beta-globin at the locus control region via the transcriptional factor Bach1 in erythroid cells.* J Biol Chem, 2004. **279**(7): p. 5480-7.

79. White, C., et al., *HRG1 is essential for heme transport from the phagolysosome of macrophages during erythrophagocytosis.* Cell Metab, 2013. **17**(2): p. 261-70.

80. Toh, S.Q., et al., *Haem uptake is essential for egg production in the haematophagous blood fluke of humans,* Schistosoma mansoni. FEBS Journal, 2015. **282**(18): p. 3632-3646.

81. Huynh, C., et al., *Heme uptake by* Leishmania amazonensis *is mediated by the transmembrane protein LHR1.* PLOS Pathogens, 2012. **8**(7): p. e1002795.

82. Rajagopal, A., et al., *Haem homeostasis is regulated by the conserved and concerted functions of HRG-1 proteins.* Nature, 2008. **453**(7198): p. 1127-31.

83. Lara, F.A., et al., *ATP binding cassette transporter mediates both heme and pesticide detoxification in tick midgut cells.* PLoS One, 2015. **10**(8): p. e0134779.

84. Pohl, P.C., et al., *In vitro establishment of ivermectin-resistant* Rhipicephalus microplus *cell line and the contribution of ABC transporters on the resistance mechanism.* Vet Parasitol, 2014. **204**(3-4): p. 316-22.

85. Pohl, P.C., et al., *ABC transporter efflux pumps: a defense mechanism against ivermectin in* Rhipicephalus (Boophilus) microplus. Int J Parasitol, 2011. **41**(13-14): p. 1323-33.

86. Pohl, P.C., et al., *ABC transporters as a multidrug detoxification mechanism in* Rhipicephalus (Boophilus) microplus. Parasitol Res, 2012. **111**(6): p. 2345-51.

87. Koh-Tan, H.H., et al., *Identification of a novel beta-adrenergic octopamine receptor-like gene (betaAOR-like) and increased ATP-binding cassette B10 (ABCB10) expression in a* Rhipicephalus microplus *cell line derived from acaricide-resistant ticks.* Parasit Vectors, 2016. **9**(1): p. 425.

88. Mangia, C., et al., *Evaluation of the in vitro expression of ATP binding-cassette (ABC) proteins in an* Ixodes ricinus *cell line exposed to ivermectin.* Parasit Vectors, 2016. **9**: p. 215.

89. Pereira, L.O., et al., *Biglutaminyl-biliverdin IX alpha as a heme degradation product in the dengue fever insect-vector* Aedes aegypti. Biochemistry, 2007. **46**(23): p. 6822-9.

90. Wegiel, B., et al., *Heme oxygenase-1: a metabolic nike.* Antioxid Redox Signal, 2014. **20**(11): p. 1709-22.

91. Wilks, A. and G. Heinzl, *Heme oxygenation and the widening paradigm of heme degradation.* Arch Biochem Biophys, 2014. **544**: p. 87-95.

92. Paiva-Silva, G.O., et al., *A heme-degradation pathway in a blood-sucking insect.* Proceedings of the National Academy of Sciences, 2006. **103**(21): p. 8030-8035.

93. Perner, J., et al., *Acquisition of exogenous haem is essential for tick reproduction.* eLife, 2016. **5**: p. e12318.

94. Al-Owais, M.M., et al., *Heme oxygenase-1 influences apoptosis via CO-mediated inhibition of K+ channels*, in *arterial chemoreceptors in physiology and pathophysiology*, C. Peers, et al., Editors. 2015, Springer International Publishing: Cham. p. 343-351.

95. Brouard, S., et al., *Heme oxygenase-1-derived carbon monoxide requires the activation of transcription factor NF-kappa B to protect endothelial cells from tumor necrosis factor-alpha-mediated apoptosis.* J Biol Chem, 2002. **277**(20): p. 17950-61.

96. Dore, S. and S.H. Snyder, *Neuroprotective action of bilirubin against oxidative stress in primary hippocampal cultures.* Ann N Y Acad Sci, 1999. **890**: p. 167-72.

97. Otterbein, L.E., et al., *Carbon monoxide has anti-inflammatory effects involving the mitogen-activated protein kinase pathway.* Nat Med, 2000. **6**(4): p. 422-8.

98. Sedlak, T.W. and S.H. Snyder, *Bilirubin benefits: cellular protection by a biliverdin reductase antioxidant cycle.* Pediatrics, 2004. **113**(6): p. 1776-82.

99. Stocker, R., *Antioxidant activities of bile pigments.* Antioxid Redox Signal, 2004. **6**(5): p. 841-9.

100. Stocker, R., et al., *Bilirubin is an antioxidant of possible physiological importance.* Science, 1987. **235**(4792): p. 1043-6.

101. Cui, L., et al., *Relevant expression of* Drosophila *heme oxygenase is necessary for the normal development of insect tissues.* Biochem Biophys Res Commun, 2008. **377**(4): p. 1156-61.

102. Ida, H., et al., *Genetic link between heme oxygenase and the signaling pathway of DNA damage in* Drosophila melanogaster. Tohoku J Exp Med, 2013. **231**(2): p. 117-25.

103. Damulewicz, M., et al., *Interactions between the circadian clock and heme oxygenase in the retina of* Drosophila melanogaster. Mol Neurobiol, 2017. **54**(7): p. 4953-4962.

104. Damulewicz, M., et al., *Haeme oxygenase protects against UV light DNA damages in the retina in clock-dependent manner.* Sci Rep, 2017. **7**(1): p. 5197.

105. Galay, R.L., et al., *Iron metabolism in hard ticks (Acari: Ixodidae): the antidote to their toxic diet.* Parasitol Int, 2015. **64**(2): p. 182-9.

106. Mandilaras, K., T. Pathmanathan, and F. Missirlis, *Iron absorption in* Drosophila melanogaster. Nutrients, 2013. **5**(5): p. 1622.

107. Dashti, Z.J.S., J. Gamieldien, and A. Christoffels, *Computational characterization of Iron metabolism in the Tsetse disease vector,* Glossina morsitans*: IRE stem-loops.* BMC Genomics, 2016. **17**(1): p. 561.

108. Tang, X. and B. Zhou, *Iron homeostasis in insects: Insights from* Drosophila *studies.* IUBMB Life, 2013. **65**(10): p. 863-72.

109. Zhou, G., et al., *Fate of blood meal iron in mosquitoes.* Journal of Insect Physiology, 2007. **53**(11): p. 1169-1178.

110. Rodrigues, V., et al., *malvolio, the* Drosophila *homologue of mouse NRAMP-1 (Bcg), is expressed in macrophages and in the nervous system and is required for normal taste behaviour.* Embo j, 1995. **14**(13): p. 3007-20.

111. Folwell, J.L., C.H. Barton, and D. Shepherd, *Immunolocalisation of the* D. melanogaster *Nramp homologue Malvolio to gut and malpighian tubules provides evidence that Malvolio and Nramp2 are orthologous.* Journal of Experimental Biology, 2006. **209**(10): p. 1988-1995.

112. Martinez-Barnetche, J., et al., *Cloning and functional characterization of the* Anopheles albimanus *DMT1/NRAMP homolog: implications in iron metabolism in mosquitoes.* Insect Biochem Mol Biol, 2007. **37**(6): p. 532-9.

113. Martínez-Barnetche, J., et al., *Cloning and functional characterization of the* Anopheles albimanus *DMT1/NRAMP homolog: implications in iron metabolism in mosquitoes.* Insect Biochem Mol Biol, 2007. **37**.

114. Xiao, G., et al., *The metal transporter ZIP13 supplies iron into the secretory pathway in* Drosophila melanogaster. Elife, 2014. **3**: p. e03191.

115. Sakurai, T. and K. Kataoka, *Basic and applied features of multicopper oxidases, CueO, bilirubin oxidase, and laccase.* Chem Rec, 2007. **7**(4): p. 220-9.

116. Lang, M., et al., *Multicopper oxidase-1 is a ferroxidase essential for iron homeostasis in* Drosophila melanogaster. Proceedings of the National Academy of Sciences, 2012. **109**(33): p. 13337-13342.

117. Liu, X., et al., *Multicopper oxidase-1 is required for iron homeostasis in malpighian tubules of* Helicoverpa armigera. Sci Rep, 2015. **5**: p. 14784.

118. Peng, Z., et al., *Multicopper oxidase-1 orthologs from diverse insect species have ascorbate oxidase activity.* Insect Biochem Mol Biol, 2015. **59**: p. 58-71.

119. Ye, Y.X., et al., *The multicopper oxidase gene family in the brown planthopper,* Nilaparvata lugens. Insect Biochem Mol Biol, 2015. **63**: p. 124-32.

120. Gorman, M.J., et al., *Characterization of the multicopper oxidase gene family in* Anopheles gambiae. Insect Biochem Mol Biol, 2008. **38**(9): p. 817-24.

121. Rosenzweig, A.C., *Metallochaperones: bind and deliver.* Chem Biol, 2002. **9**(6): p. 673-7.

122. Philpott, C.C., et al., *Cytosolic iron chaperones: Proteins delivering iron cofactors in the cytosol of mammalian cells.* J Biol Chem, 2017. **292**(31): p. 12764-12771.

123. Shi, H., et al., *A cytosolic iron chaperone that delivers iron to ferritin.* Science, 2008. **320**(5880): p. 1207-10.

124. Leidgens, S., et al., *Each member of the Poly-r(C)-binding Protein 1 (PCBP) family exhibits iron chaperone activity toward ferritin.* Journal of Biological Chemistry, 2013. **288**(24): p. 17791-17802.

125. Yanatori, I., et al., *Chaperone protein involved in transmembrane transport of iron.* Biochem J, 2014. **462**(1): p. 25-37.

126. Yanatori, I., et al., *The iron chaperone poly(rC)-binding protein 2 forms a metabolon with the heme oxygenase 1/cytochrome P450 reductase complex for heme catabolism and iron transfer.* J Biol Chem, 2017. **292**(32): p. 13205-13229.

127. Andrews, S.C., *The ferritin-like superfamily: Evolution of the biological iron storeman from a rubrerythrin-like ancestor.* Biochim Biophys Acta, 2010. **1800**(8): p. 691-705.

128. Gutierrez, L., et al., *Biophysical and genetic analysis of iron partitioning and ferritin function in* Drosophila melanogaster. Metallomics, 2013. **5**(8): p. 997-1005.

129. Pham, D.Q. and J.J. Winzerling, *Insect ferritins: Typical or atypical?* Biochim Biophys Acta, 2010. **1800**(8): p. 824-33.

130. Dunkov, B. and T. Georgieva, *Insect iron binding proteins: insights from the genomes.* Insect Biochem Mol Biol, 2006. **36**(4): p. 300-9.

131. Nichol, H., J.H. Law, and J.J. Winzerling, *Iron metabolism in insects.* Annu Rev Entomol, 2002. **47**.

132. González-Morales, N., et al., *Ferritin is required in multiple tissues during* Drosophila melanogaster *development.* PLOS ONE, 2015. **10**(7): p. e0133499.

133. Tang, X. and B. Zhou, *Ferritin is the key to dietary iron absorption and tissue iron detoxification in* Drosophila melanogaster. The FASEB Journal, 2013. **27**(1): p. 288-298.

134. Li, S., *Identification of iron-loaded ferritin as an essential mitogen for cell proliferation and postembryonic development in* Drosophila. Cell Res, 2010. **20**(10): p. 1148-57.

135. Dunkov, B.C., et al., Aedes aegypti *ferritin heavy chain homologue: feeding of iron or blood influences message levels, lengths and subunit abundance.* J Insect Sci, 2002. **2**: p. 7.

136. Geiser, D.L., et al., Aedes aegypti *ferritin.* Eur J Biochem, 2003. **270**(18): p. 3667-74.

137. Geiser, D.L., et al., *Iron loaded ferritin secretion and inhibition by CI-976 in* Aedes aegypti *larval cells.* Comp Biochem Physiol B Biochem Mol Biol, 2009. **152**(4): p. 352-63.

138. Geiser, D.L., et al., *The effect of bacterial challenge on ferritin regulation in the yellow fever mosquito,* Aedes aegypti. Insect Science, 2013. **20**(5): p. 601-619.

139. Otho, S.A., et al., *Silkworm ferritin 1 heavy chain homolog is involved in defense against bacterial infection through regulation of haemolymph iron homeostasis.* Dev Comp Immunol, 2016. **55**: p. 152-8.

140. Donohue, K.V., et al., *Heme-binding storage proteins in the Chelicerata.* J Insect Physiol, 2009. **55**(4): p. 287-96.

141. Galay, R.L., et al., *Multiple ferritins are vital to successful blood feeding and reproduction of the hard tick* Haemaphysalis longicornis. The Journal of Experimental Biology, 2013. **216**(10): p. 1905-1915.

142. Galay, R.L., et al., *Two kinds of ferritin protect* Ixodid *ticks from iron overload and consequent oxidative stress.* PLOS ONE, 2014. **9**(3): p. e90661.

143. Hajdusek, O., et al., *Knockdown of proteins involved in iron metabolism limits tick reproduction and development.* Proc Natl Acad Sci U S A, 2009. **106**(4): p. 1033-8.

144. Zhang, A.S. and C.A. Enns, *Molecular mechanisms of normal iron homeostasis.* Hematology Am Soc Hematol Educ Program, 2009: p. 207-14.

145. Yoshiga, T., et al., Drosophila melanogaster *transferrin.* European Journal of Biochemistry, 1999. **260**(2): p. 414-420.

146. Harizanova, N., et al., Aedes aegypti *transferrin. Gene structure, expression pattern, and regulation.* Insect Molecular Biology, 2005. **14**(1): p. 79-88.

147. Zhou, G., et al., *Differential regulation of transferrin 1 and 2 in* Aedes aegypti. Insect Biochem Mol Biol, 2009. **39**(3): p. 234-44.

148. Magalhaes, T., et al., *Expression of defensin, cecropin, and transferrin in* Aedes aegypti *(Diptera: Culicidae) infected with* Wuchereria bancrofti *(Spirurida: Onchocercidae), and the abnormal development of nematodes in the mosquito.* Exp Parasitol, 2008. **120**(4): p. 364-71.

149. Paily, K.P., B.A. Kumar, and K. Balaraman, *Transferrin in the mosquito,* Culex quinquefasciatus *Say (Diptera: Culicidae), up-regulated upon infection and development of the filarial parasite,* Wuchereria bancrofti *(Cobbold) (Spirurida: Onchocercidae).* Parasitology Research, 2007. **101**(2): p. 325-330.

150. Kokoza, V.A., et al., *Transcriptional regulation of the mosquito vitellogenin gene via a blood meal-triggered cascade.* Gene, 2001. **274**(1-2): p. 47-65.

151. Segraves, W.A., *Steroid receptors and orphan receptors in* Drosophila *development.* Semin Cell Biol, 1994. **5**(2): p. 105-13.

152. Thummel, C.S., *Flies on steroids*--Drosophila *metamorphosis and the mechanisms of steroid hormone action.* Trends Genet, 1996. **12**(8): p. 306-10.

153. Reinking, J., et al., *The* Drosophila *nuclear receptor E75 contains heme and is gas responsive.* Cell, 2005. **122**(2): p. 195-207.

154. Cruz, J., et al., *Distinct roles of isoforms of the heme-liganded nuclear receptor E75, an insect ortholog of the vertebrate Rev-erb, in mosquito reproduction.* Molecular and Cellular Endocrinology, 2012. **349**(2): p. 262-271.

155. Pierceall, W.E., et al., *E75 expression in mosquito ovary and fat body suggests reiterative use of ecdysone-regulated hierarchies in development and reproduction.* Mol Cell Endocrinol, 1999. **150**(1-2): p. 73-89.

156. Segraves, W.A. and C. Woldin, *The E75 gene of* Manduca sexta *and comparison with its* Drosophila *homolog.* Insect Biochem Mol Biol, 1993. **23**(1): p. 91-7.

157. Aicart-Ramos, C., et al., *Covalent attachment of heme to the protein moiety in an insect E75 nitric oxide sensor.* Biochemistry, 2012. **51**(37): p. 7403-7416.

158. Girvan, H.M. and A.W. Munro, *Heme sensor proteins.* J Biol Chem, 2013. **288**(19): p. 13194-203.

159. Farrugia, G. and J.H. Szurszewski, *Carbon monoxide, hydrogen sulfide, and nitric oxide as signaling molecules in the gastrointestinal tract.* Gastroenterology, 2014. **147**(2): p. 303-13.

160. Gullotta, F., et al., *CO metabolism, sensing, and signaling.* BioFactors, 2012. **38**(1): p. 1-13.

161. Jeffrey Man, H.S., A.K. Tsui, and P.A. Marsden, *Nitric oxide and hypoxia signaling.* Vitam Horm, 2014. **96**: p. 161-92.

162. Gudderra, N.P., et al., *Developmental profile, isolation, and biochemical characterization of a novel lipoglycoheme-carrier protein from the American dog tick,* Dermacentor variabilis *(Acari: Ixodidae) and observations on a similar protein in the soft tick,* Ornithodoros parkeri *(Acari: Argasidae).* Insect Biochemistry and Molecular Biology, 2001. **31**(4): p. 299-311.

163. Maya-Monteiro, C.M., et al., *HeLp, a heme lipoprotein from the hemolymph of the cattle tick,* Boophilus microplus. Journal of Biological Chemistry, 2000. **275**(47): p. 36584-36589.

164. Logullo, C., et al., *Binding and storage of heme by vitellin from the cattle tick,* Boophilus microplus. Insect Biochemistry and Molecular Biology, 2002. **32**(12): p. 1805-1811.

165. Black Iv, W.C., et al., *Flavivirus susceptibility in* Aedes aegypti. Archives of Medical Research, 2002. **33**(4): p. 379-388.

166. Gubler, D.J. and G.G. Clark, *Dengue/dengue hemorrhagic fever: the emergence of a global health problem.* Emerging Infectious Diseases, 1995. **1**(2): p. 55-57.

167. Rothman, A.L. and F.A. Ennis, *Immunopathogenesis of dengue hemorrhagic fever.* Virology, 1999. **257**(1): p. 1-6.

168. Murray, N.E.A., M.B. Quam, and A. Wilder-Smith, *Epidemiology of dengue: past, present and future prospects.* Clinical Epidemiology, 2013. **5**: p. 299-309.

169. Wilder-Smith, A. and D.J. Gubler, *Dengue vaccines at a crossroad.* Science, 2015. **350**(6261): p. 626-627.

170. Oliveira, J.H.M., et al., *Blood meal-derived heme decreases ROS levels in the midgut of* Aedes aegypti *and allows proliferation of intestinal microbiota.* PLoS Pathog, 2011. **7**(3): p. e1001320.

171. Vincent, S. *Oxidative effects of heme and porphyrins on proteins and lipids*. in *Seminars in hematology*. 1989.

172. Kogan, P.H., *Substitute blood meal for investigating and maintaining* Aedes aegypti *(Diptera: Culicidae).* Journal of Medical Entomology, 1990. **27**(4): p. 709-712.

173. Galun, R., Y. Avi-Dor, and M. Bar-Zeev, *Feeding response in* Aedes aegypti*: Stimulation by adenosine triphosphate.* Science, 1963. **142**(3600): p. 1674-1675.

174. Wolters, D.A., M.P. Washburn, and J.R. Yates, *An automated multidimensional protein identification technology for shotgun proteomics.* Analytical Chemistry, 2001. **73**(23): p. 5683-5690.

175. Distler, U., et al., *Drift time-specific collision energies enable deep-coverage data-independent acquisition proteomics.* Nat Meth, 2014. **11**(2): p. 167-170.

176. Liao, Z., et al., *IsoQuant: A software tool for SILAC-based mass spectrometry quantitation.* Analytical chemistry, 2012. **84**(10): p. 4535-4543.

177. Vizcaíno, Juan A., et al., *2016 update of the PRIDE database and its related tools.* Nucleic Acids Research, 2016. **44**(22): p. 11033-11033.

178. Bonizzoni, M., et al., *RNA-seq analyses of blood-induced changes in gene expression in the mosquito vector species,* Aedes aegypti. BMC Genomics, 2011. **12**(1): p. 82.

179. Reimand, J., et al., *g:Profiler—a web-based toolset for functional profiling of gene lists from large-scale experiments.* Nucleic Acids Research, 2007. **35**(suppl 2): p. W193-W200.

180. Reimand, J., T. Arak, and J. Vilo, *g:Profiler—a web server for functional interpretation of gene lists (2011 update).* Nucleic Acids Research, 2011. **39**(suppl 2): p. W307-W315.

181. Whiten, S.R., et al., *Characterization of the adult* Aedes aegypti *early midgut peritrophic matrix proteome using LC-MS.* PLOS ONE, 2018. **13**(3): p. e0194734.

182. Ribeiro, J.M.C., et al., *A deep insight into the sialome of male and female* Aedes aegypti *mosquitoes.* PLoS ONE, 2016. **11**(3): p. e0151400.

183. Conway, M.J., et al., Aedes aegypti *D7 saliva protein inhibits dengue virus infection.* PLoS Negl Trop Dis, 2016. **10**(9): p. e0004941.

184. Ribeiro, J.M.C., et al., *An annotated catalogue of salivary gland transcripts in the adult female mosquito,* Aedes ægypti. BMC Genomics, 2007. **8**: p. 6-6.

185. Noriega, F.G., et al., Aedes aegypti *midgut early trypsin is post-transcriptionally regulated by blood feeding.* Insect Molecular Biology, 1996. **5**(1): p. 25-29.

186. Barillas-Mury, C.V., F.G. Noriega, and M.A. Wells, *Early trypsin activity is part of the signal transduction system that activates transcription of the late trypsin gene in the midgut of the mosquito,* Aedes aegypti. Insect Biochemistry and Molecular Biology, 1995. **25**(2): p. 241-246.

187. Noriega, F.G. and M.A. Wells, *A molecular view of trypsin synthesis in the midgut of* Aedes aegypti. Journal of Insect Physiology, 1999. **45**(7): p. 613-620.

188. Lowenberger, C., *Innate immune response of* Aedes aegypti. Insect Biochemistry and Molecular Biology, 2001. **31**(3): p. 219-229.

189. Hanington, P.C. and S.M. Zhang, *The primary role of fibrinogen-related proteins in invertebrates is defense, not coagulation.* Journal of Innate Immunity, 2011. **3**(1): p. 17-27.

190. Conus, S. and H.-U. Simon, *Cathepsins and their involvement in immune responses.* Swiss Med Wkly, 2010. **140**(w13042).

191. Matsumoto, F., et al., *Cathepsins are required for Toll-like receptor 9 responses.* Biochemical and Biophysical Research Communications, 2008. **367**(3): p. 693-699.

192. Yorke, W. and J. Macfie, *The action of the salivary secretion of mosquitoes and of* Glossina tachinoides *on human blood.* Ann Trop Med Parasitol, 1924. **18**: p. 103-108.

193. Beier, M.S., et al., *Ingestion of* Plasmodium falciparum *sporozoites during transmission by Anopheline mosquitoes.* Am J Trop Med Hyg, 1992. **47**(2): p. 195-200.

194. Hudson, A., *Some functions of salivary glands of mosquitoes and other blood-feeding insects.* Canadian Journal of Zoology, 1964. **42**(1): p. 113-120.

195. Mellink, J.J. and W. Vandenbovenkamp, *Functional-aspects of mosquito salivation in blood feeding of* Aedes aegypti. Mosquito News, 1981. **41**(1): p. 115-119.

196. Champagne, D.E., et al., *The salivary gland-specific apyrase of the mosquito* Aedes aegypti *is a member of the 5'-nucleotidase family.* Proceedings of the National Academy of Sciences of the United States of America, 1995. **92**(3): p. 694-698.

197. Juhn, J., et al., *Spatial mapping of gene expression in the salivary glands of the dengue vector mosquito,* Aedes aegypti. Parasites & Vectors, 2011. **4**: p. 1-1.

198. Hawkins, R.I., *Factors affecting blood clotting from salivary glands and crop of* Glossina austeni. Nature, 1966. **212**: p. 738-9.

199. Devenport, M., et al., *Identification of the* Aedes aegypti *peritrophic matrix protein AeIMUCI as a heme-binding Protein.* Biochemistry, 2006. **45**(31): p. 9540-9549.

200. Tsutsui, K. and G.C. Mueller, *Affinity chromatography of heme-binding proteins: An improved method for the synthesis of hemin-agarose.* Analytical Biochemistry, 1982. **121**(2): p. 244-250.

201. Radyuk, S.N., et al., *The peroxiredoxin gene family in* Drosophila melanogaster. Free Radical Biology and Medicine, 2001. **31**(9): p. 1090-1100.

202. Peterson, T.M.L. and S. Luckhart, *A mosquito 2-Cys peroxiredoxin protects against nitrosative and oxidative stresses associated with malaria parasite infection.* Free radical biology & medicine, 2006. **40**(6): p. 1067-1082.

203. Akbari, O.S., et al., *The developmental transcriptome of the mosquito* Aedes aegypti, *an invasive species and major arbovirus vector.* G3: Genes|Genomes|Genetics, 2013. **3**(9): p. 1493-1509.

204. González-Lázaro, M., et al., Anopheles gambiae *Croquemort SCRBQ2, expression profile in the mosquito and its potential interaction with the malaria parasite*

Plasmodium berghei. Insect biochemistry and molecular biology, 2009. **39**(0): p. 395-402.

205. Bonizzoni, M., et al., *Complex modulation of the* Aedes aegypti *transcriptome in response to dengue virus infection.* PLOS ONE, 2012. **7**(11): p. e50512.

206. Liew, J.W.K., M.Y. Fong, and Y.L. Lau, *Quantitative real-time PCR analysis of* Anopheles dirus *TEP1 and NOS during* Plasmodium berghei *infection, using three reference genes.* PeerJ, 2017. **5**: p. e3577.

207. Sun, J., et al., *Lipophorin as a yolk protein precursor in the mosquito,* Aedes aegypti. Insect Biochemistry and Molecular Biology, 2000. **30**(12): p. 1161-1171.

208. van Heusden, M.C., F. Thompson, and J. Dennis, *Biosynthesis of* Aedes aegypti *lipophorin and gene expression of its apolipoproteins.* Insect Biochemistry and Molecular Biology, 1998. **28**(10): p. 733-738.

209. Zhang, L. and L. Guarente, *Heme binds to a short sequence that serves a regulatory function in diverse proteins.* The EMBO Journal, 1995. **14**(2): p. 313-320.

210. Immenschuh, S., et al., *The rat and human hemopexin genes contain an identical interleukin-6 response element that is not a target of CAAT enhancer-binding protein isoforms.* Journal of Biological Chemistry, 1994. **269**(17): p. 12654-61.

211. Chandor-Proust, A., et al., *The central role of mosquito cytochrome P450 CYP6Zs in insecticide detoxification revealed by functional expression and structural modelling.* Biochemical Journal, 2013. **455**(Pt 1): p. 75-85.

212. Feyereisen, R., *Arthropod CYPomes illustrate the tempo and mode in P450 evolution.* Biochimica et Biophysica Acta (BBA) - Proteins and Proteomics, 2011. **1814**(1): p. 19-28.

213. Untergasser, A., et al., *Primer3—new capabilities and interfaces.* Nucleic Acids Research, 2012. **40**(15): p. e115-e115.

214. Liu, W. and D.A. Saint, *A new quantitative method of real time reverse transcription polymerase chain reaction assay based on simulation of polymerase chain reaction kinetics.* Analytical Biochemistry, 2002. **302**(1): p. 52-59.

215. Tsujimoto, H., et al., *Identification of candidate iron transporters from the ZIP/ZnT gene families in the mosquito* Aedes aegypti. Frontiers in Physiology, 2018. **9**(380).

216. Isoe, J., et al., *Defects in coatomer protein I (COPI) transport cause blood feeding-induced mortality in yellow fever mosquitoes.* Proceedings of the National Academy of Sciences, 2011. **108**(24): p. E211–E217.

217. Schindelin, J., et al., *Fiji - an open source platform for biological image analysis.* Nature methods, 2012. **9**(7): p. 10.1038/nmeth.2019.

218. Kaplan, L.A.E., et al., *A comparison of RT-PCR and northern blot analysis in quantifying metallothionein mRNA levels in killifish exposed to waterborne cadmium.* Marine Environmental Research, 1995. **39**(1): p. 137-141.

219. Taracena, M.L., et al., *Regulation of midgut cell proliferation impacts* Aedes aegypti *susceptibility to dengue virus.* PLOS Neglected Tropical Diseases, 2018. **12**(5): p. e0006498.

APPENDIX A

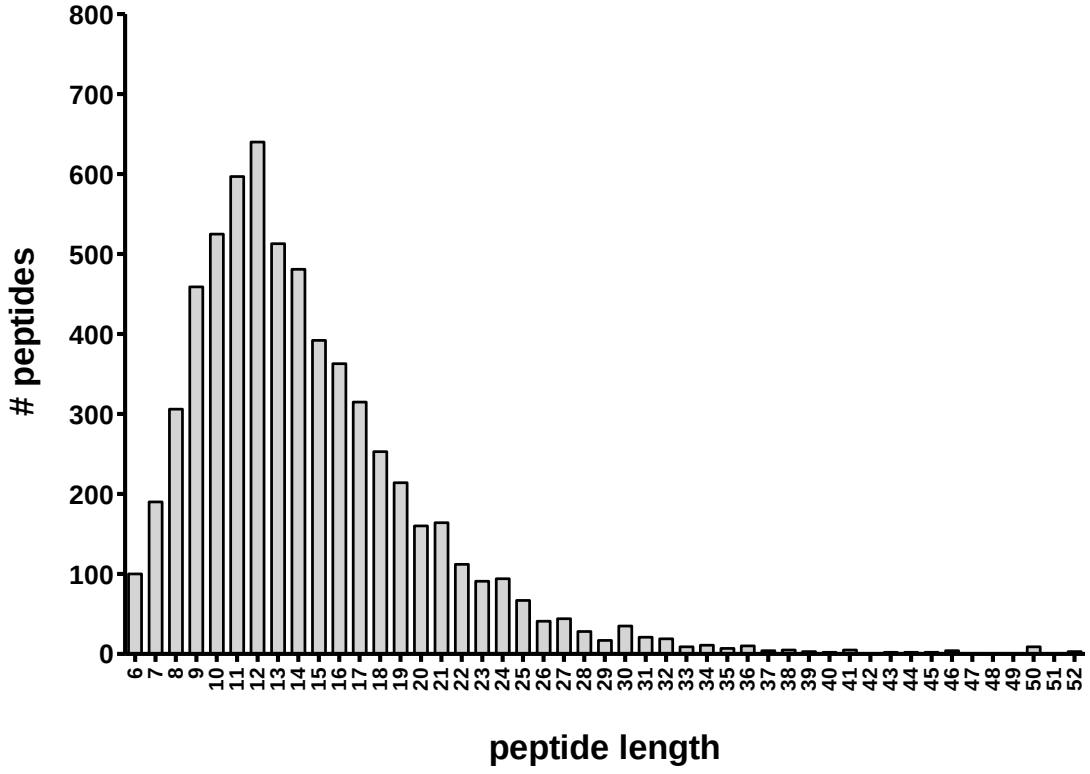

A-1. Peptide length distribution. Frequency distribution of peptide length versus abundance for all 6319 peptides obtained from *Ae. aegypti* peritrophic matrix and contents [181].

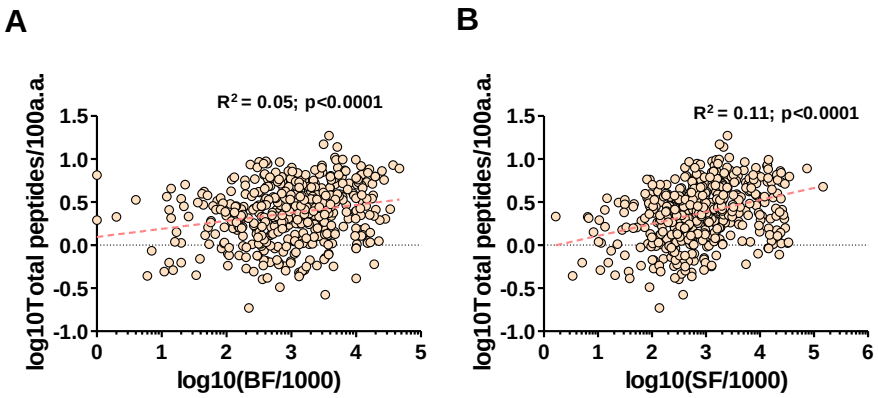

A-2. Peptide recovery from peritrophic matrix is only weakly correlated with transcript abundance. Relationship between the length-normalized transcript abundance in bloodfed **(A)** or sugar-fed **(B)** mosquitoes [181].

B-1. C_q values for gene expression patterns for known and putative adult *Ae. aegypti* peritrophic matrix peritrophins determined by quantitative PCR using primer sets. Adapted from Tsujimoto et al. [215].

Biological replicate ↓		2467			2495			6953		
	Technical replicate →	1	2	3	1	2	3	1	2	3
1	NBF	21.74	21.80	21.99	17.98	18.07	17.95	22.51	22.75	22.36
	2HRS	16.31	16.39	16.35	17.44	17.38	17.31	24.88	25.19	24.86
	4HRS	17.74	17.77	17.85	19.33	19.25	19.13	25.21	25.44	25.26
	8HRS	18.06	18.18	18.06	19.03	18.71	18.64	22.82	23.06	22.78
	12HRS	18.14	18.26	18.21	18.68	18.47	18.42	24.37	24.42	24.47
	18HRS	19.70	19.69	19.84	19.73	19.88	19.53	24.85	25.08	24.82
	24HRS	19.52	19.49	19.53	18.87	18.7	18.59	26.75	26.72	26.74
	48HRS	18.14	18.11	17.99	16.72	17.11	17.16	23.05	23.16	23.09
2	NBF	19.69	19.48	19.51	17.03	17.11	17.11	26.56	26.39	26.54
	2HRS	18.51	18.87	18.57	18.85	18.85	18.73	26.17	26.31	26.24
	4HRS	17.72	17.92	17.77	18.49	18.74	18.57	23.66	23.59	23.68
	8HRS	18.09	18.34	18.08	18.74	18.96	18.94	23.97	24.04	23.99
	12HRS	19.67	20.04	19.93	19.81	20.03	19.98	23.22	23.2	23.29
	18HRS	19.87	19.96	19.86	20	19.79	19.86	23.72	23.77	23.7
	24HRS	18.73	18.84	18.87	19.14	19.08	19.04	22.63	22.6	22.59
	48HRS	21.82	21.35	21.33	20.68	20.61	20.72	28.6	28.83	29.19
3	NBF	20.17	20.18	20.49	15.82	16	16	22.05	22.24	22.21
	2HRS	17.5	17.44	17.62	17.37	17.5	17.41	23.43	23.41	23.55
	4HRS	16.28	16.37	16.53	17.24	17.45	17.35	23.3	23.17	23.52
	8HRS	16.27	16.23	16.29	16.34	16.58	16.47	23.51	23.48	23.57
	12HRS	20.5	20.77	20.69	20.52	20.76	20.82	24.79	24.68	25.09
	18HRS	20.36	20.36	20.35	19.48	19.7	19.63	25.17	25.05	25.41
	24HRS	20.51	20.5	20.53	19.49	19.67	19.6	28.11	28.05	28.73
	48HRS	21.76	21.06	21.16	18.56	18.92	18.79	26.35	26.45	26.55

B-2. Calculated expression patterns for known and putative adult *Ae. aegypti* peritrophic matrix peritrophins determined by quantitative PCR using primer sets. Adapted from Tsujimoto et al. [215].

Biological replicate ↓		**2467** Expression	**2495** Expression	**6953** Expression
1	NBF	15.50	13.72	0.65
	2HRS	197.11	13.66	0.09
	4HRS	254.34	11.20	0.19
	8HRS	129.29	9.03	0.57
	12HRS	126.50	11.16	0.21
	18HRS	128.26	11.84	0.36
	24HRS	116.85	18.33	0.09
	48HRS	83.42	18.87	0.32
2	NBF	39.45	18.72	0.04
	2HRS	198.36	18.43	0.13
	4HRS	314.01	21.23	0.72
	8HRS	212.13	14.52	0.47
	12HRS	80.63	6.89	0.74
	18HRS	109.94	9.84	0.73
	24HRS	88.10	7.43	0.69
	48HRS	106.52	13.43	0.06
3	NBF	16.40	24.39	0.38
	2HRS	218.33	27.51	0.48
	4HRS	300.67	21.77	0.40
	8HRS	231.30	27.98	0.25
	12HRS	163.12	12.79	0.78
	18HRS	118.64	16.36	0.38
	24HRS	88.14	13.37	0.04
	48HRS	54.09	22.00	0.13

B-3. C_q values for gene expression for single-injection RNAi-mediated knockdown midguts determined by quantitative PCR using primer sets. Adapted from Tsujimoto et al. [215].

Biological replicate ↓		2467			CAT			FER			S7		
	Technical replicate →	1	2	3	1	2	3	1	2	3	1	2	3
1	ds2467	20.47	20.25	20.37	25.04	24.74	24.78	22.46	22.21	22.47	24.39	24.28	24.2
	dsGFP	16.88	16.85	17.13	22.49	22.46	22.43	20.25	20.27	20.24	21.27	21.31	20.65
2	ds2467	23.65	23.68	24.34	24.19	24.35	24.39	22.11	22.3	22.36	23.14	23.22	23.23
	dsGFP	15.30	15.73	16.61	21.34	21.41	21.43	19.16	19.03	19.05	20.76	20.88	20.73
3	ds2467	18.11	18.05	18.06	21.27	21.19	21.20	18.49	18.38	18.35	20.05	20.15	20.05
	dsGFP	17.29	17.24	17.12	21.32	21.47	21.45	18.71	18.59	18.37	19.84	20.05	19.81

Biological replicate ↓		2495			CAT			FER			S7		
	Technical replicate →	1	2	3	1	2	3	1	2	3	1	2	3
1	ds2495	21.34	21.19	21.35	22.9	22.95	23.14	20.12	20.09	20.33	21.25	21.36	21.32
	dsGFP	19.09	19.17	19.45	22.49	22.46	22.43	20.25	20.27	20.24	21.27	21.31	20.65
2	ds2495	N/A	20.7	20.85	22.28	22.27	22.95	19.4	19.75	19.83	20.27	21.29	21.41
	dsGFP	16.2	16.44	17.11	21.34	21.41	21.43	19.16	19.03	19.05	20.76	20.88	20.73
3	ds2495	23.02	22.99	22.92	21.91	21.92	21.69	19.47	19.42	19.36	21.13	20.87	21.01
	dsGFP	19.35	19.9	19.93	21.32	21.47	21.45	18.71	18.59	18.37	19.84	20.05	19.81

Biological replicate ↓		6953			CAT			FER			S7		
	Technical replicate →	1	2	3	1	2	3	1	2	3	1	2	3
1	ds6953	29.85	29.79	29.84	23.91	23.82	23.68	21.06	21.16	21.1	22.28	22.38	22.22
	dsGFP	24.76	24.77	24.71	22.49	22.46	22.43	20.25	20.27	20.24	21.27	21.31	20.65
2	ds6953	26.53	27.02	27.02	22.15	22.24	22.7	19.82	19.9	19.91	21.12	21.2	21.69
	dsGFP	20.18	19.98	21.11	21.34	21.41	21.43	19.16	19.03	19.05	20.76	20.88	20.73
3	ds6953												
	dsGFP	29.3	29.84	29.8	21.32	21.47	21.45	18.71	18.59	18.37	19.84	20.05	19.81

B-4. Calculated expression values for gene expression for single-injection RNAi-mediated knockdown midguts determined by quantitative PCR using primer sets. Adapted from Tsujimoto et al. [215].

Biological replicate ↓		**2467** Expression	**CAT** Expression	**FER** Expression
1	ds2467	634.79	1.10	10.17
	dsGFP	397.56	0.58	4.26
2	ds2467	43.36	0.73	5.05
	dsGFP	577.02	1.00	7.66
3	ds2467	106.65	0.68	7.27
	dsGFP	148.34	0.52	5.76

Biological replicate ↓		**2495** Expression	**CAT** Expression	**FER** Expression
1	ds2495	3.39	0.47	5.29
	dsGFP	11.17	0.58	4.26
2	ds2495	3.80	0.53	5.98
	dsGFP	52.45	1.00	7.66
3	ds2495	0.90	0.85	7.11
	dsGFP	3.47	0.52	5.76

Biological replicate ↓		**6953** Expression	**CAT** Expression	**FER** Expression
1	ds6953	0.02	0.55	5.73
	dsGFP	0.28	0.58	4.26
2	ds6953	0.08	0.75	6.62
	dsGFP	3.96	1.00	7.66
3	ds6953	N/A	N/A	N/A
	dsGFP	0.005	0.52	5.76

B-5. C_q values for gene expression for multiplex injection RNAi-mediated knockdown midguts determined by quantitative PCR using primer sets. Adapted from Tsujimoto et al. [215].

Biological replicate ↓		2467			2495			6953			CAT			FER			S7		
	Technical replicate →	1	2	3	1	2	3	1	2	3	1	2	3	1	2	3	1	2	3
1	dsMix	21.55	21.82	21.88	19.49	19.65	19.64	25.83	26.01	26.26	22.76	22.64	22.45	20.24	20.15	20.21	21.46	21.53	21.13
	dsGFP	22.02	22.01	22.12	17.12	17.71	19.52	26.49	27.23	27.6	25.95	25.16	25.46	23.66	22.36	23.41	24.73	24.38	24.46
2	dsMix	21.33	21.42	21.27	21.06	21.23	21.17	26.62	26.83	26.83	22.14	22.19	21.95	19.49	19.45	19.32	21.09	21.18	20.95
	dsGFP	16.58	16.67	16.69	17.79	17.61	17.74	22.74	22.68	22.68	21.31	21.39	21.3	17.88	17.92	17.75	19.46	19.62	19.47
3	dsMix	20.05	20.24	20.2	19.96	20.04	19.86	25.83	25.9	25.7	22.57	22.34	22.39	19.91	19.71	19.89	21.02	21.01	21.03
	dsGFP	15.17	15.35	15.87	18.57	18.68	18.59	24.8	24.37	24.24	23.83	23.36	23.24	20.68	20.86	20.85	21.25	21.47	21.47

B-6. Calculated expression values for gene expression for multiplex injection RNAi-mediated knockdown midguts determined by quantitative PCR using primer sets. Adapted from Tsujimoto et al. [215].

Biological replicate ↓		2467	2495	6953	CAT	FER
		Expression	Expression	Expression	Expression	Expression
1	dsMix	37.17	10.92	0.15	0.65	5.47
	dsGFP	301.85	276.83	0.69	0.81	7.17
2	dsMix	37.34	3.14	0.07	0.75	7.46
	dsGFP	153.18	9.98	0.35	0.42	7.05
3	dsMix	67.74	6.68	0.13	0.57	5.42
	dsGFP	1115.94	21.21	0.42	0.36	3.72